Prenatal THC exposure has lasting detrimental effects on the rat hippocampus

by

Hannah Margaret Olivia Reid

BSc, University of Victoria, 2019

A Dissertation submitted in Partial Fulfillment of the Requirements for the Degree of

DOCTOR OF PHILOSOPHY

in the Division of Medical Sciences

PRENATAL THC EXPOSURE HAS LASTING DETRIMENTAL EFFECTS ON THE RAT HIPPOCAMPUS

by

Hannah Margaret Olivia Reid

BSc, University of Victoria, 2019

Supervisory Committee

Dr. Brian R. Christie, Division of Medical Sciences

Supervisor

Dr. Leigh Anne Swayne, Division of Medical Sciences

Departmental Member

Dr. Ryan J. McLaughlin, Washington State University

Outside Member

Abstract

Prenatal cannabis exposure is as common as prenatal alcohol exposure, and yet it is understudied. With the recent legalization of cannabis, it is doubly important to elucidate these effects. The hippocampus is rich in cannabinoid type 1 receptors, which are targeted by the psychoactive component of cannabis. The hippocampus is central to learning and memory and is known to be affected acutely by this drug. In this dissertation, I examine how prenatal THC exposure affects different populations of hippocampal interneurons, how morphological characteristics of microglia are altered, and hippocampal synaptic plasticity is affected, and how inhibitory and excitatory markers My findings show not only that there are alterations in all these areas, but that there are regional and sex differences in many of these changes. These results suggest that there is increased $GABA_A$ recruitment via increased gephyrin cluster sizes. In absence of other receptor changes this shows that the balance of inhibition and excitation is shifted towards inhibition. Dendritic spines decreases are consistent with human clinical findings with similar psychiatric outcomes. As interneuron densities are static compared with other outcome measures, early perturbations in the endocannabinoid system likely drive the observed interneuron alterations, which then drive spine, receptor, and plasticity alterations. This work shows that there are consequences of prenatal cannabis exposure into adulthood.

Table of Contents

2 A Systematic Review of the Effects of Perinatal Alcohol Exposure and Perinatal Marijuana Exposure on Adult Neurogenesis in the Dentate Gyrus

List of Figures

List of Tables

Abbreviations

A/C	**Alcohol and THC**
Abcam	Antibodies Cambridge
abGCs	Adult born granule cells
aCSF	Artificial cerebrospinal fluid
AEA/ANA	Anandamide
AM251	1-(2,4-Dichlorophenyl)-5-(4-iodophenyl)-4-methyl-N-(1-piperidyl)pyrazole-3-carboxamide, CB1 antagonist, weak CB2 antagonist
AMPA	α-Amino-3-hydroxy-5-methyl-4-isoxazolepropionic acid
AMPAR	α-Amino-3-hydroxy-5-methyl-4-isoxazolepropionic acid receptor
ANOVA	Analysis of Variance
BrdU	5-bromo-2'-deoxyuridine
CA	Cornu ammonis
CA1	Cornu Ammonis 1
CA2	Cornu Ammonis 2
CA3	Cornu Ammonis 3
CB1	Cannabinoid receptor type 1

CB2	Cannabinoid receptor type 2
CCAC	Canadian Council on Animal Care
CCK	Cholecystokinin
CGE	Caudal Ganglionic Eminence
CNS	Central nervous system
DAG	Diacylglycerol
DAGL	Diacelglyeroldiacylglycerol lipase
DG	Dentate Gyrus
EC	Entorhinal cortex
eCB	Endocannabinoid
EtOH	Ethanol
FASD	Fetal Alcohol Spectrum Disorder
GABA	γ-Aminobutyric acid
GABAA	Gamma-aminobutyric acid receptor type A
GABAB	Gamma-aminobutyric acid receptor type B
GCL	Granule cell layer
GD	Gestational day
$G_{i/o}$	G protein inhibitory type

GPCR	G-protein coupled receptor
KCC2	Potassium-Chloride Cotransporter 2
Ki-67	Marker of proliferation
LTD	Long-Term Depression
MAGL	Monoacylglycerol lipase
MGE	Medial Ganglionic Eminence
mGluR	Metabotropic glutamate receptor
MPEP	2-Methyl-6-(phenylethynyl)pyridine, Metabotropic glutamate receptor antagonist
NDS	Normal donkey serum
NGS	Normal goat serum
NIDA	National Institute on Drug Abuse
NMDA	N-Methyl-D-aspartate
NPY	Neuropeptide Y
PAE	Perinatal alcohol exposure
PBS	Phosphate-buffered saline
PBST	Phosphate Buffered Saline with Tween 20
PD/PND	Postnatal Day

PFA Paraformaldehyde

PRISMA Preferred Reporting Items for Systematic Reviews and Meta-Analyses

PSD95 Postsynaptic density protein 95

PV Parvalbumin

r-TMS Repetitive Transcranial Magnetic Stimulation

SAM Simultaneous alcohol and marijuana

Smo Smoothened protein

SOM Somatostatin

SP Stratum pyramidale

THC Δ^9-tetrahydrocannabinol

TERRITORY ACKNOWLEDGEMENT

We acknowledge and respect the lək^{w}əŋən peoples on whose traditional territory the university stands and the Songhees, Esquimalt and W̱SÁNEĆ peoples whose historical relationships with the land continue to this day.

ACKNOWLEDGEMENTS

I would first and foremost like to thank my supervisor, Dr. Brian Christie, for his mentorship and support. Thank you for always being available to answer my questions and for encouraging me to form my own opinions (and challenging them to make sure they are sound). Thank you for letting me try strange things and go off on research tangents and side projects. Thank you for affording me the ability to publish and to attend conferences.

I would like to thank Taylor Snowden, Penelope Young, and Alejandra Rauldales- my cohort. Whether it was coffee walks to discuss research or decompress, celebrating over beers, or just chatting, I am a much happier and healthier person for all of the love and care you have shown me. Taylor you are such a ray of sunshine thank you for always brightening my day. Penny, thank you for being my (creative) writing buddy and teacher. Maybe one day we can both publish non-sciencey things. Ale, you are such a sweetheart, thank you for always being such a kind and calming presence. Erin Gräfe, thank you for being my desk buddy, fielding all of my ephys questions, and letting me drag you into the world of Dungeons and Dragons. Jenessa Johnston and Kaylene Schiel, thank you for being the most fun people ever. Jenessa thank you answering all of my molecular questions, and tolerating my never ending stream of depression jokes regarding your work.

To the Christie lab members past and present, thank you for making coming to work everyday an enjoyable experience. To the post docs and senior members of the lab and of the DMS, thank you for taking the time to mentor me, and for letting be bounce questions off of your heads, I am a much better scientist for it. Thank you to all of the wonderful office staff for being so on top of things!

Katie Neale, I would not be a scientist without you. You are such a wonderful and true friend I am so happy that I met you. Thank you for all of your mentorship inside and outside the lab. I'd like to think that some of your good habits rubbed off on me (I hope).

To the undergraduates, volunteers, techs, and FLEX students that I have had the pleasure of working with over the years: Allyson Gross, Sara Winger, Katherine Ball, Polina Poberezhnyk, Colin Murray, Emily Funnikoter, Kate Conway, Nathen Chen-Mack, Owen Trepanier, Emily Bosdachin. Thank you! It really takes a village and I appreciate the heck out of all of you.

To my family: Esther, Jock, and Hailey. Thank you for you love and support through graduate school and also over the years. I think its safe to say you are the reason I both finished my undergraduate degree and made it through graduate school. Mom, thank you for always taking the time to explain the natural world when I was a kid, and for encouraging me to question everything always. Dad, thank you for fostering my love of reading and for always telling me to stay in school "as long as possible." Hailey, thank you for dealing with the craziness of my wedding at the end of my degree, for being my lowkey lawyer, and for the friendly facetime calls.

To my friends near and far, thank you for keeping me sane over the years. Ellen I appreciate your phone calls, checking in on me. Charlotte you were the best lab partner ever! Julia, Laura and Kate, thank you for being my other family. Erin (Mcdons) you are going to be the best doctor I can't wait to see what you do next.

I would like to thank my husband, Anthony. From before graduate school now to everything that comes next, you have always had my back. Thank you for learning and growing with me, and for always making an effort, no matter the endeavor. Thank you for brining me food and for listening to me talk about my research (especially during this last whirlwind of writing).

I would finally like to acknowledge all of the rats that made this work possible.

This work is dedicated to

Our little spark of madness, and may we never lose it

CHAPTER 1

Introduction

1.1 Preface

The papers contained in this dissertation all pertain to the study of prenatal cannabis exposure in a rat model. The central mechanism to which all others are linked is that of the direct and indirect actions of the CB1 receptor, and how alterations in this receptor create downstream effects in prenatal THC exposure. It has been known for some time that prenatal THC exposure can alter CB1 receptors (1). In the case of interneurons this could affect their migration, as the CB1 receptor is involved in migration and axon guidance (2). The CB1 receptor is also implicated in neuroinflammation, and so this dissertation touches on microglia (3,4). Finally, the CB1 receptor is implicated in hippocampal synaptic plasticity, and so long-term depression is assayed (5,6). Together these results show that prenatal cannabis exposure has long-lasting, sex-dependent effects in the rat hippocampus.

1.2 The hippocampus

The hippocampus is primarily made up of two main structures, the cornu ammonis region (subdivided into CA1, CA2, CA3, and CA4 or hilus regions), and the dentate gyrus (DG) (7). The subiculum (divided into the para-, pre-, post-, and prosubiculum) is often treated as part of the CA1 subfield in research, although it is a distinct subfield (7). The hippocampus lends itself well to the study of synaptic plasticity, as it is a uni-directional circuit with stereotypic cytoarchitecture that is preserved in hippocampal sections.

Projections from the entorhinal cortex (EC) project to the hippocampus, around the circuit, and back out again (7). More specifically, layer II of the medial EC projects to the dentate gyrus through the perforant path (7). The perforant path can be broken down into the medial and lateral perforant path; the medial tends to contain spatial information while the lateral tends to carry information about novel objects (8,9). From there, the mossy fibers of the commissural pathway project to the CA3 subfield, and from there Schaffer collaterals project to the CA1 subfield (7). The CA3 also makes reciprocal connections to the neocortex, hypothalamus, and brain stem via the fimbria-fornix pathway (10). The mossy fibers of the dentate gyrus further project medially to the other hemisphere (7). This entire circuit is part of the larger Papez circuit, which also includes among other things, the amygdala (11).

1.3 The endocannabinoid system

Under basal conditions, the CB1 receptor is acted upon by endogenous cannabinoids (eCBs) (12). Anandamide (ANA, AEA) is synthesized through a complex biochemical pathway, but is largely controlled by N-acylphosphatidylethanolamine-specific phospholipase D (NAPE-PLD or NAT) (13). This enzyme catalyzes AEA synthesis by creating N-arachidonoyl-phosphatidylethanolamine (NAPE) from phosphatidylethanolamine and arachidonic acid (13). Hydrolysis of NAPE forms AEA (13). The other main eCB, 2- arachidonoyl glycerol, is created when diacylglycerol lipase (DAGL), breaks down diacylglycerol (DAG) (14). DAGL has two isoforms, α and β. Like the CB1 and CB2 receptors, the first is primarily in the brain and the second is primarily peripheral (15,16). 2-AG is also regulated by monoacylglycerol lipase (MAGL) (14). MAGL acts to degrade 2-AG (14). Interestingly, and because of the properties of lipids,

eCBs cannot be stored (17). Thus, the ability to regulate their production in a tight timeline on demand is an important feature of the eCB system. The regulation of this metabolism is not fully characterized and is an exciting frontier of research. The endocannabinoid system is also affected by metabotropic glutamate receptors (mGluRs) (6). The activation of mGluRs in the postsynaptic neuron can stimulate the production of eCBs (6).

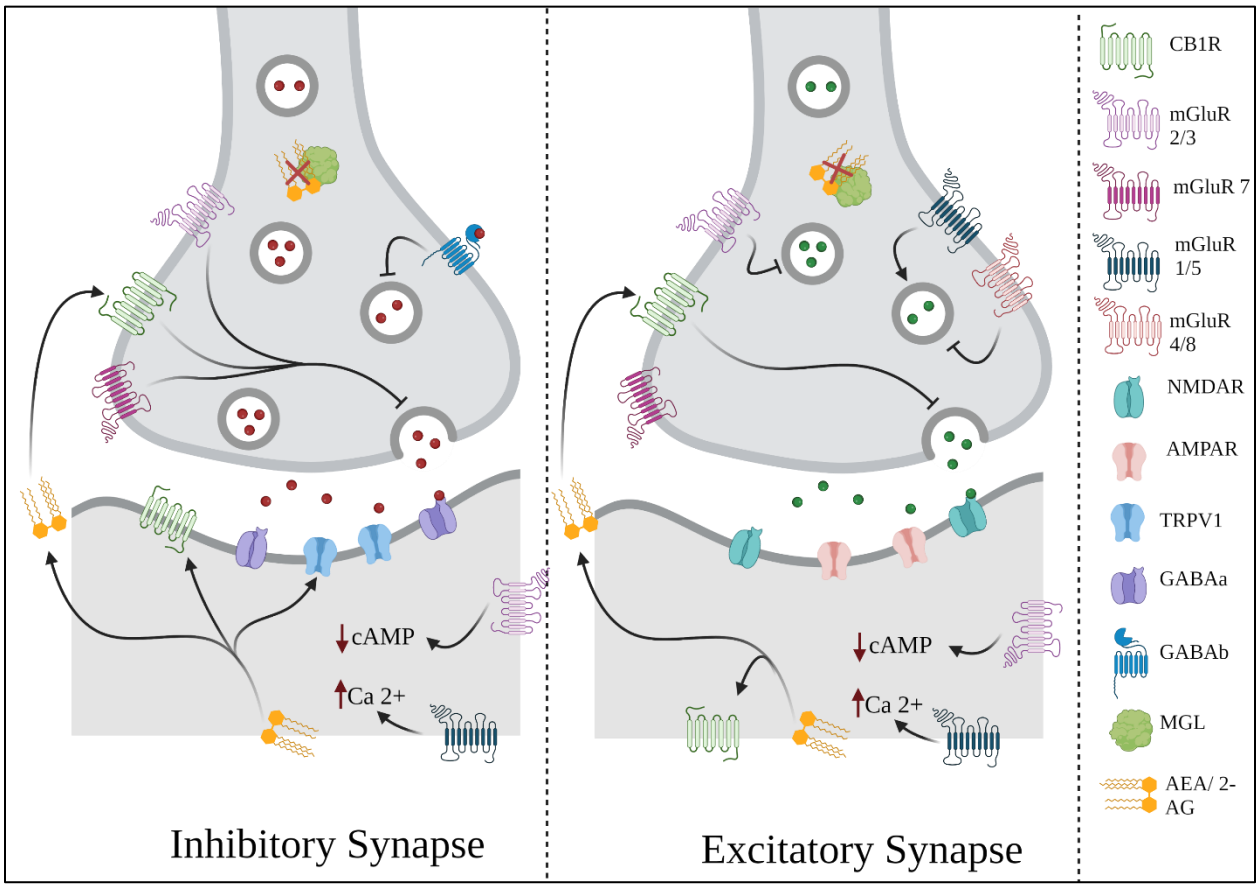

Figure 1.1 *The endocannabinoid system at the synapse. Created with Biorender.*

1.4 Interneurons

Interneurons are a diverse population of cells that release γ-aminobutyric acid (18). Unlike principal neurons, all interneurons are born in the caudal and medial ganglionic

eminences and must migrate to their final location in the brain (19). Some interesting work out of Harvard showed that interneurons are programmed to a specific marker profile very early, but their shape is context dependent (20). Dysregulation of hippocampal interneurons has been identified in psychiatric disorders, and their tight regulation of neuronal networks is necessary for proper signal transmission and fidelity (18). There are many subtypes of interneuron, in the hippocampus and elsewhere in the brain. Parvalbumin (PV) interneurons are integral for large-scale network oscillations, while somatostatin (SOM) interneurons synapse onto dendritic tufts and fine-tune input (18). Neuropeptide Y (NPY) interneurons are involved with basal inhibitory tone, as they secrete GABA into the extracellular matrix to signal metabotropic $GABA_B$ receptors (21). CB1 receptors are primarily found on interneurons, and further also likely aid in their migration (22,23).

1.5 Microglia and neuroinflammation

Microglia are the resident immune cells of the brain, involved with homeostasis and are responsive to neurological insults (24). Many postnatal studies have assayed the effect of cannabis on brain inflammation, mainly thought to be mediated by the CB2 receptor (25,26). However, microglia also express CB1 receptors and have been shown to respond to eCBs in their environment in a phagocytic manner (27). One postnatal study has shown that acute THC exposure can exert immunosuppressive effects on microglia (28). As both responders to excitotoxicity and other insults, as well as effectors of inflammation, are an important piece of prenatal cannabis research.

1.6 Hippocampal Plasticity: Long-Term Depression

Long-term depression is a type of synaptic plasticity that acts as a signal to decrease future signal strength (29). And so LTD is the process by which less firing begets even less firing. It was originally proposed to be a mechanism of forgetting (30). The induction of LTD usually involves group I mGluRs, which lead to the activation of phosphatases such as calcineurin (31). Phosphatases and kinases are common cellular switches, where kinases add a phosphate group, while phosphatases remove the phosphate group (32). The dephosphorylation leads to the removal of α-amino-3-hydroxy-5-methyl-4-isoxazolepropionic acid (AMPA) receptors from the plasma membrane of the synapse (33). On a larger scale LTD can lead to a decrease in synaptic connections altogether, which allows the neurons involved with working memory to be plastic since existing connections can be rewritten.

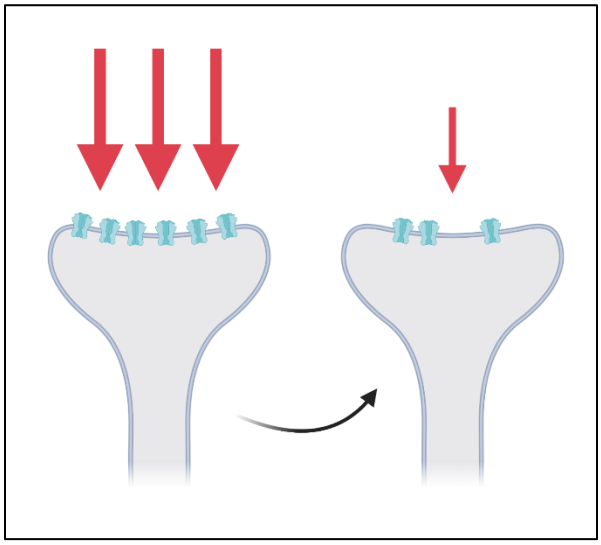

Figure 1.2 *Simplified LTD Schematic*
Less firing leads to the removal of post-synaptic receptors.

CHAPTER 2

Published: **A Systematic Review of the Effects of Perinatal Alcohol Exposure and Perinatal Marijuana Exposure on Adult Neurogenesis in the Dentate Gyrus.**

2.1 Abstract

2.1.1 Background: Marijuana and alcohol are both substances that, when used during pregnancy, may have profound effects on the developing fetus. There is evidence to suggest that both drugs can affect working memory, one function of the hippocampal formation, however, there is a paucity of data on how perinatal exposure to alcohol or cannabis impacts the process of adult neurogenesis.

2.1.2 Methods: This systematic review examines immunohistochemical data from adult rat and mouse models that assess perinatal alcohol or perinatal marijuana exposure. A comprehensive list of search terms was designed and used to search three separate databases. All results were imported to Mendeley and screened by two authors. Consensus was reached on a set of final papers that met the inclusion criteria and their results were summarized.

2.1.3 Results: Thirteen papers were identified as relevant, ten of which pertained to the effects of perinatal alcohol on the adult hippocampus, and three pertained to the effects of perinatal marijuana on the adult hippocampus. Cellular proliferation in the dentate gyrus was not affected in adult rats and mice exposed to alcohol perinatal. In general, perinatal alcohol exposure did not have a significant and reliable effect on the maturation and survival of adult born granule neurons in the dentate gyrus. In contrast,

interneuron numbers appear to be reduced in the dentate gyrus of adult rats and mice exposed perinatal to alcohol. Perinatal marijuana exposure was also found to reduce inhibitory interneuron numbers in the dentate gyrus.

2.1.4 Conclusions: Perinatal alcohol exposure and perinatal marijuana exposure both act on inhibitory interneurons in the hippocampal formation of adult rats. These findings suggest simultaneous perinatal alcohol and marijuana exposure (SAM) may have a dramatic impact on inhibitory processes in the dentate gyrus.

2.2 Introduction

With the relaxation of cannabis restrictions across North America, a growing proportion of young adults (19 – 30 years of age) are reporting the **S**imultaneous use of **A**lcohol and **M**arijuana (SAM), and indications are that this trend will continue to rise (34). ***This age demographic also coincides with the peak fertility period for males and females*** (35)***, and SAM significantly increases the risk of unplanned pregnancies*** (36). Moreover, the use of illicit drugs in this age group is more common, with cannabis being the most commonly used drug by pregnant women (37). Approximately half of all marijuana users also report alcohol use (38–40), with recent statistics indicating that over 30% of women of reproductive age have consumed alcohol and marijuana (40,41). Although the prevalence rates for SAM are likely to rise (38), the effects of combined perinatal ethanol exposure and THC (Δ9-tetrahydrocannabinol) exposure on the developing brain are not well understood. Previous studies have shown that working memory is impaired by perinatal alcohol exposure (42,43) and similar deficits have been observed in adults exposed to marijuana

(43–45). Ethanol is a teratogen and so alcohol consumption during pregnancy can disrupt development leading to facial dysmorphology, pre- and postnatal growth deficiencies, and central nervous system (CNS) dysfunction (46,47). Heavy drinking in the second trimester, particularly the 10th to 20th weeks of human pregnancy, when the brain is growing dramatically, is associated with an increase in the severity of many clinical features (48,49). In rodent models, a portion of the developmental stages that are congruous with the human third trimester occurs up to post-natal day nine (43). For the purpose of this review postnatal day ten and older will be considered to be postnatal while rodents at postnatal day nine and younger will be taken as perinatal. Perinatal alcohol literature contains experiments using multiple exposure paradigms. E1-E20 and P4-9 are both common models (43,50). A benefit of the E1-E20 model is that alcohol can be integrated into the mother's diet without the need for gavage or injection. P4-9 exposure isolated effects on the brain growth spurt and with recent advancements pups can be exposed using vaporized ethanol, which can also decrease the stress related to injection or gavage. For our review, we have chosen to discuss pre- and postnatal exposure paradigms that range from the first gestational day to the ninth postnatal day in rodent models, as these dates coincide with the first to third-trimester equivalent in humans (51).

It has long been known that the hippocampus is a brain area that is particularly sensitive to the effects of perinatal alcohol exposure (PAE). PAE induces significant cell loss in the hippocampus (52–54), and even brief periods of binge exposure can produce significant changes in hippocampal structure and function (55–57). Both $GABA_A$ and NMDA receptors have been implicated in the mechanism of alcohol-related neurodegeneration; $GABA_A$ receptors have been shown to become hyperexcitable while

NMDARs are blocked (58). Since GABA signaling is thought to be integral to the spatial and temporal integration of new neurons, it is logical that aberrations of this system lead to severe developmental consequences (59). Long-term potentiation deficits have also been reported, and the histamine H_3 receptor has been implicated (60).

Marijuana is one of the most commonly used recreational drugs during pregnancy, yet little is known about how it affects the development of the brain (61). THC is the major psychoactive ingredient in marijuana and is known to readily cross the placental barrier impacting fetal development (62). Evidence is emerging that perinatal THC, like perinatal alcohol, can impair the cognitive functioning of offspring– possibly throughout the lifespan (63). Cannabinoid receptors and their endogenous ligands have been detected at the earliest stages of embryonic development; this indicates that maternal marijuana use can impact the developing brain (64,65). The two primary cannabinoid receptors, known as CB_1 and CB_2, can both act to reduce adenylyl cyclase activity in cells (66). Their activation, primarily on interneurons, thus leads to the prevention of GABA release at the synapse. CB_2 receptors are expressed sparsely in microglia, macrophages, and some neurons in the central nervous system, but are more ubiquitous in the peripheral nervous system (67). There is evidence that alcohol acts to reduce endogenous cannabinoid levels through a CB_2 receptor-mediated pathway and that this mechanism is important in alcohol use disorders (68,69). CB_1 receptors are expressed in both inhibitory and excitatory neurons, at perinatal time points in the rodent cortex, basal forebrain, and telencephalon (70). Because CB_1 receptors are expressed perinatally, and in the hippocampus (part of the telencephalon), it is likely that CB_1 receptors will be the major players when it comes to developmental THC exposure (71). CB_1 receptor activation can impact interneuron development, neuronal

proliferation, migration, morphogenesis, synaptogenesis, and the balance of excitation and inhibition in the hippocampus (72–74). A recent paper found that fetal THC exposure can cause altered hippocampal oscillations, brain hyperexcitability, and spatial memory impairment (75). In this review, we will systematically explore what is known about the effects of perinatal alcohol and marijuana exposure in the dentate gyrus. The entire hippocampus was included in the search parameters however the papers returned mainly concerned the dentate gyrus. The dentate gyrus is a good target of this research as it is one of two sites in the rodent brain that has adult neurogenesis (76). Adult neurogenesis in the dentate gyrus is thought to be necessary for the formation of spatial memory (77). It is worth noting that, while well-established in rodents, the existence of adult neurogenesis is still debated in humans due to the type and parameters of assays available for use in humans (78). Spatial memory is affected by both THC and alcohol consumption in humans and so its corresponding brain structure a logical place to assess deficits caused by these drugs (79,80).

It is important to consider the actions of both substances alone, as well as in combination, as some work has suggested that the detrimental effects of perinatal alcohol and perinatal marijuana may be synergistic (81–83). Our initial systematic search to investigate documented changes in adult neurogenesis following SAM exposure returned a single result in the hippocampal formation, indicating there is a paucity of data for understanding the cellular consequences of perinatal SAM exposure. This singular paper found that perinatal cannabinoid exposure causes birth defects similar to perinatal alcohol exposure and implicated CB1-Hedgehog interactions as the cause (84). While this paper is worth mentioning, it did not satisfy all of the inclusion/exclusion criteria in this review and will not be part of the final result tables.

This paper also succinctly discusses the differences between THC and CBD, the two main cannabinoids present in marijuana, versus synthetic cannabinoids, which can be hundreds of times more potent and much longer lasting than THC and CBD (84). And while it is also worth mentioning that there are many other cannabinoids and terpenes in cannabis, this review will focus on THC and synthetic cannabinoids that bind with the CB_1 receptor (71).

This review will compare cellular data in adult offspring of rats or mice perinatally exposed to alcohol or marijuana. Our goal is to identify how perinatal SAM exposure impacts the structure and function of the adult hippocampus in hopes of directing future research.

2.3 Materials and Methods

This review was carried out using the stylistic criteria for Preferred Reporting Items for Systematic Reviews and Meta-Analyses (PRISMA), with minor amendments to the traditional process (e.g. exclusion of bias scoring) due to the nature of cellular studies (85). The literature on adult neurogenesis changes in the hippocampal formation after perinatal marijuana exposure is limited; for this reason, marijuana papers selected were compared to selected perinatal alcohol exposure instead of being separately analyzed. This method was used to provide an objective starting point for SAM research aimed at targeting the cellular basis for any developmental changes. In particular, this study was designed to target all papers that investigate adult neurogenic changes in the hippocampal formation under perinatal alcohol conditions or perinatal cannabis conditions. PRISMA search terms were designed to broadly include any

cellular study in any age of exposed offspring and then papers were selected based on the inclusion and exclusion criteria (S1). Five blocks of search terms were used. Each block included similar terms that contained "OR" as an operator. Between search blocks an "AND" operator was used. The blocks of search terms used here required papers to 1) include perinatal drug exposure 2) mention the hippocampal formation 3) provide immunohistochemical and other cellular results 4) specify alcohol use, and 5) specify marijuana use (**see Supplementary table 2.1**). Three databases were selected based on their ability to return cellular-level research. The first and second authors individually performed two searches, one for perinatal alcohol (search blocks 1,2,3,4) and the other for perinatal marijuana (search blocks 1,2,3,5) using the same terms, then exported all the citations to Mendeley. Duplicates were removed and all papers were screened using the inclusion/exclusion criteria (**Supplementary table 2.2**). Papers selected in the screening process were read in full and assessed for eligibility as defined by the search criteria, and final papers selected were compared between authors. Any discrepancies in paper selection were resolved by discussion. Although outside the scope of this review, the main methods and findings of short-listed papers have been included as a supplementary table (**Supplementary table 2.2).** The final article numbers for each step of this review are included in **Figure 2.1**. The search period included was January 1st 2000-March 13th 2020.

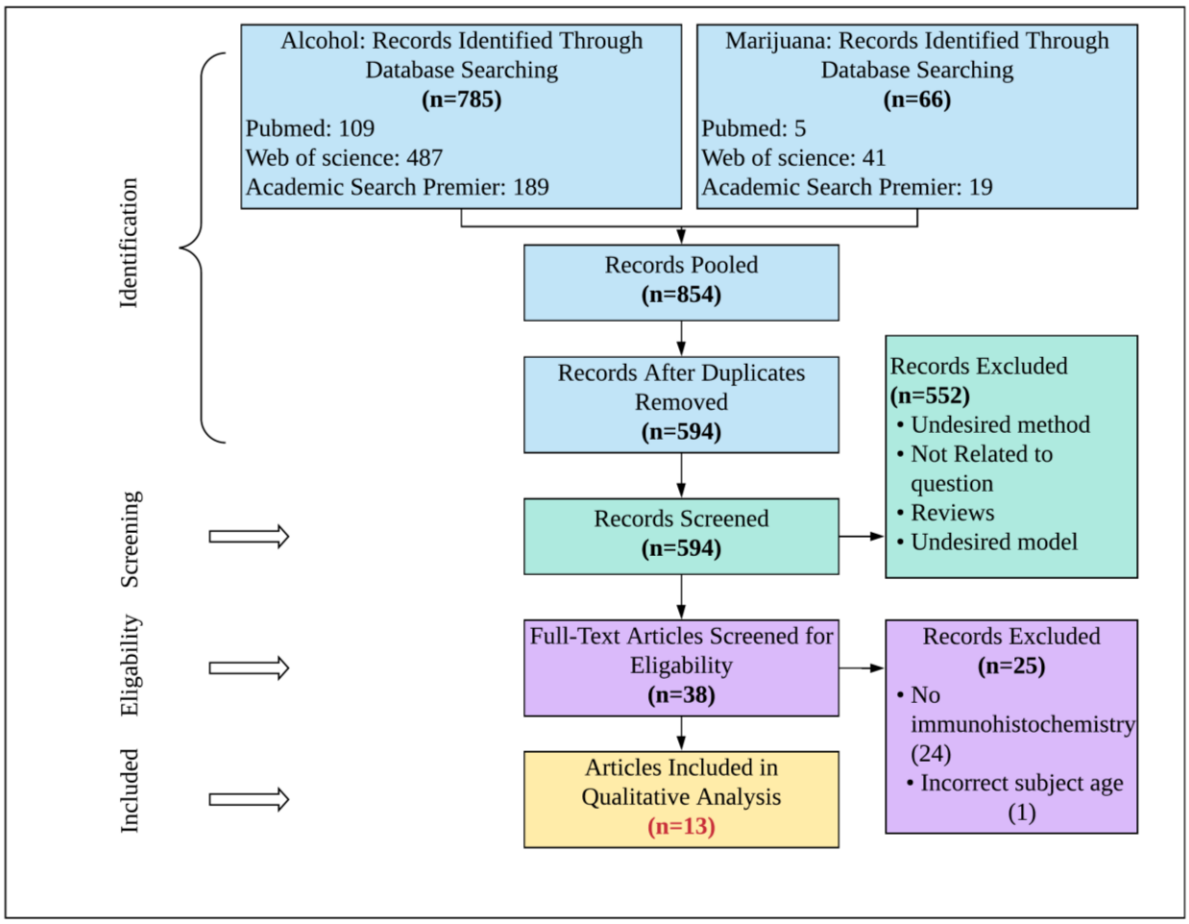

Figure 2.1 *PRISMA flow diagram*

2.4 Results

A total of thirteen studies were identified using a pre-defined criteria (S1), with ten studies focused on perinatal alcohol exposure and three on perinatal marijuana

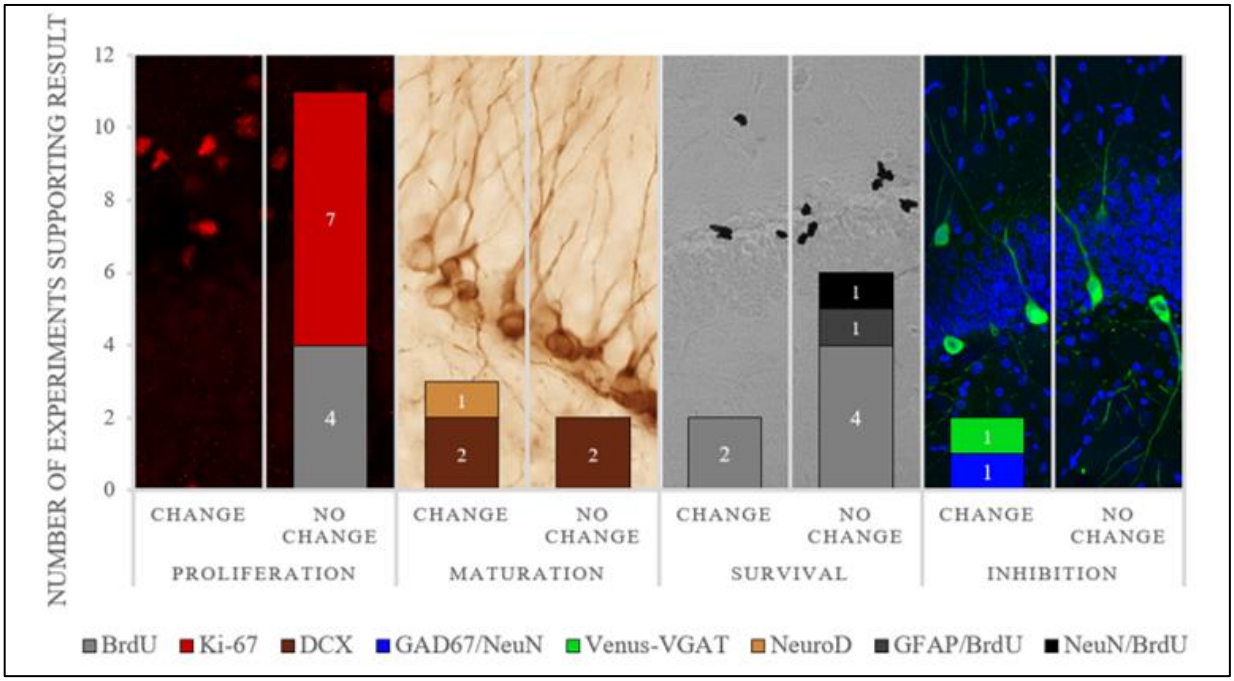

Figure 2.2 *Visual representation of literature. Each histology image from left to right: Ki-67, DCX, BrdU, and parvalbumin.*

exposure. Eleven of the twelve studies identified included an evaluation of the dentate gyrus subfield of the hippocampus. Datasets for papers that did not satisfy the inclusion and exclusion criteria are not reported in this table.

2.4.1 Perinatal Alcohol Exposure

2.4.1.1 Cellular Proliferation

The protein Ki-67, an endogenous S phase marker for cell proliferation in the brain, can be used in conjunction with the administration of BrdU, and exogenous marker that is taken up by the DNA of dividing cells during mitosis, to quantify cell proliferation in the brain (86–88). As is depicted in **Figure 2.2**, there were 11 experiments across 10 papers that used Ki-67 or BrdU alone, or in combination, to label proliferating cells in the adult dentate gyrus (**Table 1**).

Table 2.1: Summary of perinatal alcohol exposure experiments concerning proliferation. In the exposure age and Test Age column "P" indicates postnatal day and "E" indicates embryonic day.

Paper	Exposure Age	Model	Sex	Test Age	Marker/ Stain Used	Main Finding
(Gil-Mohapel et al., 2011)	E1-P9	Rat	M	P78-82	BrdU	No Change
					Ki-67	No Change
(Gil-Mohapel et al., 2014)	E1-21	Rat	MF	P386	Ki-67	No Change
(Hamilton et al., 2011b)	E1-P10	Rat	MF	P60	BrdU 2 hours	No Change
					Ki-67	No Change
				P90	Ki-67	No Change
(Klintsova et al., 2007)	P4-9	Rat	M	P50	BrdU	No Change
					Ki-67	No Change
(Olateju et al., 2018)	E7-E17	Mouse	MF	P56	Ki-67	No Change
(Sliwowska et al., 2010)	E1-21	Rat	M	P60-65	BrdU	No Change
(Uban et al., 2010)	E1-21	Rat	F	P60-65	BrdU	No Change

Seven experiments used the intrinsic marker for cell proliferation, Ki-67, to study how perinatal ethanol exposure affected cell proliferation in the adult hippocampus, but none of the studies showed any change in the number of Ki-67 immunopositive cells. Similarly, the four studies that used bromodeoxyuridine (BrdU; 50-200 mg/kg), a thymidine analogue that is injected and incorporated into the DNA of actively dividing cells, failed to document any changes following perinatal ethanol exposure. Thus,

whether endogenous or exogenous markers for cell proliferation were quantified, the results are in agreement that BrdU does not induce significant changes in this process in young adult animals.

2.4.1.2 Cell Maturation

Table 2.2: Summary of perinatal alcohol exposure experiments concerning maturation. In the exposure age and Test Age column "P" indicates postnatal day and "E" indicates embryonic day.

Paper	Exposure Age	Model	Sex	Test Age	Marker/ Stain Used	Main Finding
(Elibol-Can et al., 2014)	E7-E20	Rat	M	P60	DCX	No Change
(Gil-Mohapel et al., 2011)	E1-P9	Rat	M	P78-82	DCX	No Change
				P115	DCX	No Change
(Gil-Mohapel et al., 2014)	E1-21	Rat	MF	P386	DCX	Decrease in F
(Hamilton et al., 2011b)	P4-P9	Rat	MF	P60	NeuroD	Decrease
				P90	NeuroD	Decrease
(Olateju et al., 2018)	E7-E17	Mouse	MF	P56	DCX	Decrease

Doublecortin (DCX) is a microtubule-associated protein expressed by neuronal precursor cells and immature neurons. Thus, DCX positive cells represent a set cells across a broad developmental spectrum, ranging from immature neural progenitor (INP) cells (also known as Type 2B cells) to immature granule neurons (IGN) (89). Four papers assessed DCX immunoreactivity in the dentate gyrus (**Table 2.2**) following

perinatal ethanol exposure (90–93). Two papers showed no change in DCX immunoreactivity (90,92), one showed a significant decrease in DCX positive cells that was restricted to females (91), and one paper found a decrease in DCX cells in both males and females (93) (see **Figure 2.2**). To better elucidate changes in cellular maturation following perinatal ethanol exposure, we also examined papers that examined the basic helix loop helix transcription factor NeuroD (neurogenic differentiation factor 2). NeuroD is a marker expressed continuously by type 2b immature granule neurons once they begin to mature. We found that only one paper used NeuroD as a marker of maturation, and this work found that there was a decrease in the number of NeuroD positive cells in both male and female rats perinatally exposed to alcohol (52). This work provides some convergent evidence to support the conclusion that perinatal ethanol exposure does negatively impact neuronal maturation.

2.4.1.3 Cell Survival

Table 2.3: Summary of perinatal alcohol exposure experiments concerning survival. In the exposure age and Test Age column "P" indicates postnatal day and "E" indicates embryonic day; in the Marker/Stain Used column, "P" indicates the post natal day when subjects were injected with BrdU.

Paper	Exposure Age	Model	Sex	Test Age	What was Investigated?	Marker/ Stain Used	Main Finding
(Gil-Mohapel et al., 2011)	E1- P9	Rat	MF	P90	Dividing Cells	BrdU, P60	No Change
(Hamilton et al., 2011b)	P4-9	Rat	MF	P115	Dividing Cells	BrdU P80	Decrease

(Klintsova et al., 2007)	P4-9	Rat	M	P80	Dividing Cells	BrdU P50	Decrease
(Sliwowska et al., 2010)	E1-21	Rat	M	P81-86		BrdU P60-65	No Change
(Uban et al., 2010)	E1-21	Rat	F	P81-86	Dividing Cells	BrdU P60-65	No Change
					0-3 Week Old Glia	GFAP/BrdU P60-65	No Change
					0-3 Week Old Mature Granule Neurons	NeuN/BrdU P60-65	No Change

BrdU can be used to examine cell survival if it is injected 3-6 weeks prior to tissue being collected for histology (94). This allows sufficient time for new cells to develop and become functional (76). BrdU is only available to be incorporated into dividing cells within 2-3 hours of being injected (87), so it does not stain cells that are born after this time point; allowing researchers to compare the number of cells stained initially (in the immediate perfusion group) to the number of cells present after a given amount of time (a second experimental group). There were seven papers where BrdU assays were conducted on brain samples collected to study cell survival (see **Table 2.3**). In one study, where rats were injected with BrdU (200 mg/kg) at postnatal day 80 (P80) and their brains were collected at P115, a decrease was found in the number of BrdU positive cells in animals exposed to alcohol perinatally (52) . In a second paper, two BrdU experiments were reported. In this work, BrdU (50 mg/kg) was injected every second

day from P30-P50 and then brains are collected at either P50 or P80 (95). The number of BrdU positive cells was found to be equivalent in animals assessed at P50, but a decrease in numbers was observed at P80. One study was performed where BrdU was injected at P60 and brains collected at P90 and no change in BrdU immunoreactivity was found (91). Two studies injected BrdU between P60 and P65 and analyzed the brains between P81 and P86 (three weeks later) and found no change in the number of BrdU labeled cells relative to controls (96,97). One study utilized double labelling to assess the survival of new glial cells (GFAP/BrdU) as well as the survival of new granule neurons (NeuN/BrdU) and found no change in the proportion of each, relative to control, in either condition (97). Thus, the majority of studies indicate that perinatal alcohol exposure does not have a significant impact on cell survival.

2.4.1.4 Inhibitory Neuron Numbers

Table 2.4: Summary of perinatal alcohol exposure experiments concerning interneurons. In the exposure age and Test Age column "P" indicates postnatal day and "E" indicates embryonic day.

Paper	Exposure Age	Model	Sex	Test Age	What was Investigated?	Marker/ Stain Used	Main Finding
(Lu et al., 2018b)	E9-20	Rat	M	P84	GABAergic Mature Neurons	NeuN and GAD67	Increase
					Glutamatergic Mature Neuron	NeuN and Glutamate	Decrease
(Elibol-Can et al., 2014)	E7-E21	Rat	MF	P60	Venus-VGAT	CA1	Decreased in M
						CA3	Decreased in M
						GCL	Decreased in MF
						Hilus	Decreased in M

Ethanol is known to directly impact inhibitory cells in the brain, however only a few studies have examined the impact of perinatal ethanol exposure on these cells in the dentate gyrus (see **Table 2.4**). In one study, a transgenic mouse model (Venus-VGAT) was used that allowed them to directly visualize inhibitory (GABAergic) interneurons (98). This paper found a decrease in the number of interneurons in the granule cell layer (GCL) of the dentate gyrus. The other paper took a more traditional histological approach and labelled cells with NeuN, a mature neuron marker, a marker for the excitatory neurotransmitter glutamate, or with a GAD67, a marker of inhibitory interneurons. This study only assessed males, but in these they found an increase in neurons double-labelled with NeuN and Glutamate, and an decrease in cells double-labelled with NeuN and GAD67 (99). Thus, both studies assessing inhibition found perinatal alcohol exposure to result in decreased numbers of interneurons in the granule cells layers.

2.4.2 Perinatal Marijuana

Two studies assessing the effects of perinatal marijuana exposure in adult rats and mice were found. One perinatal marijuana study assayed two types of interneuron counts in transgenic mouse lines. They found that CCK positive Caudal Ganglionic Eminence Derived Interneurons decreased in adult mice perinatally exposed to THC but Medial Ganglionic Eminence Derived Interneurons showed no change (100). The other perinatal marijuana study assayed CB1 receptor levels and found an increase in the CA1 area of the Hippocampus (1).

Table 2.5: Results of PRISMA showing the impact of perinatal marijuana and perinatal alcohol in the Hippocampal formation of adult

rats and mice. A/M indicates if the perinatal exposure is alcohol(A) or marijuana(M). M and F in the "Main Finding" column indicate when there are sex differences in the results. Exposure and test ages are reported as embryonic (E) days of age or postnatal (P) days of age. Abbreviations are as follows: Immature neural progenitor (INP), immature granule neurons (IGN), gamma-aminobutyric acid (GABA), Cornu Ammonis area 1 (CA1), Cornu Ammonis area 2 (CA2), Cornu Ammonis area 3 (CA3), dentate gyrus (DG), and granule cell layer (GCL). Marker purposes are as follows: DCX (doublecortin, a neuronal migration protein), Venus-VGAT (a transgenic construct that labels GABAergic neurons), BrdU (bromodeoxyuridine, a thymidine analogue that labels DNA synthesis), Ki-67 (antigen Ki-67, a marker of proliferation), GFP (green fluorescent protein), CB1R (cannabinoid receptor type 1), NeuroD (Neurogenic differentiation factor 2, a marker of type 2b immature up to mature granule neurons), NeuN (neuronal nuclei, a mature neuron marker), and GAD67 (glutamate decarboxylase 67 kilodalton isoform).

	A/M	**Exposure Age**	**Model**	**Sex**	**Test Age**	**What was Investigated?**	**Marker/ Stain Used**	**Hippocampal Subregion**	**Main Finding**
1	A	P2-P9	Mouse	MF	P90	GABA Interneurons	Venus-VGAT	CA1	Decreased in M
								CA3	Decreased in M
								GCL	Decreased in MF
								Hilus	Decreased in M
2	A	E7-E21	Rat	M	P60	Type 2b INP to Immature Granule Neuron	DCX	CA1	No Change
								CA2+3	No Change

								DG	No Change
3	M	E10.5-E17.5	Mouse	MF	P20-P60	Cannabinoid receptor type 1	CB1R	CA1	Decrease in M
						Cholecystokinin interneurons	CCK	CA1	Decrease in M
4	A	E1-21	Rat	M	P78-82	Dividing Cells	BrdU	DG	No Change
						Type 2b INP to IGN	DCX	DG	No Change
						Dividing Cells	Ki-67	DG	No Change
					P115	Dividing Cells	BrdU, P80	DG	Decrease
						Type 2b INP to IGN	DCX	DG	No Change
5	A	E1-P9	Rat	MF	P386	Type 2b INP to IGN	DCX	DG	Decrease in F
						Dividing Cells	Ki-67	DG	No Change
6	A	P4-9	Rat	MF	P60	Dividing Cells	BrdU 2 hours	DG	No Change
						Dividing Cells	Ki-67	DG	No Change
						Type 2b INP to Mature Granule Neuron	NeuroD	DG	Decrease

					P90	Dividing Cells	BrdU P60	DG	No Change
						Dividing Cells	Ki-67	DG	No Change
						Type 2b INP to Mature Granule Neuron	NeuroD	DG	Decrease
7	A	P4-9	Rat	M	P80	Dividing Cells	BrdU	DG	Decrease
					P50	Dividing Cells	BrdU	DG	No Change
					P50	Dividing Cells	Ki-67	DG	No Change
8	A	E9-20	Rat	M	P84	GABAergic Mature Neurons	NeuN and GAD67	CA3	Increase
								DG	Increase
						Glutamatergic Mature Neuron	NeuN and Glutamate	CA3	Decrease
								DG	Decrease
9	A	E7-E17	Mouse	MF	P56	Type 2b INP to Immature Granule Neuron	DCX	DG	Decrease
						Dividing Cells	Ki-67	DG	No Change
10	A	E1-21	Rat	M	P60-65	Dividing Cells	BrdU	GCL	No Change

								Hilus	No Change
					P81-86		BrdU P60-65	GCL	No Change
								Hilus	No Change
11	M	E5.5–E17.5	Rat	M	P120	CB1 Positive Boutons	CB1R	CA1	Increase
12	A	E1-21	Rat	F	P60-65	Dividing Cells	BrdU	GCL	No Change
					P81-86	Dividing Cells	BrdU P60-65	GCL	No Change
						0-3 Week Old Glia	GFAP/BrdU P60-65	GCL	No Change
						0-3 Week Old Mature Granule Neurons	NeuN/BrdU P60-65	GCL	No Change
13	M	E10.5-E18.5	Mouse	MF	P30	Caudal Ganglionic Eminence Derived Interneurons	GFP (5HT3AR-GFP transgenic line)	DG/ Hilar Border	Decrease
						Medial Ganglionic Eminence Derived Interneurons	GFP (NKX2.1-cre:RCE-GFP	DG/ Hilar Border	No Change

		transgenic line)
1. (98)		
2. (90)		
3. (75)		
4. (92)		
5. (91)		
6. (101)		
7. (95)		
8. (102)		
9. (93)		
10. (96)		
11. (1)		
12. (97)		
13. (100)		

2.5 Discussion

2.5.1 Perinatal Alcohol in the Dentate Gyrus

This review found that in adult rats and mice perinatally exposed to alcohol, most components of adult neurogenesis do not appear to be significantly affected, but there is evidence for changes in interneurons in the hippocampus (**Table 2.5**). This review intended to investigate changes in the hippocampus caused by perinatal alcohol and marijuana exposure, however, a paucity of papers devoted to this topic required a focus on the review of perinatal alcohol exposure effects alone, although two papers on perinatal marijuana exposure did meet our criteria. To date, only one paper has been published that assesses the interaction of perinatal administration of these substances at the cellular level, but no papers have assessed this in the developing hippocampus (84). As this area of research is in its infancy, this review hopes to shed light on possible

directions for future SAM and perinatal cannabis research, based upon likely points of interaction.

DCX is first expressed in type 2b immature neural progenitor cells but is produced continuously until the cell is an immature granule neuron (103). BrdU and Ki-67 are both markers of proliferation and the results of one are often used to validate the other (104). To this end, it can be seen that in rats and mice perinatally exposed to alcohol, there is no large long-lasting effect on the number of actively dividing cells in the dentate gyrus. NeuroD is also a marker of maturation and in the prior study that utilized it as a marker, a decrease was found.

BrdU is injected before the animal is euthanized. Cells that incorporate BrdU are actively dividing at the time of injection (104). Therefore, when collecting tissue at advanced time-points, BrdU can assay temporally discrete populations of cells undergoing DNA synthesis (104). The studies that used BrdU to assess proliferation (injection immediately before euthanasia) found no change in proliferation, however half of the studies which followed an adult population of cells over a month-long window found a decreased number of BrdU-stained cells. This indicates that the population of cells dividing at the time of BrdU injection are not surviving in the same proportions of survival rates observed in control animals.

In perinatal alcohol exposure, research suggests that most damage happens due to cell loss early in development, and although some recovery occurs in terms of medically observable phenotype, this is caused by a slow recovery of the affected cell population throughout the individual's life (105). A second mechanism proposed suggests that cell death is caused by a loss of inhibitory interneurons and subsequent excitotoxicity or

aberrant dendritic pruning (106). Two papers were found on this subject; one showed a statistically significant change in the balance of inhibitory and excitatory neurons in the dentate gyrus, and the other suggested that one specific type of interneuron is decreasing (99,100).

2.5.2 Perinatal Marijuana in the Dentate Gyrus

Three papers that assessed the adult effects of perinatal marijuana exposure were identified. One found a decrease in cholecystokinin (CCK) positive interneurons that arise from the caudal ganglionic eminence, and no change in interneurons arising from the medial ganglionic eminence in the dentate gyrus of mice (100). This suggests that moving forward, more research is required to understand the effects on interneuron subtypes and their implications in disease. The second paper discussed the cannabinoid receptor type 1 (1). This receptor is expressed in inhibitory neurons, so an increase in CB1 expression could indicate either that the number of interneurons is increasing, or that CB1 is being upregulated (107). A new paper found a significant decrease in CB1R expression in males but not females, which is opposite to findings of an increase in CB1-positive boutons (1,75). De Salas-Quiroga *et al.* also found that there was a marked decrease in the number of CCK-positive interneurons in the CA1 region of the hippocampus, which agrees with other published work, however, the effect was only significant in males (61,75).

The data found in this review suggests that the balance between inhibition and excitation may be where the largest effect will be seen in emerging SAM models. It is tempting to hypothesize that the actions of simultaneous perinatal alcohol and marijuana exposure will be synergistic because it appears these substances target two

different sites. Specifically, alcohol appears to primarily target post-synaptic GABA receptors, whereas cannabinoids seem to target presynaptic CB1 receptors (23,108). Studies done on these receptors in the absence of SAM conditions also support this finding (109–112).

2.6 Conclusions

This systematic literature review, conducted using PRISMA-style search criteria, suggests that an interaction of alcohol and marijuana in a SAM model of exposure could influence inhibitory interneurons of the dentate gyrus. This study found that in adult rats and mice perinatally exposed to alcohol, within the dentate gyrus, proliferation is not affected but migration, maturation, survival, and interneurons are all affected. The papers pertaining to marijuana exposure suggested differences in interneurons, thus interneurons are the likely point of convergence of these two drugs. Specifically, CB_1 receptors are expressed largely in the second trimester in the hippocampus, are presynaptic, and their activation leads to decreased GABA release. GABA is integral to the spatiotemporal integration of developing neurons. Perinatal THC exposure and perinatal alcohol exposure overlap in their ability to affect the maturation and integration of pyramidal neurons in the dentate gyrus. Therefore, future studies may show circuit integration and cell survival in pyramidal neurons in the dentate gyrus of SAM-exposed animals. As research begins to acknowledge the patients exposed to both alcohol and marijuana perinatally, an understanding of the underlying mechanism will allow clinicians to better diagnose, and hopefully treat, this understudied population.

CHAPTER 3

Published: **Prenatal alcohol and cannabis exposure can have opposing and region-specific effects on parvalbumin interneuron numbers in the hippocampus.**

3.1 Abstract

3.1.1 Background: We have recently shown that alcohol and cannabis can interact prenatally, and in a recent review paper we further identified interneurons in the hippocampus as a potential point of convergence for these teratogens.

3.1.2 Methods: A 2 (EtOH, Air) x 2 (THC, Vehicle) design was used to expose pregnant Sprague-Dawley rats to either EtOH or air, in addition to either THC or the inhalant vehicle solution, from gestational days 5-20. Immunohistochemistry was performed to detect parvalbumin-positive interneurons in one male and one female pup from each litter at post-natal day (PND) 70.

3.1.3 Results: Significant between-group, and sub-region specific, effects were found in the dorsal CA1 subfield, as well as the ventral DG. In the dorsal CA1 subfield, there was an increase in the number of PV interneurons in both the EtOH and EtOH + THC groups, but only a possible decrease with THC alone. There were fewer changes in interneuron numbers overall in the DG, however, a sex difference was found, and a decrease in the number of PV interneurons in the THC-exposed group was observed in the male ventral DG. There was also an increase in cell layer volume between the EtOH

+ THC group and control group in the DG, and an increase from the control and THC group to the EtOH group in the CA1 region.

3.1.4 Conclusions: Prenatal alcohol and prenatal THC exposure differentially affect parvalbumin interneuron numbers in the hippocampus, indicating that both individual and combined exposure can impact the balance of excitation and inhibition in a structure critically involved in learning and memory processes.

3.2 Introduction

With the legalization of cannabis in many regions of the world, there is increasing interest in the potential for cannabis, particularly its psychoactive component Δ^9-tetrahydrocannabinol (THC), to have teratogenic effects (113). Approximately 3% of women use alcohol and/or cannabis heavily throughout pregnancy (40,114,115), so it is important to understand the effects of each compound alone, as well as any potential synergy between THC and alcohol (40,115). Indeed, our recent studies indicate that the simultaneous consumption of alcohol and THC (A/C) during pregnancy can affect blood alcohol levels (116).

Both THC and alcohol (ethanol, EtOH) affect the hippocampus, which plays a central role in learning and memory processes (117–120). The hippocampal formation is a brain region that consists of two main subdivisions, the dentate gyrus (DG) and the cornu ammonis (CA) (121). The DG is known to play a role in spatial memory and object recognition (122,123), whereas the CA subfield is implicated in autobiographical and social memory (124,125).

We have recently published a systematic review (126) that suggested that hippocampal interneurons may be a focal point for the actions of both THC and ethanol in the developing brain. In part, this is because THC activates CB1 receptors, which can change GABA release, and further. After all, repeated THC exposure causes a change in CB1 receptor levels (127,128). CB1 receptors are $G_{i/o}$ coupled receptors activated by the endogenous cannabinoids anandamide and 2-arachidonoylglycerol under normal conditions (129). Their activation in excitatory cells inhibits adenylyl cyclase activity, preventing neurotransmitter release at the synapse (129). For the CB1 receptors on interneurons, this means that cannabinoid binding suppresses GABA release during acute activation. However, repeated exposure to exogenous cannabinoids (e.g., THC) can cause downregulation of these receptors and therefore increase GABA release (130). Although there is a ~20-fold increase in CB1 receptors in GABAergic cells compared with other cell types, CB1 receptors also exist on astrocytes, microglia, and glutamatergic cells (131,132). When glutamatergic and astroglial CB1 receptors are activated in the hippocampus, a signal transduction cascade is activated that causes the removal of AMPA receptors (133). $GABA_A$ receptors are chloride ion channels found post-synaptically (121). In most cases, the extracellular chloride concentration is much higher than the intracellular concentration of an excitatory neuron. This means that when GABA is released and the $GABA_A$ channel opens, negatively charged chloride ions travel into the cell along its concentration gradient and cause the cell to become hyperpolarized and unable to propagate excitatory inputs. However, in development, the KCC2 receptor (a potassium-chloride co-transporter), is not yet upregulated (134), so these inputs act as excitatory inputs because the intracellular chloride concentration

is higher than the extracellular concentration. This is an important process for circuit establishment, and also a reason for hyperexcitability with prenatal A/C exposure.

Interneurons play an important role in the hippocampus, controlling excitatory cells through $GABA_A$ receptors, and research suggests that they can also exhibit synaptic plasticity (118). While there are several immunohistochemically distinct interneurons in the hippocampus (18), the parvalbumin (PV) interneurons play a distinct role in hippocampal memory-related processes (see **Figure 3.1** for PV cell location). They coordinate excitatory networks in memory consolidation (135), are essential for spatial working, but not reference, memory (136), and act as a discriminator in social memory

(137). PV-positive interneurons are also integral in producing gamma oscillations and are considered central to the maintenance of the inhibitory/excitatory balance (138).

In this paper, we assess the effect of prenatal alcohol exposure, prenatal THC exposure, and the combination of the two on PV interneuron numbers in the CA1 and DG subfields of the hippocampal formation. PV interneurons are fast-spiking, integral to the

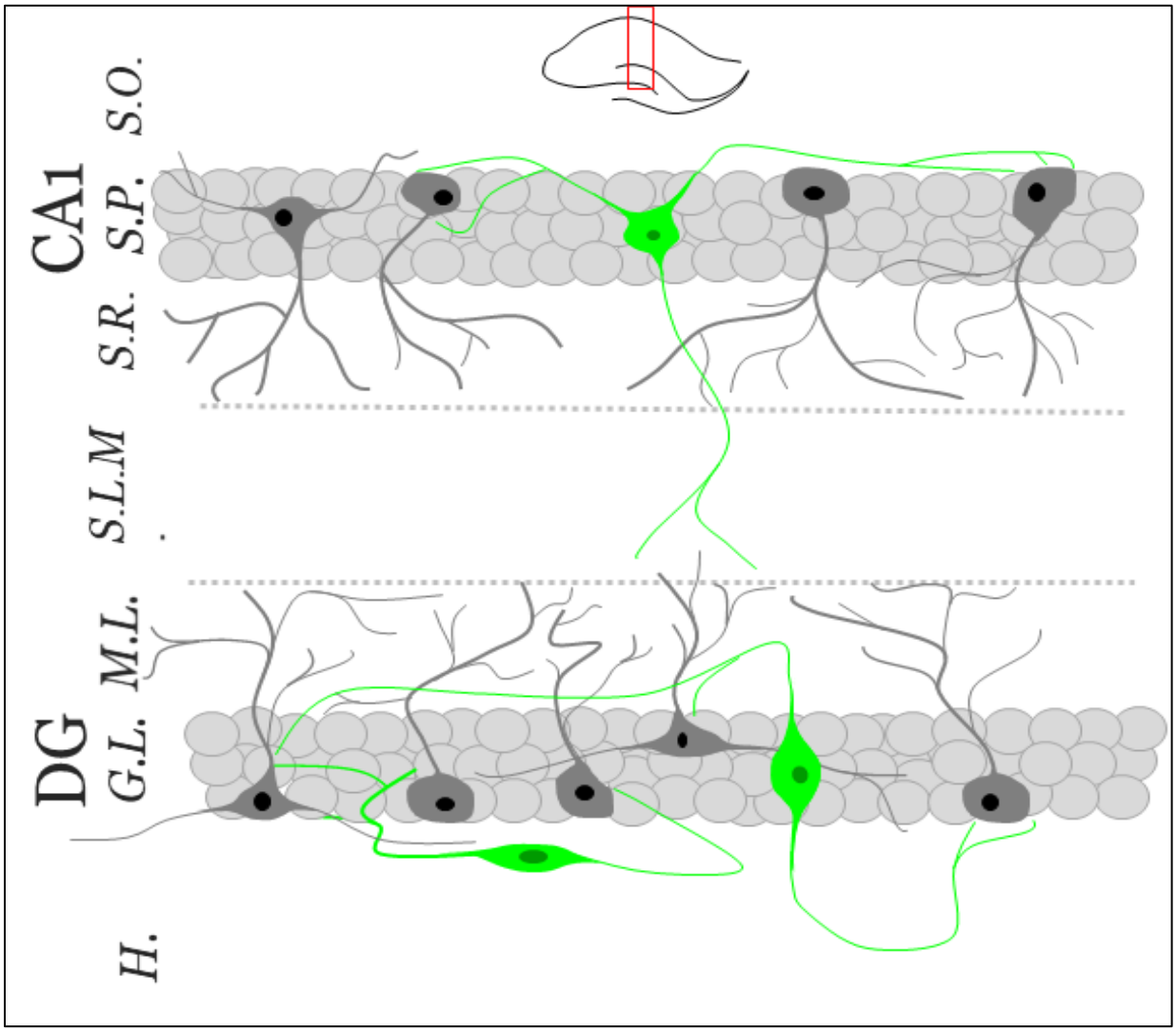

Figure 3.1 *Schematic of Parvalbumin positive cell axonal and dendritic position in the hippocampus. (A) Schematic showing the relative position of PV positive cells in the CA1 and DG of the hippocampus. Note how the majority of connections are located in the CA1 and DG cell layers. S.O.: stratum oriens; S.P.: stratum pyramidales; S.R.: stratum radiatum; S.L.M.: stratum lacunosum moleculare; M.L.: molecular layer; G.L.: granule layer; H.: hilus.*

processes of feedforward, feedback, and lateral inhibition, and are abundant in the stratum pyramidale (SP) layer of CA1 and the granule cell layer (GCL) of the DG (139). Loss of these interneurons has been associated with schizophrenia, Lewy Body Dementia, and chronic stress (140–142). Further, these cells are thought to influence adult neurogenesis and play a role in spatial working memory, novel object exploration, and novel object location recognition (143,144). This work seeks to investigate population changes in PV interneurons in adult rats that were prenatally exposed to prenatal ethanol vapor, THC vapor, or a combination of both.

3.3 Materials and Methods

Female Sprague-Dawley rats (n=24) were assigned to receive 1 of 4 experimental conditions (EtOH or Air), and (THC or Vehicle (VEH; propylene glycol, Sigma-Aldrich; see **Figure 3.2**). Thus, there were 4 total conditions: EtOH + THC (n=6), EtOH + VEH (EtOH; n=6), Air + THC (THC; n=5) and Air + VEH (VEH; n=6). Pregnancy was confirmed in all dams by the presence of a seminal plug, and this was designated as gestational day (GD) 0. Pregnant rats were exposed to their assigned drug exposure condition once daily from GD 5 to GD 20 in a vapor inhalation chamber (La Jolla Alcohol Research Incorporated, La Jolla, CA).

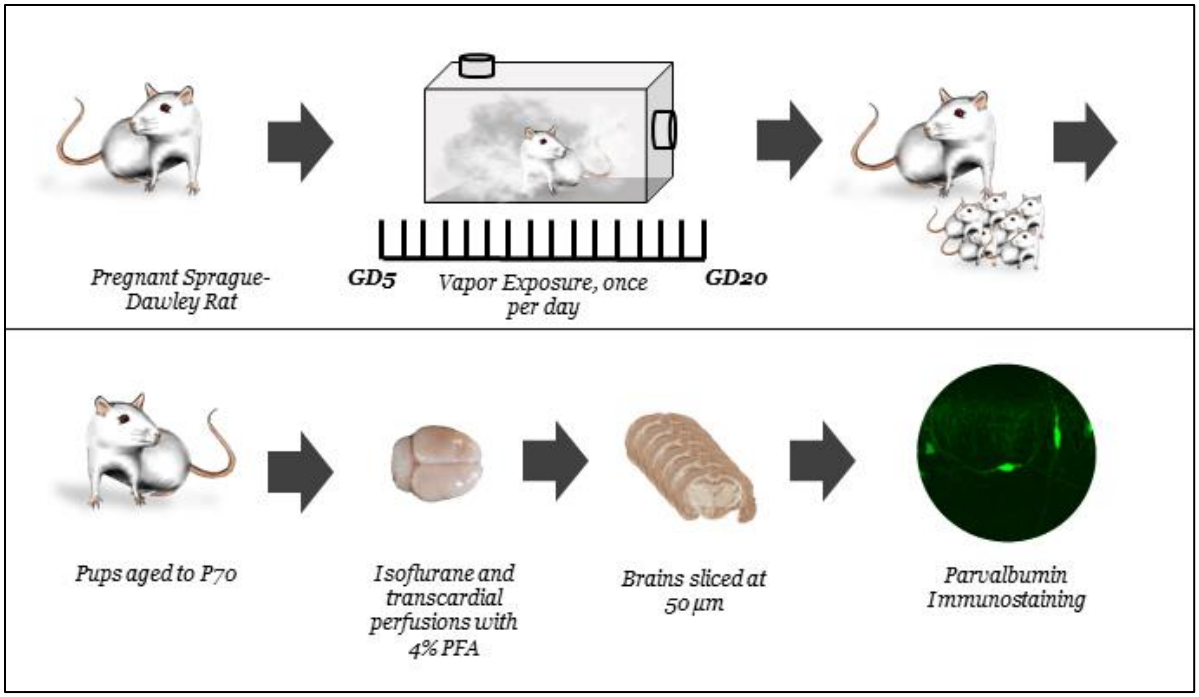

Figure 3.2 *Pregnant rats were exposed to 95% EtOH or Air for 3 consecutive hours at an airflow of 2 L/min. Afterwards, all rats were either exposed to THC or propylene glycol vehicle at an airflow of 2mL/min. Blood samples were taken on GDs 5, 10, 15, and 20. Between PD60-70, the adult offspring were deeply anesthetized with lethal ketamine (67 mg/mL) and xylazine (6.7 mg/mL) and underwent transcardiac perfusion. Brains were collected and post-fixed in 4% paraformaldehyde for 24 hours. Brains were sliced at 50 µm for histology.*

Pregnant rats were exposed to 95% EtOH (68 mL/hour; Sigma-Aldrich) or Air for 3 consecutive hours at an airflow of 2 L/min. Then, subjects were either exposed to THC (100 mg/mL; NIDA Drug Supply Program) or the VEH (propylene glycol; Sigma-Aldrich) at an airflow rate of 2 L/min; THC and VEH were administered in single 6-second puffs every 5 min for a 30-min period (7 puffs total). An additional 10 minutes of airflow was administered before opening the chambers to remove any residual vaporized drug. Dams gave birth on GD 22, and litters were culled on postnatal day (PD) 2. One male and one female pup from each dam were used in this study. All animals used in this study had previously been tested in an open field (PD 31-34); measuring

activity levels in the open field is not expected to influence hippocampal interneurons (81).

Between PD 60-70, the adult offspring were deeply anesthetized with a lethal ketamine (67 mg/mL) and xylazine (6.7 mg/mL) dose (0.001 mL/g) and transcardially perfused with cold saline followed by 4% paraformaldehyde (PFA) in a phosphate buffer. Brains were extracted and post-fixed in 4% PFA for 24 hours. Brains were sectioned using a Leica vibratome into 50 μM slices. Immunohistochemistry was performed using a 1 in 6 series of tissue. A 5-minute incubation in 1% sodium borohydride in PBS was used for antigen retrieval. MilliporeSigma mouse anti-PV antibody (MAB1572) was used at 1:1000 in 3% normal goat serum (NGS) and 0.5 % Triton X-100 in PBS (0.5% PBST) for 48 hours at 4 °C with shaking. Biotinylated goat anti-mouse secondary antibody (ThermoFisher # 31804) was used at 1:500 in 3% NGS and 0.5% PBST for 2 hours at room temperature with shaking. Development for light microscopy was performed with Vectastain ABC Elite avidin-biotin-peroxidase complex and 3,3'-Diaminobenzidine (Vector laboratories Burlingame, CA). ABC and DAB were prepared as per supplier instructions. For fluorescent microscopy, Alexa 488 conjugated goat anti-mouse secondary (ThermoFisher # A-11001) was used at a 1:500 concentration in 3% NGS and 0.5% PBST. Cresyl Violet staining was performed on a 1 in 12 section of tissue from the same set of brains as described previously (145). Profile counts of PV cells were performed at 40x using an Olympus brightfield CX21 microscope (Olympus Corporation, Center Valley, PA, USA), and images for area analysis were taken using an Olympus brightfield BX51TF microscope (MBF Bioscience, Williston, VT, USA) using StereoInvestigator software version 11.03 (MBF Bioscience, Williston, VT, USA), area

analysis was performed using FIJI-Image J (Version 1.52p, National Institutes of Health, USA) (see figure **S1** for areas measured and **S2** for representative DAB stained images). Fluorescent images were taken using an Olympus BX61WI confocal laser scanning microscope and Olympus FluoView FV10-ASW 1.7c software (Olympus Corporation, Center Valley, PA, USA). Reconstruction of PV cell density was performed in two steps. First, each cell count in a given slice, side, and area (for example the left granule cell layer in the DG of one slice) was divided by the measured area, in mm^2. Following this, the cell densities were averaged for each brain in the dorsal CA1, ventral CA1, dorsal DG, and ventral DG. A calculation of per region was done by multiplying the average density by 2400 μM, the normalized length for half of an adult rat hippocampus (146). To add context to any observed changes in PV cell density, the number of overall cells was also assessed by way of Cresyl Violet staining. Cresyl Violet analysis occurred as follows: an image of the dorsal and ventral granule and pyramidal cell layers (in the DG and CA1 respectively) were taken using StereoInvestigator 03 (MBF Bioscience, Williston, VT, USA) and an Olympus BX51TF microscope. Images were analyzed in FIJI-ImageJ (Version 1.52p, National Institutes of Health, USA (**Figure S 3.3**)) to allow analysis to be completed from home computers. Stained sections were assessed by counting the cells in 3 2000 μm^2 boxes per animal in both the dorsal and ventral regions. We took one box aligned from the top, middle, and bottom of the cell layer for this analysis, so that if there were changes in density through the layer, we were measuring it evenly. Within that, we took boxes in as random a fashion as possible. A comparison between the number of PV neurons and the Cresyl Violet stained cells was calculated by dividing the density of PV neurons in the pyramidal layer of the CA1, or the granule layer of the DG, by the density of Cresyl Violet stained cells in the total

sample area of 6000 μm² in the same respective cell layers. The resulting number is reported as the inhibitory ratio. Dorsal and ventral slices were classified using the Matt Gaidica Rat Brain Atlas where dorsal was bregma -1.88 to -4.16 and ventral was bregma -4.52 to -6.04. These coordinates were chosen by taking the entire length of the hippocampus and dividing by two then using the closest plate to those numbers in the atlas. All statistics using the general linear model were done using IBM SPSS statistics software and estimation statistics and figures were made using R (147,148). A 95% confidence interval was used as the statistical threshold in this study, and all post-hoc tests were performed using a Tukey test.

3.4 Results

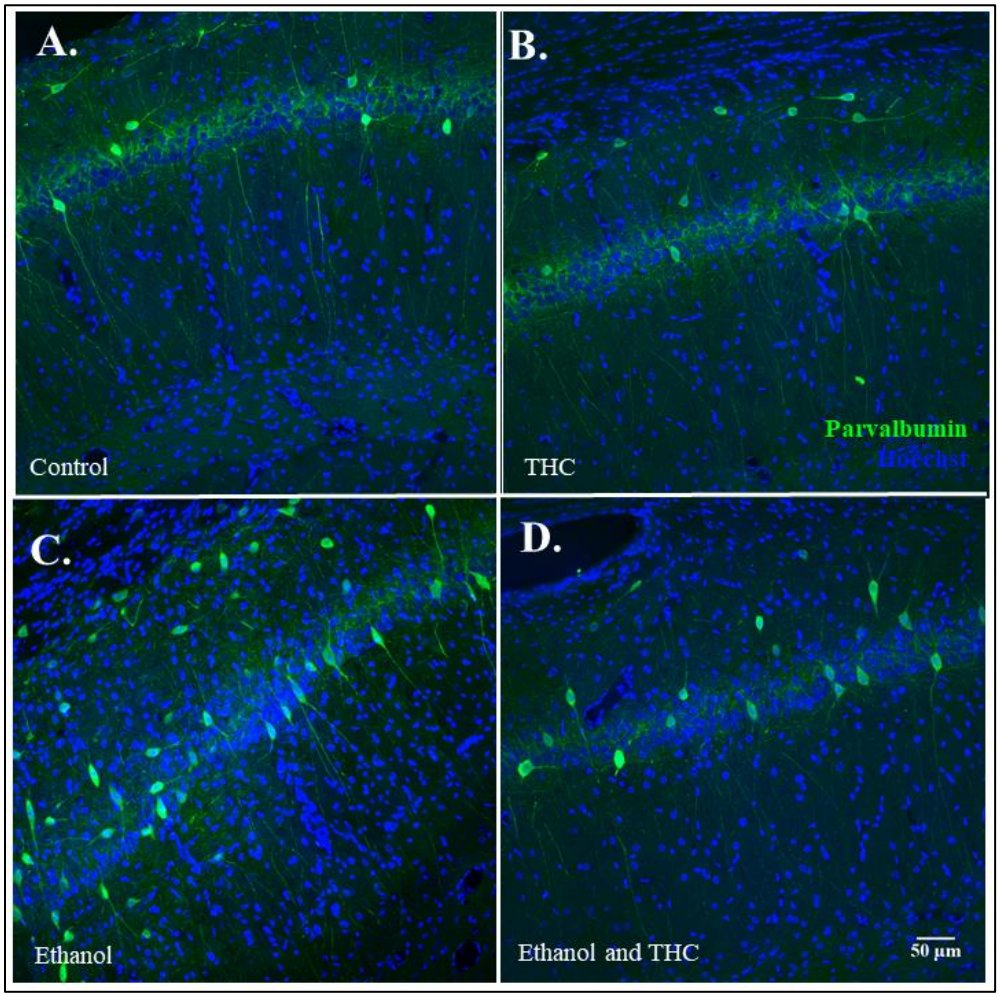

Figure 3.3 *Representative confocal images of cells positive for parvalbumin (green) in the CA1 region of the hippocampus in P70 Sprague-Dawley rats, counterstained with Hoechst (blue). The images show representative examples of stained sections from (A) the air alone exposure group; (B) the THC exposure group; (C) the EtOH exposure group; and (D) the EtOH + THC exposure group. Scale bar = 50 microns.*

Data were analyzed with a multi-way ANOVA with Tukey post-hoc tests, and supported with estimation statistics.

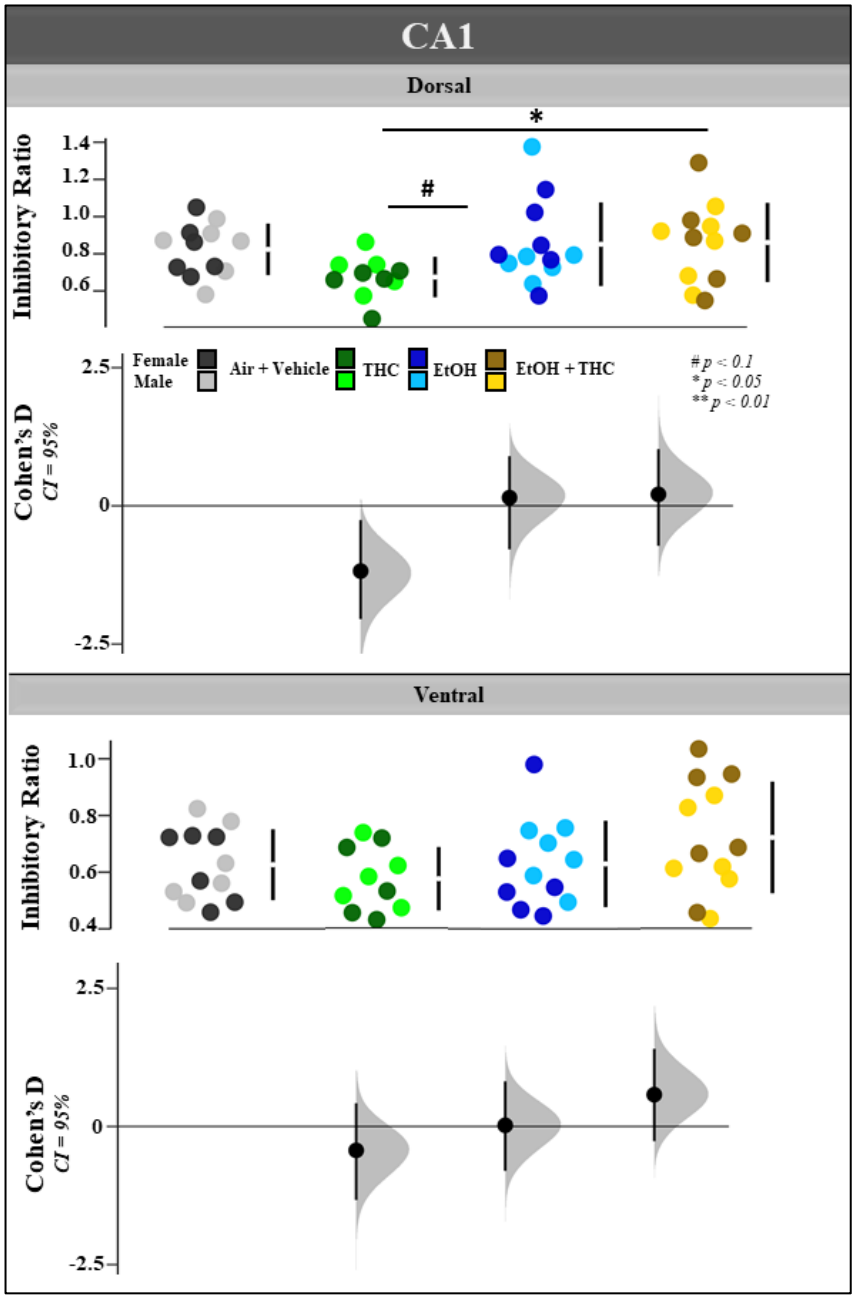

Figure 3.4 *Representative confocal images of PV cells in the DG of P70 Sprague-Dawley rats. Calculated numbers of parvalbumin-positive cells in rats exposed to air, THC, EtOH, and EtOH + THC from GD5-20 in the dorsal and ventral CA1 hippocampal region. Animals assessed at P70. Data collected as profile counts of a DAB stained 1 in 6 series of tissue. Cohen's D of effect size shown where each experimental group is compared with control.*

An initial multivariate analysis of variance (ANOVA) showed a statistically significant effect of dorsal versus ventral location and a significant effect of treatment in the CA1 and DG for parvalbumin-positive cell density ($p = 0.008$, $p = 0.003$, see **Supplementary Tables 3.1 and 3.2**). Power analysis performed with G* Power software based on cell counts showed a large effect size and suggest the number of animals and number of slices per animal was appropriate.

In the dorsal CA1, there was a trend towards increase in the inhibitory ratio of PV cells in the EtOH group (p = 0.081) compared with the THC alone group, and a significant increase in the EtOH + THC groups compared with the THC group (p = 0.021) (**Figures 3 and 4**).

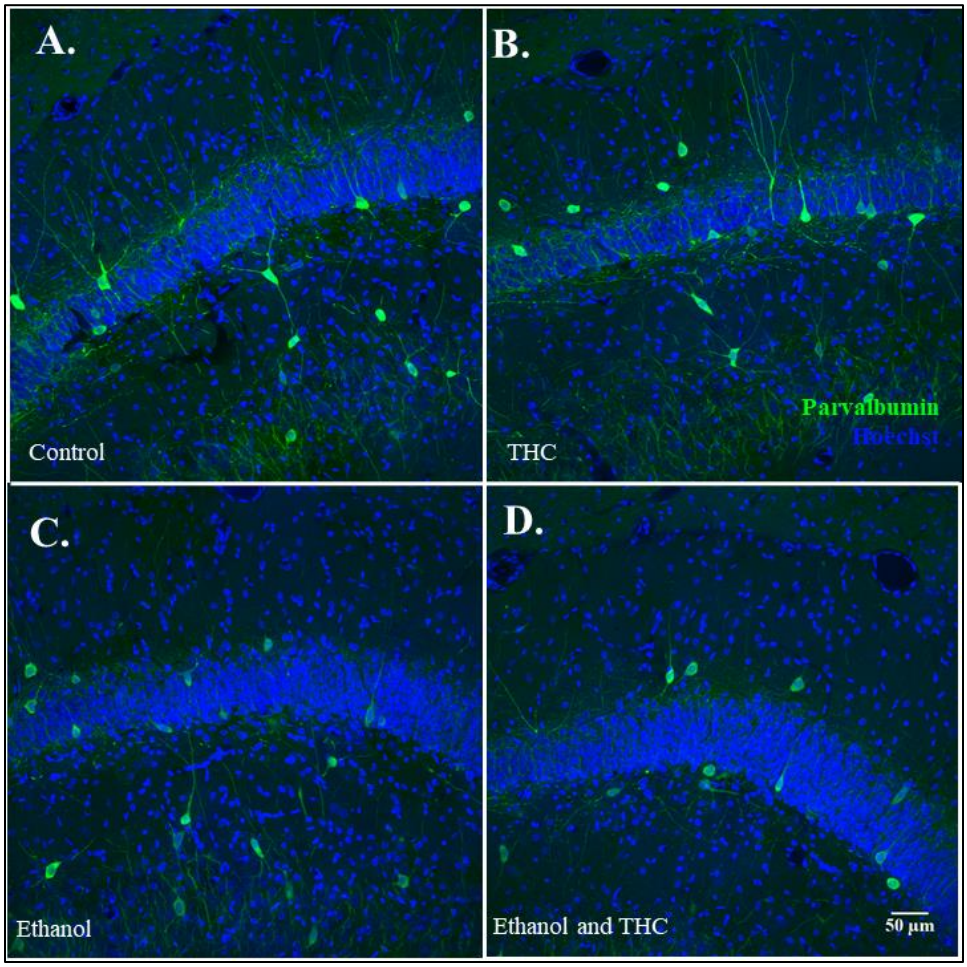

Figure 3.5 *Representative confocal images of PV cells in the DG of P70 Sprague-Dawley rats, counterstained with Hoechst. A. Air exposure group. B. THC exposure group. C. EtOH exposure group. D. EtOH + THC exposure group.*

There was no significant difference between the Air + Vehicle group and the THC exposed group in the Tukey post hoc test, however, estimation statistics suggest that there may be a decrease in the number of cells (**Figure 3.4**). This is also reflected in cell count data (reconstructed without area measurement) (**Figure S 3.4**).

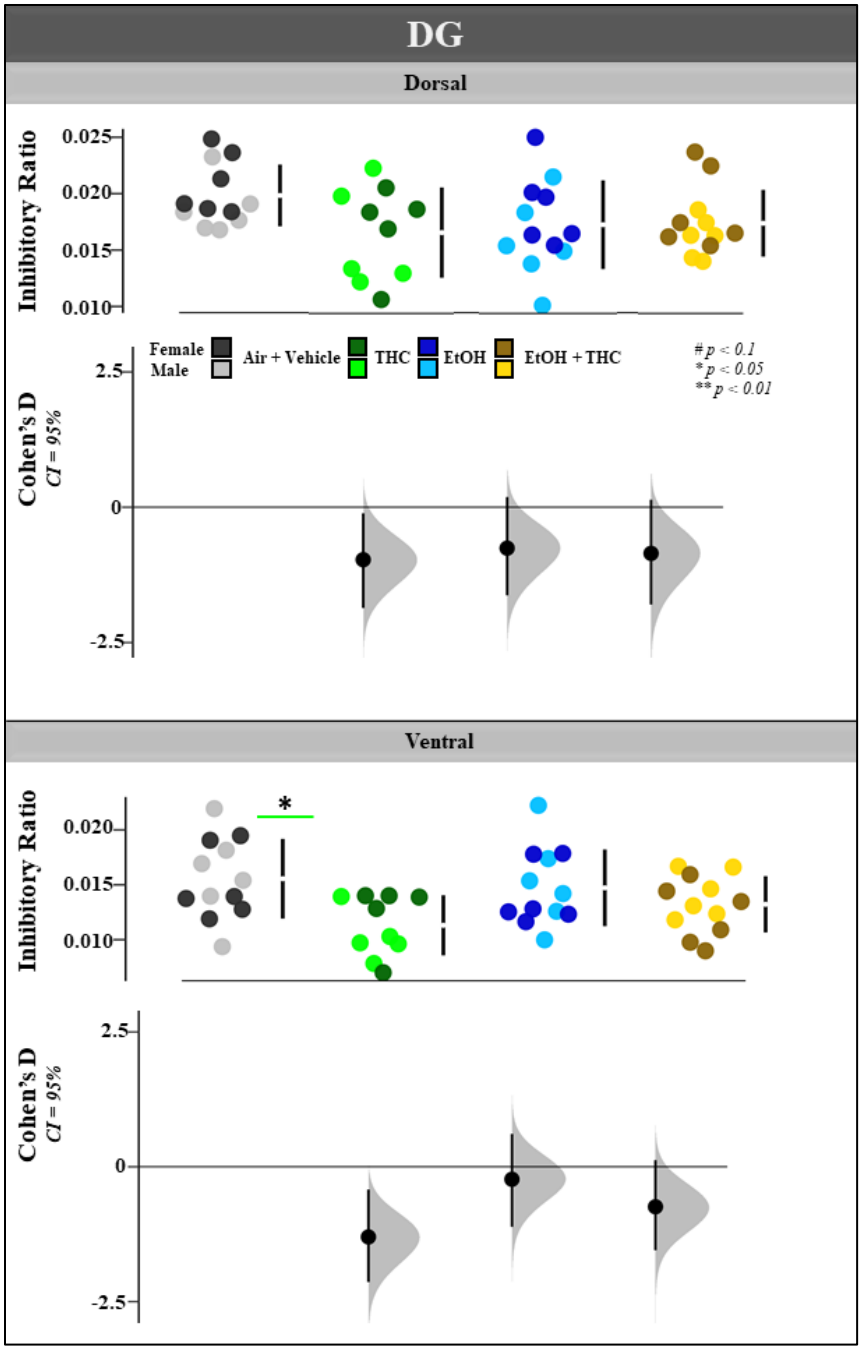

Figure 3.6 *Calculated numbers of parvalbumin-positive cells in rats exposed to air, THC, EtOH, and EtOH + THC from GD5-20 in the dorsal and ventral dentate gyrus. Animals assessed at P70. Data collected as profile counts of a DAB stained 1 in 6 series of tissue. Cohen's D of effect size shown where each experimental group is compared with control.*

In the ventral CA1, in contrast to the dorsal CA1, no significant effects were found in the density of PV interneurons (**Figures 3.3 and 3.4**). Interestingly, there was a significant increase in the cell layer volume between the Air + Vehicle and THC groups when compared with the Ethanol alone group (**Figure S 3.5**). Further, the cell count data alone (**Figure S 3.4**), reflected the trend of dorsal CA1 with the exception that the decrease in cell number from control to THC reached the threshold of significance. When the number of Cresyl Violet stained cells

was sampled in three 2000 μm² boxes of the cell layer, no differences were found (**Figure S 3.6**).

The initial three-way ANOVA in the dentate gyrus showed a potential interaction between sex and dorsal or ventral location relative to PV neuron density ($p = 0.054$), so for this analysis, results were split by both sex and dorsal or ventral location (Cohen's D = -0.738). Tukey post-hoc analysis showed no changes were observed in the dorsal DG in any groups (**Figures 3.5 and 3.6**). In the ventral DG, there was a trend toward a decrease in the number of PV cells in the THC exposed group ($p = 0.057$). The likelihood of this trend being real is supported by estimation statistics with a Cohen's D value of -1.49. There was a significant increase in granule cell layer volume between the EtOH + THC group and the control group in the dentate gyrus ($p = 0.004$, **Figure S 3.5**).

We also investigated the relative change between the density of PV interneurons in the dorsal and ventral regions relative to each exposure group (**Figure S 3.7**). There was a trend toward a decrease between the THC-alone and Ethanol-alone groups in the male dentate gyrus ($p = 0.092$).

3.5 Discussion

To our knowledge, this is the first paper to study PV interneurons using this model. Although we are unable to compare directly with previous research, the present findings are in line with those by Lu *et al.* who used a similar model with the more general interneuron marker glutamic acid decarboxylase 67 (149). Between estimation and ANOVA statistics, there is likely a decrease in PV interneuron density in the dorsal CA1 region, suggesting that in our model, there is a main effect of THC that is not seen

in the dual exposure (**Figures 3.3 and 3.4**). Given that there is an increase in the cell layer volume in the EtOH group but no change in cell numbers, there could be an increase in the overall number of cells in the ethanol group not seen in the EtOH + THC group.

Unlike the CA1 region, there were probable sex differences in the DG. This suggests that neurogenesis is differently affected in males and females exposed to these teratogens. The only significant change seen in this group in the density of PV interneurons was a decrease in the THC exposed group compared with all other groups in the male ventral region (**Figures 3.5 and 3.6**). However, the fact that there is also an increase in the cell layer volume in the EtOH + THC group compared with the control group, and no change in the overall cell density, suggests that there are more cells in the EtOH and THC group.

Considering that prenatal alcohol exposure is known to cause $GABA_A$ receptor hyperexcitability, these results are perhaps surprising, as one might expect that PV interneurons may be downregulated in response to the increased efficacy of GABA (58). However, one must also consider that the net effect of FASD is network hyperexcitability, which is seen clinically as a comorbidity with epilepsy in more extreme cases (150). Further, the greatly differing effects of prenatal versus postnatal exposure must be considered. Prenatal exposure not only effects circuit development, but also occurs at a time before the GABA switch, a process where KCC2 chloride receptors are upregulated (134). Before this upregulation, the intracellular concentration of chloride is so high that when the existing chloride channels open, the ions exit the cell along its concentration gradient, causing interneurons to have an

excitatory effect *in utero* (134). Lastly, interneurons in the hippocampus all migrate from either the caudal or medial ganglionic eminences during development and the cannabinoid system has been implicated in this (128). Therefore, it is possible that an upregulation of the number of neurons is a response to prenatal ethanol exposure that is inhibited by THC– leading to worse behavioral outcomes (113). Further research is required to parse out what changes occur due to the initial teratogenic insult and what effects, if any, result from the body's attempt to mitigate the injury.

THC tended to cause either a trend towards a decrease or a significant decrease in the number of PV cells. While no completely parallel literature was identified, Vargish *et al.* found a decrease in the number of cholecystokinin-positive positive interneurons in the DG, however only in those derived from the caudal ganglionic eminence (128). It is important to note that while cholecystokinin-positive and PV interneurons are found in the hippocampus, most cannabinoid receptor 1 (CB1) receptors are found on cholecystokinin-positive positive interneurons and not PV positive interneurons (75), although there is evidence of this outside the hippocampus (151). This is relevant because THC acts predominantly on CB1 receptors thus it is expected that THC would affect PV and CCK interneurons differently. CB1 receptors are $G_{i/o}$ coupled; CB1 receptor activation results in a signal cascade that inhibits the release of neurotransmitter vesicles at the synapse (70). For these reasons, future work should assess cholecystokinin-positive interneurons. Work by Tortoriello *et al.* found an increase in the number of CB1 receptors the CA1 of adult rats exposed to THC prenatally (1). While more research is needed to strengthen these results, it possible that the decreased number of cholecystokinin-positive interneurons each express relatively more

CB1 receptors. This is relevant to PV interneurons as interactions between cholecystokinin-positive interneurons and PV interneurons may be a good line of enquiry for future research to determine why this drop in PV interneurons is observed. Loss of PV interneurons could be directly from prenatal THC exposure, or could be selective degeneration as the brain's attempt to curb excessive inhibition. Fish *et al.* recently published a paper suggesting that prenatal cannabinoids interact with alcohol through a CB1-smoothened (Smo) pathway. Smo is a G-protein coupled receptor (GPCR) that acts to lower adenylyl cyclase activity (113). Specifically, they found that prenatal ethanol exposure inhibits sonic hedgehog (Shh) signalling, thereby increasing intracellular oxysterol, which then activates the smoothened protein (113). CB1 is found in heteromeric subunits with Smo, therefore overall adenylyl cyclase activity is decreased by a CB1 mechanism during prenatal THC exposure, and Smo via prenatal alcohol exposure, thus GABA is further released due to a loss of inhibition of neurotransmitter vesicle fusion (113).

After our initial results we were curious if differing numbers of inhibitory neurons could reflect a differing requirement for inhibition. So, to contextualize our results we analyzed the area measurements collected alone as well as a sampled density of Cresyl Violet stained cells. Interestingly, we found no change in density in any region, but an increase in cell layer volume in the dentate gyrus of EtOH + THC exposed animals and in the CA1 pyramidal layer of EtOH exposed animals. This suggests that in these cases that the numbers of total cells are increasing in this layer, which may speak to changes in neurogenesis, in the case of the dentate gyrus. But, considering that the changes are also seen in CA1, future research should take early timepoints into account. As a caveat,

it is worth noting that the magnitude of these changes is not resolvable with our analysis, and could partially be attributed to the changes in interneuron number. Further work is needed to elucidate the immediate and latent effects of combined prenatal alcohol and cannabis.

PV interneurons have been implicated in lateral inhibition, network synchrony, and neurogenesis (137,139,144). A decrease in the density of PV interneurons in adulthood could therefore decrease the efficacy of lateral inhibition, decrease network synchrony, and decrease neurogenesis while an increase in the density of PV interneurons could lead to too much lateral inhibition, over-inhibition of basal network repression, and a loss of cell survival. Regarding neurogenesis, contacts from PV interneurons on adult born granule cells (abGCs) in the DG are thought to be necessary for cell survival. It would therefore be interesting to investigate the correlation between changes in PV interneuron density and neurogenesis (144). Further, it is possible that the greater or lesser density of cells have altered amounts of synaptic connections in order to overcome an abundance or loss of inhibition so electrophysiological and ultrastructural studies would further elucidate the consequences of the changes in PV interneuron density seen in prenatal THC, ethanol, and combined exposure.

3.6 Conclusions

This study assessed the effects of prenatal alcohol, THC, and their combination on the number of PV cells in the rat hippocampus. While no sex differences were found, differences in the dorsal and ventral dentate gyrus, and the dorsal and ventral CA1 were observed. These dorsal-ventral differences should be considered in future work, as they reflect differences between neocortical versus amygdalar inputs. Significant effects were

found in the dorsal and ventral CA1, as well as the ventral DG. In the dorsal CA1, there was an increase in the number of PV interneurons in both the EtOH and EtOH + THC groups, and no change in the THC group. In the ventral CA1, there was a decrease in the number of PV interneurons in the THC group, an increase in the EtOH group, and no change from air-exposed in the EtOH + THC group. In the ventral dentate gyrus there was a decrease in the number of PV interneurons in the THC exposed group but not in either of the other two groups. More work is required to better understand the underlying mechanisms of the current results, and further work should address other interneuron types in the hippocampus.

CHAPTER 4

Prenatal ethanol and cannabis exposure have sex and region-specific effects in somatostatin and neuropeptide Y interneurons in the rat hippocampus.

4.1 Abstract

Cannabis is becoming increasingly legalized and socially accepted around the world. Accompanying this is an increase of *in utero* cannabis exposure. In addition, given that many people who consume cannabis also tend to drink at the same time, a subset of individuals exposed to cannabis during gestation are also exposed to alcohol. We have recently shown that combined exposure to these two teratogens can alter the density of interneurons that express parvalbumin in the hippocampus. In this paper we investigate the effects of *in utero* alcohol and cannabis exposure on somatostatin-positive interneurons, separate classes of cells that are important for network synchrony and basal inhibition in the hippocampus. Here we find that dual alcohol and cannabis exposure does not seem to have an additive effect, however, we did find that exposure to THC *in utero* had region-specific and sex-specific effects on the density of somatostatin-positive interneurons in the adult rat hippocampus. In neuropeptide Y interneurons we found a female-specific decrease in cell density in the CA1 with THC exposure that is not present with both teratogens; however, we also found impacts of combined exposure in the ventral dentate gyrus of females. These results further illustrate how alcohol and

cannabis exposure *in utero* may affect hippocampal function by altering inhibitory processes.

4.2 Introduction

Individuals who use illicit (and licit) drugs can face many health and social challenges. These challenges are further compounded during pregnancy when substance use affects both the mother and the developing fetus (152). Unfortunately, the social stigma surrounding drug use during pregnancy can often prevent individuals from seeking and receiving help, further contributing to drug exposure (152). One compound of concern is alcohol. Although it is generally recognized that alcohol harms the developing fetal brain (153,154), almost 14% of women in Canada report drinking during pregnancy when anonymously surveyed, and 10% worldwide (155–160). Children exposed prenatally to alcohol may exhibit a range of outcomes referred to as fetal alcohol spectrum disorder (FASD), including craniofacial abnormalities, low birth weight, persistent health challenges, and cognitive/behavioral problems (161). Impairments in learning and memory are among the cognitive effects of prenatal alcohol exposure and are often characterized by delayed developmental milestones, difficulty learning from consequences, and challenges in spatial memory (162).

With the legalization of cannabis in many jurisdictions, there has also been a persistent increase in simultaneous alcohol and cannabis (A/C) use in young adults between 19 and 30 years of age, the demographics associated with peak fertility (34,35,38,39,163). As alcohol and cannabis are both known to inhibit working and spatial memory in adults and since prenatal ethanol exposure causes learning and memory deficits,

memory deficits following concurrent prenatal exposure are likely (114,164,165). Moreover, since the hippocampus is central to learning and memory, it is pertinent to look for cellular and molecular changes in this region (166). Previous work has shown that cannabis and alcohol can individually impact the hippocampus (6,128,167–170), and that ethanol exposure can impact cannabinoid receptor activity in the hippocampus (171–173).

We have recently published a systematic review that suggested that hippocampal interneurons may be a focal point for the actions of both THC and ethanol in the developing brain (166). THC, the active component in cannabis, binds to presynaptic CB1 receptors, while ethanol acts on post-synaptic $GABA_A$ receptors (1,127). A potential mechanism for the synergy of these drugs can be speculated based on what is already known about their respective mechanisms of action. THC, the active component in cannabis, binds predominantly to presynaptic CB1 receptors, whereas ethanol acts on postsynaptic $GABA_A$ receptors (among its many actions) (1,127). The presynaptic CB1 receptors are $G_{i/o}$ coupled receptors and they can also be activated by the endogenous cannabinoids anandamide and 2-arachidonoylglycerol (2-AG) (129). The activation of CB1 receptors works to inhibit adenylyl cyclase activity, leading to reduced neurotransmitter release at the synapse (129). On the other hand, ethanol binds to $GABA_A$ receptors which are chloride ion channels found post-synaptically (121). In the adult brain, the extracellular chloride concentration is usually much higher than the intracellular concentration in mature excitatory neurons. Thus, when $GABA_A$ receptors are activated, negatively charged chloride ions travel into the cell along their concentration gradient, hyperpolarizing the cell and reducing its capacity to propagate excitatory signals. However, prior to birth, and particularly early in gestation, the KCC2

receptor, a potassium-chloride co-transporter, has yet to be upregulated, so the intracellular concentration of chloride can be much higher than the extracellular concentration(134). Thus, activation of these "inhibitory receptors" can be “excitatory” as they depolarise the cell under these conditions. This excitatory phase is essential for establishing circuits during normal development; however, exposure to alcohol in the prenatal environment can leave these cells subject to the effects of hyperexcitability (166). Taken together, we hypothesized that prenatal THC and EtOH exposure would affect hippocampal interneuron populations, possibly in a synergistic fashion.

Somatostatin-positive (SOM) interneurons tend to be found in the hippocampus and contribute to the creation of theta and gamma oscillations, which are important for cognition and memory (174–176). SOM interneurons are also important in feed-forward inhibition and promote neuronal synchrony in the neonatal hippocampus (177). Some studies have also shown that SOM interneurons express CB1 receptors; however, more research is needed to validate this work (178). Interestingly, SOM interneurons tend to be decreased in Alzheimer’s disease (AD) brains (174–176), interfering with their role in maintaining hippocampal-prefrontal synchrony and spatial encoding and further suggesting a role for SOM interneurons in processes related to cognition and memory (179,180). There is evidence that FASD produces structural changes in SOM interneurons, but it is not clear if there are also changes in the density of SOM interneurons in these studies (181,182). The density of SOM interneurons in the dentate gyrus is decreased in adult animals exposed to alcohol (183), so this is a realistic possibility.

Neuropeptide-Y (NPY) is a 36 amino acid polypeptide that is expressed widely in the brain, particularly in the hippocampus and hypothalamus (184). NPY-positive

interneuron changes have been found in studies of long-term stress, epilepsy, Alzheimer's disease, PTSD, and prenatal ethanol exposure (185–189). In the hippocampus, NPY has been implicated in neurogenesis, acting through the Y_1 receptor, and previous research has found both that NPY peptide levels are increased after a learning and memory task and that exogenous application of the NPY peptide can increase neurogenesis (190–192). Interestingly, a proposed mechanism for how NPY interneurons affect neurogenesis involves a requirement that young adult-born granule cells (abGCs) express the Y_1 receptor (190). This mirrors studies that show that parvalbumin (PV) interneuron and SOM innervation is required for the survival of new abGCs (193,194). The NPY receptor is $G_{i/o}$ coupled, and while the pathway that regulates neurogenesis is thought to proceed through the Y_1 receptor subtype, there are also receptor subtypes 2-6 — however, 6 is rodent specific and a pseudogene in humans (195,196). A subtype of NPY interneuron called the neurogliaform cell contains *en passant* boutons that release GABA into the extracellular space which largely act on extrasynaptic $GABA_B$ receptors to maintain basal inhibition in the brain (18,197,198). Given their impact on neurogenesis and the inhibition/excitation balance, NPY interneurons are a good target of study in prenatal cannabis and alcohol exposure.

4.3 Methods

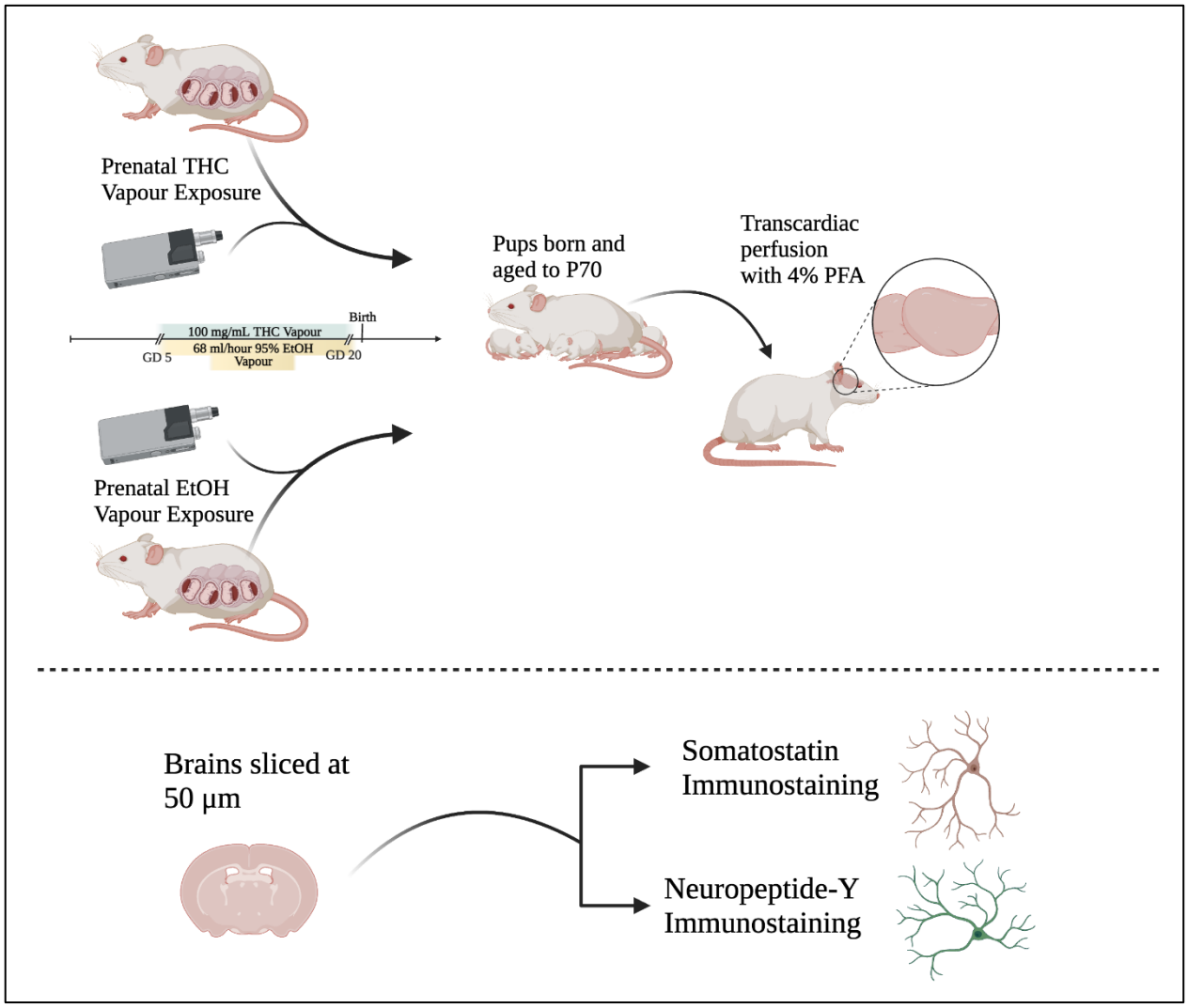

Figure 4.1 *Pregnant rats were exposed to 95% EtOH or Air for 3 consecutive hours at an airflow of 10 L/min. Afterwards, all rats were either exposed to THC or propylene glycol vehicle at an airflow rats of 2mL/min. Between PD60-70, the adult offspring were deeply anesthetized with lethal ketamine (67 mg/mL) and xylazine (6.7 mg/mL) and underwent transcardiac perfusion. Brains were collected and post-fixed in 4% paraformaldehyde for 24 hours. Brains were sliced at 50 µm for histology. Created with Biorender.*

Female Sprague-Dawley rats (n=24) were assigned to receive one of four experimental conditions (EtOH or Air) and (THC or Vehicle (VEH; propylene glycol, Sigma-Aldrich; see **Figure 4.1)).** Thus, there were 4 total conditions: EtOH + THC (n=6), EtOH + VEH (EtOH; n=6), Air + THC (THC; n=5) and Air + VEH (VEH; n=6). Subjects were bred at

the Center for Behavioral Teratology breeding colony at San Diego State University; pregnancy was confirmed in all dams by the presence of a seminal plug, which designated gestational day (GD) 0. Pregnant rats were exposed to their assigned drug condition daily from GD 5 to GD 20 in a vapor inhalation chamber (La Jolla Alcohol Research Incorporated, La Jolla, CA). Pregnant rats received 95% EtOH (68 mL/hour; Sigma-Aldrich) or Air for three consecutive hours at an airflow of 10 L/min. Then, subjects were either exposed to THC (100 mg/mL; NIDA Drug Supply Program) or the VEH (propylene glycol; Sigma-Aldrich) at an airflow rate of 2 L/min via an e-cigarette tank (SMOK TFV8 X-Baby); THC and VEH were administered in 6-second puffs every 5 min for a 30-min period (7 puffs total). An additional 10 minutes of airflow were delivered before opening the chambers to remove any residual vaporized drug. Dams gave birth on GD 22, and litters were pseudo-randomly culled to eight pups on postnatal day (PD) 2. This study used one male and one female pup from each dam. All animals used in this study were tested in an open field (PD 31-34) prior to being sacrificed for histology (data published in Breit *et al.*2019, amalgamated with other behavior tests); there is no evidence to suggest that measuring activity levels in the open field influences hippocampal interneurons (199). Maternal data, as well as plasma levels of drugs, are reported in (Breit et al., 2019).

Between PD 60-70, adult offspring were deeply anesthetized with a lethal dose of ketamine (67 mg/mL) and xylazine (6.7 mg/mL) dose (0.001 mL/g) prior to perfusing the subjects transcardially with cold saline, followed by 4% paraformaldehyde (PFA) in a phosphate buffer. Brains were extracted, post-fixed in 4% PFA for 24 hours, and then sectioned at 50 μM using a Leica VT1000S vibratome. All immunohistochemistry was

performed using a 1 in 6 series of tissue sections. A separate 1-in-6 series from these animals were used in a recent study of parvalbumin-positive interneurons (200). Tissue samples with DG present were sorted into a new 12-well dish and washed in PBS 3 times for 5 minutes, followed by a 2-hour pre-incubation in 3% NGS in 0.5 PBST. Subsequently, the tissues were incubated for 48 hours in 3% NGS in 0.5 PBST with a 1:200 dilution of α -somatostatin (GeneTex, GTX71935, and 0.14mg/ml) or 1:1000 α – NPY antibody (Abcam ab30914). The brains were left to incubate in a 4° C fridge on a "Belly Dancer" shaker. After 48 hours, the brain tissue was washed three times for 5 minutes in PBS. Following this was a 2-hour 2° C incubation in a 1:500 dilution of biotinylated goat α-rabbit (GenTex GTX71935) at room temperature in 3% NGS and 0.5% PBST. Vectastain ABC Elite avidin-biotin-peroxidase complex (Vector Laboratories Burlingame, CA) was used according to the supplied instructions, and tissue was incubated in this solution for 10 minutes at room temperature. After the incubation, brain tissue was washed three times for 10 minutes in PBS and then developed in 3,3'-Diaminobenzidine (Vector Labs, SK-4100).

Profile counts of SOM and NPY cells were performed at 40x using an Olympus brightfield CX21 microscope (Olympus Corporation, Center Valley, PA, USA). Images were obtained using an Olympus brightfield BX51TF microscope (MBF Bioscience, Williston, VT, USA) using StereoInvestigator software version 11.03 (MBF Bioscience, Williston, VT, USA), and FIJI-Image J (Version 1.52p, National Institutes of Health, USA) was used for area analysis.

We used a two-step process to determine cell density. First, each cell count in each slice, hemisphere, and region (for example, the left granule cell layer in the DG of one slice) was divided by its unique measured area. Next, the cell densities for individual slices

were calculated for the dorsal and ventral aspects of the CA1 and DG subfields. We classified dorsal and ventral regions using the Matt Gaidica Rat Brain Atlas (146). The dorsal region was from bregma -1.88 to -4.16, and the ventral region was from bregma -4.52 to -6.04. These coordinates were calculated by taking the entire length of the hippocampus and using the closest plates from the atlas to divide the hippocampus into two (i.e. half).

All statistics were performed using the general linear model in IBM SPSS statistics software, and figures were made using R and BioRender (147,148). A 95% confidence interval was used as the statistical threshold in this study, and all post-hoc tests were performed using a Tukey test. Males and females were evaluated separately as an omnibus ANOVA suggested sex differences.

4.4 Results

For SOM interneurons, an omnibus ANOVA showed a significant effect of treatment ($p = 0.029$), location along the dorsal-ventral axis ($p = 0.002$), brain region ($p > 0.001$) as well as an interaction between treatment and dorsal-ventral location ($p > 0.001$), dorsal-ventral location and region ($p = 0.001$), and treatment by dorsal-ventral location by region ($p = 0.007$). Because there are sex differences in counts before relative brain sizes were accounted for as well as interactions with treatment ($p = 0.02$ and $p > 001$ respectively), sexes were kept separate for post-hoc analysis.

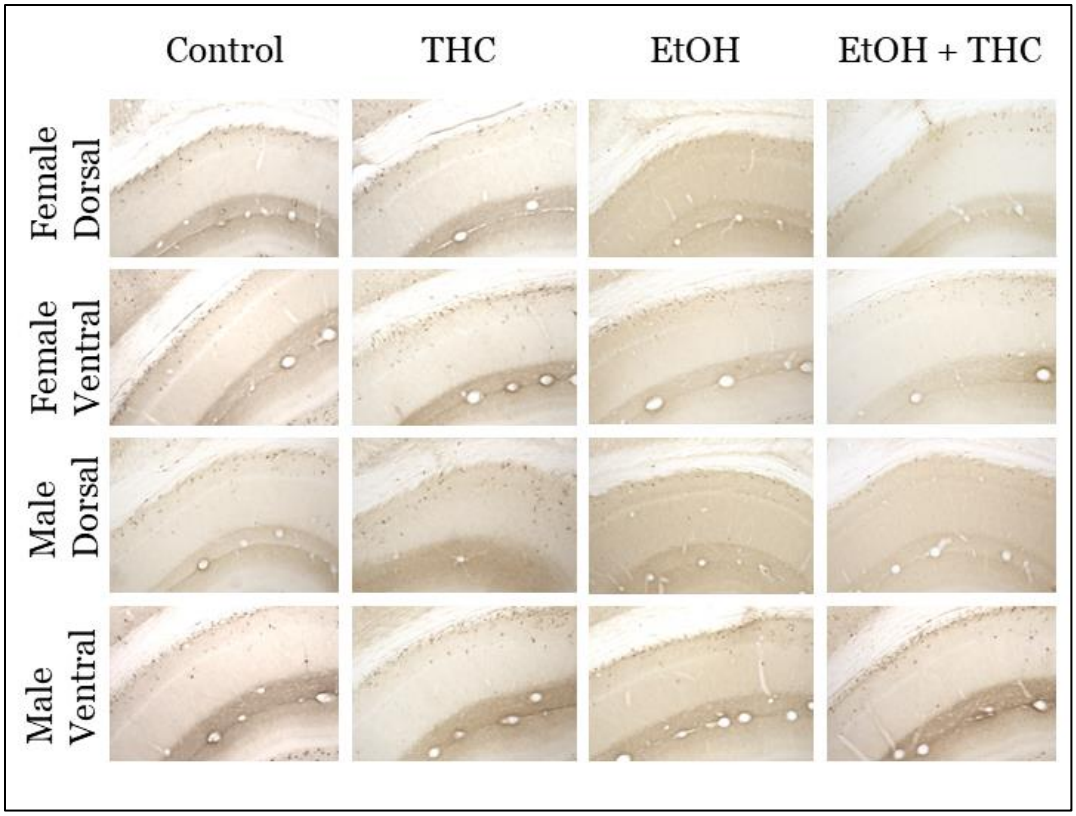

Figure 4.2 *10x representative images of somatostatin interneurons in the CA1 of male and female rats in each exposure group.*

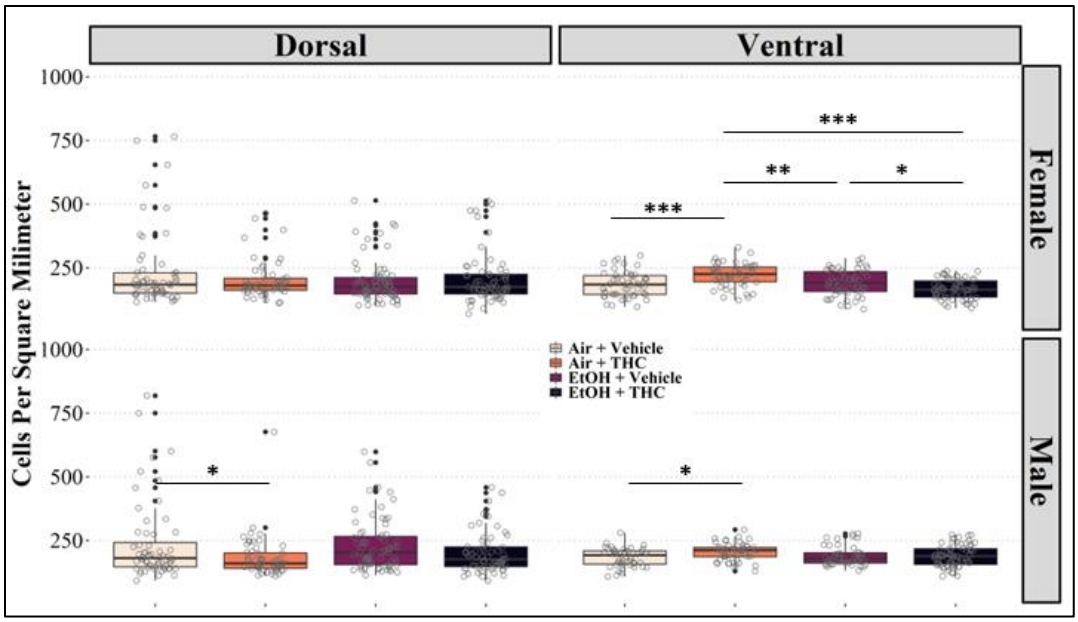

Figure 4.3 *Calculated density of somatostatin-positive cells in rats exposed to air, THC, EtOH, and EtOH + THC from GD5-20 in the dorsal and ventral CA1. Dorsal and ventral results were pooled as no effect of dorsal or ventral location was found. Animals assessed at P70. Data collected as profile counts of a DAB stained 1 in 6 series of tissue and area measurements of each cell layer. Each count was divided by its area.*

There was a significant increase in the density of SOM interneurons in the ventral CA1 of male and female animals ($p = 0.046$ and $p < 0.001$) in the THC-exposed group relative to the control group. However, females in the THC group, were also significantly higher than both the ethanol (EtOH) group ($p = 0.005$) and the combined exposure group ($p < 0.001$) (**Figures 4.2 and 4.3**). The EtOH group was also significantly increased relative to the combined group in the ventral CA1 of females ($p = 0.035$). In the males, a dorsal decrease in the density of SOM interneurons was also observed with THC exposure ($p = 0.046$), however, in the ventral CA1 there was an increase in cell density in the THC group relative to control ($p = 0.034$) We did not observe changes in SOM cell density in the dentate gyrus/hilar region (**Figures 4.4 and 4.5**).

NPY interneurons saw a different trend. The omnibus test revealed a significant effect of sex ($p < 0.001$), treatment ($p < 0.001$), dorsal-ventral location ($p < 0.001$), and brain region ($p < 0.001$). There was a significant interaction between sex and treatment ($p = 0.002$), treatment and region ($p < 0.001$), and dorsal-ventral location and region ($p < 0.001$). In the CA1, females showed a significant decrease in the density of NPY interneurons with THC both dorsally ($p = 0.011$) and ventrally ($p = 0.20$) (**Figures 4.6 and 4.7**).

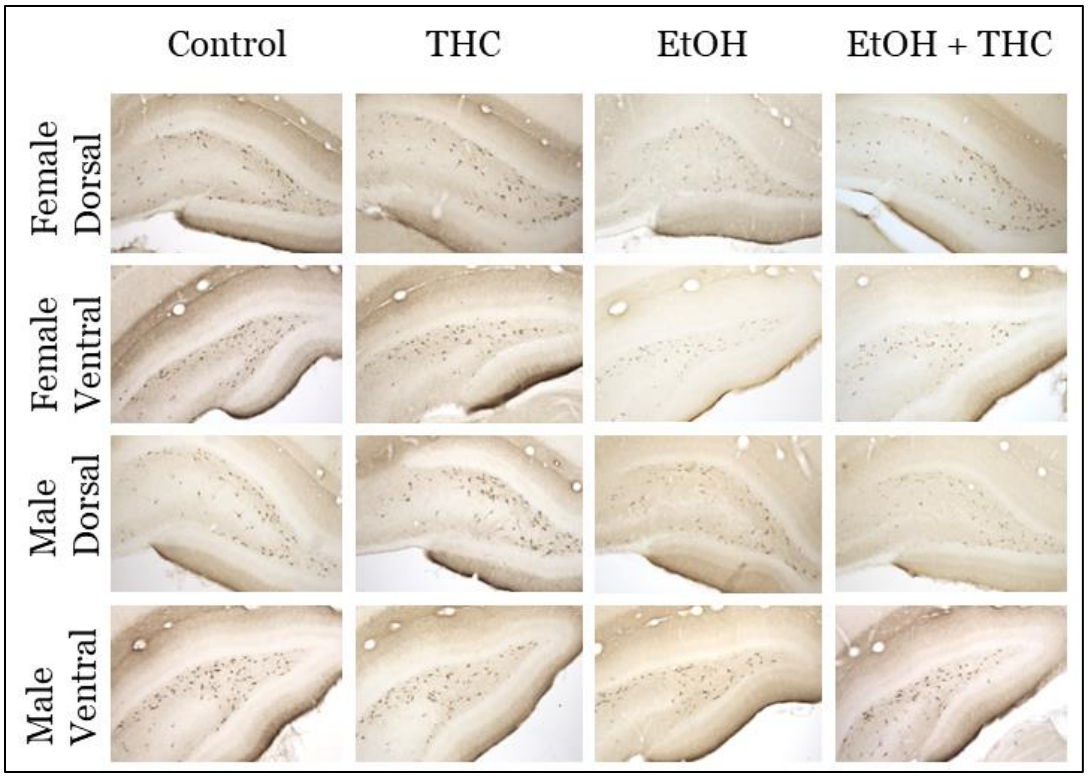

Figure 4.4 *10x representative images of somatostatin interneurons in the DG of male and female rats in each exposure group.*

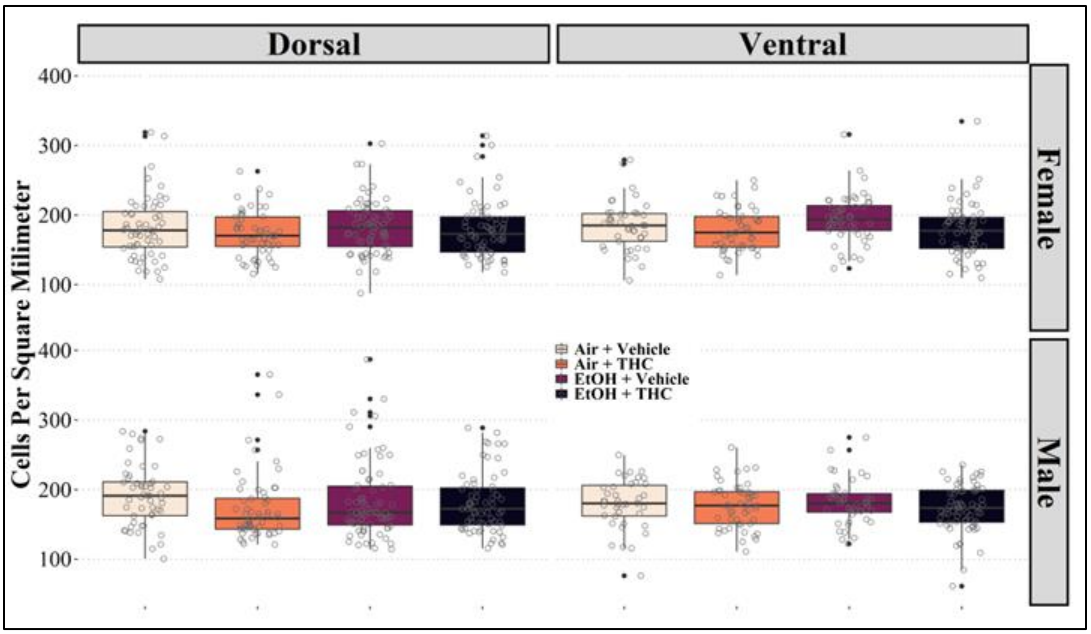

Figure 4.5 *Calculated density of somatostatin-positive cells in rats exposed to air, THC, EtOH, and EtOH + THC from GD5-20 in the dentate gyrus. Dorsal and ventral results were pooled as no effect of dorsal or ventral location was found. Animals assessed at P70. Data collected as profile counts of a DAB stained 1 in 6 series of tissue and area measurements of each cell layer. Each count was divided by its area.*

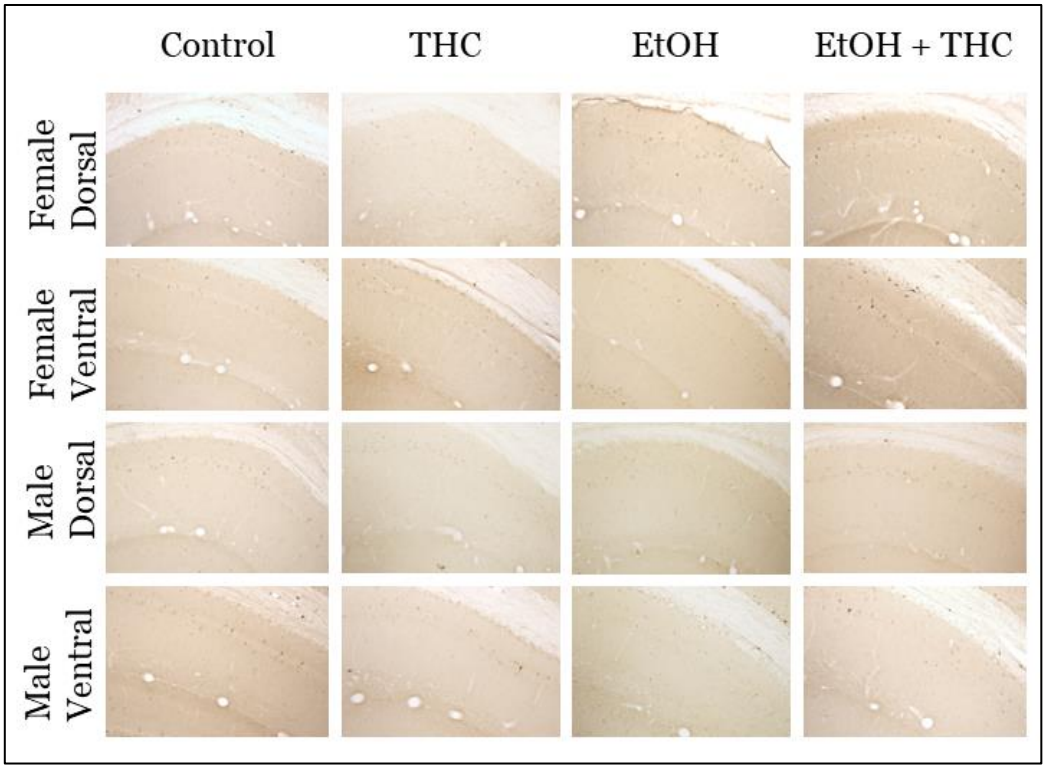

Figure 4.6 *10x representative images of neuropeptide Y interneurons in the CA1 of male and female rats in each exposure group.*

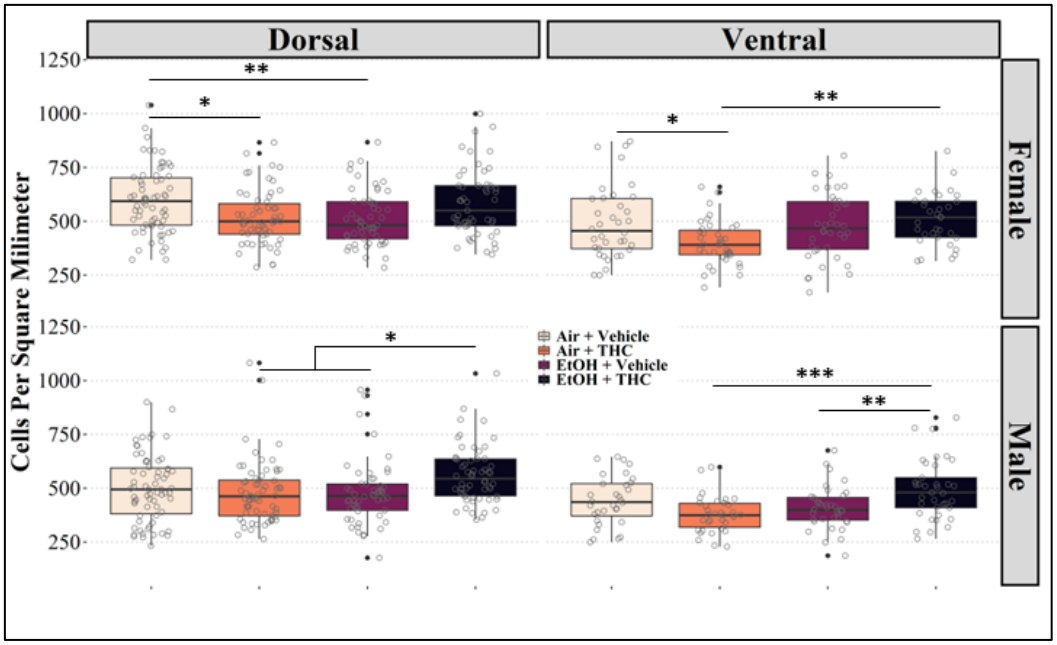

Figure 4.7 *Calculated density of NPY-positive cells in rats exposed to air, THC, EtOH, and EtOH + THC from GD5-20 in the dorsal and ventral CA1. Dorsal and ventral results were pooled as no effect of dorsal or ventral location was found. Animals assessed at P70. Data collected as profile counts of a DAB stained 1 in 6 series of tissue and area measurements of each cell layer. Each count was divided by its area.*

In the dorsal region, NPY interneuron density was also decreased in females exposed to EtOH only ($p = 0.009$). Ventrally, the decrease in the THC group was also significantly different than the combined exposure group ($p = 0.005$). In the dorsal CA1 of males, there was no significant decrease from control to THC or EtOH, and no significant increase between control and combined, but there was a significant increase from both the THC and EtOH group relative to the control group ($p = 0.010$ and $p = 0.012$ respectively). This trend was also observed ventrally; there was no significant difference between control and THC, but there was a significant increase from both THC ($p < 0.001$), and EtOH ($p = 0.007$) exposure relative to combined exposure. The dentate gyrus showed different sex-specific trends (**Figures 4.8 and 4.9**).

In the dorsal dentate gyrus of males, the EtOH group was significantly decreased compared with all other groups (control ($p < 0.001$), THC ($p = 0.030$), and combined exposure ($p = 0.002$)). The only interaction in the ventral dentate gyrus of males was a higher density in the combined exposure group relative to the THC group ($p = 0.004$), although there was a trend towards a reduction in density in the THC group compared to the control group ($p = 0.052$). In the dorsal dentate gyrus of females, the density of NPY interneurons was decreased in all three drug-exposed groups relative to the control ($p < 0.001$ in all cases). Ventrally, there was a decrease in density between controls and EtOH ($p = 0.049$) as well as controls and combined exposure compared with controls ($p < 0.001$).

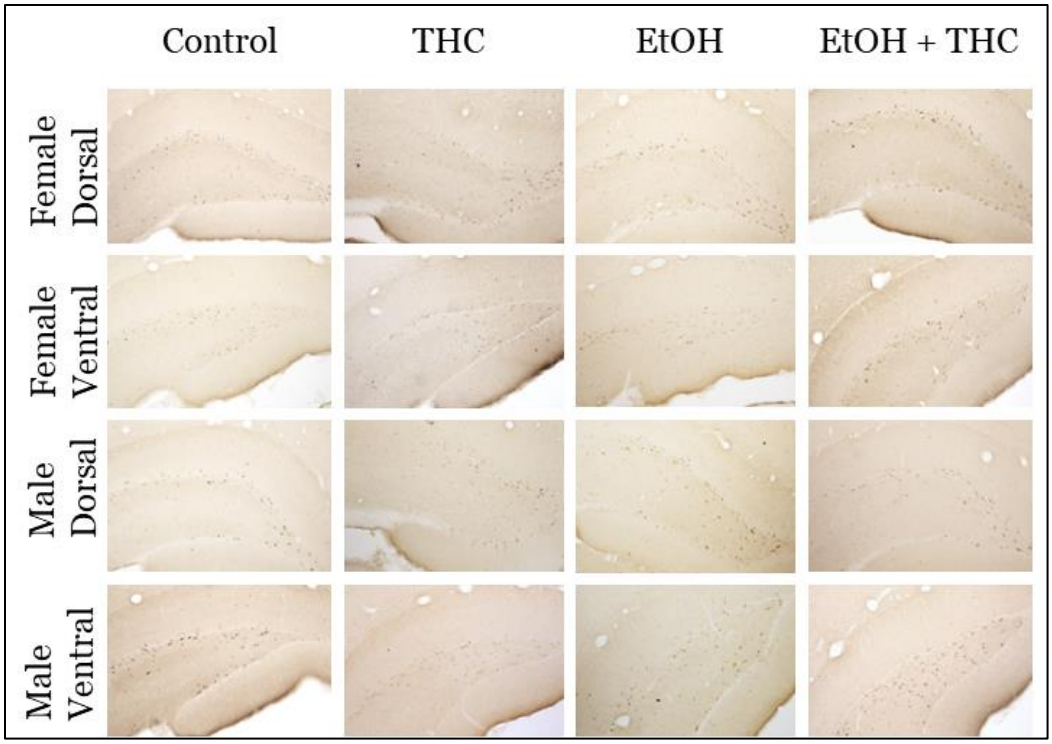

Figure 4.8 *10x representative images of neuropeptide Y interneurons in the DG of male and female rats in each exposure group.*

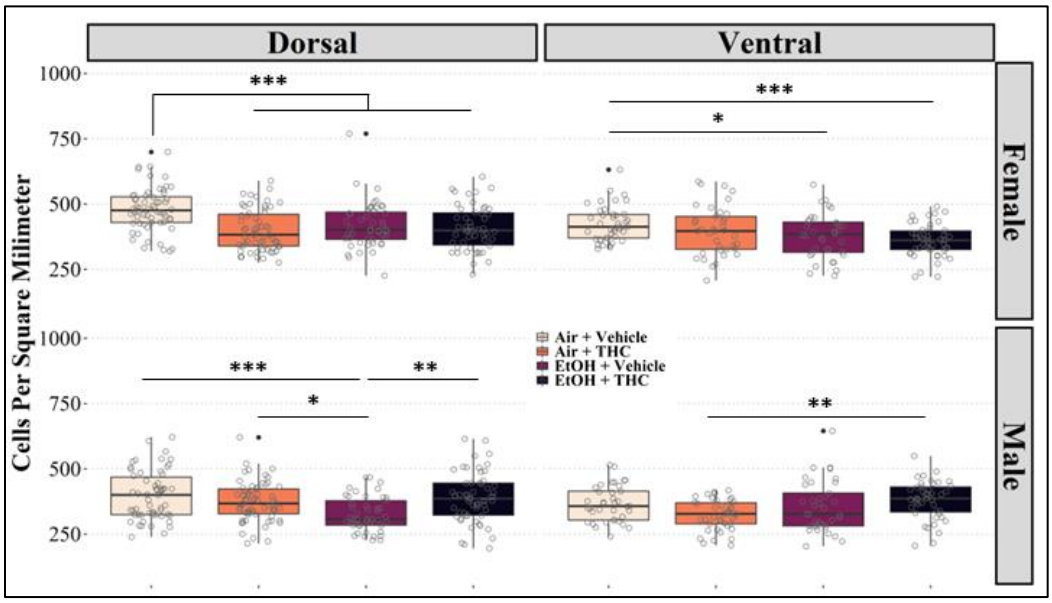

Figure 4.9 *Calculated density of NPY-positive cells in rats exposed to air, THC, EtOH, and EtOH + THC from GD5-20 in the dentate gyrus. Dorsal and ventral results were pooled as no effect of dorsal or ventral location was found. Animals assessed at P70. Data collected as profile counts of a DAB stained 1 in 6 series of tissue and area measurements of each cell layer. Each count was divided by its area.*

4.5 Discussion

4.5.1 Somatostatin

Our results suggest that the main effector for changes in SOM interneuron numbers is prenatal THC exposure. These changes were restricted to the CA1 region, where we found a ventral increase in SOM interneurons in both sexes. A dorsal decrease was also observed in males. Other developmental work in interneurons shows that prenatal ethanol exposure can cause cell death in the caudal ganglionic eminence (CGE) and the medial ganglionic eminence (MGE), the structures from which all interneurons in the brain are generated, but it is also known that individuals with FASD often experience symptoms that improve over time and given that we examined interneurons in adulthood, there may be compensatory changes (18,201). Cannabis is primarily perceived to be a more benign drug than alcohol and has even gained some acceptance in the general population as being safe to use during pregnancy (115,166). Our work challenges the perception that cannabis use during pregnancy is safe, as our results indicate that prenatal cannabis exposure may cause changes in interneuron numbers that persist into the adult brain. It should be noted that these changes occurred in a paradigm that represents moderate consumption. Indeed, equivalent THC consumption for a human relative to our model is approximately 10 mg of THC, assuming a linear dose-response extrapolated from the work of Grabenauer and Wilson (202), which is at the low end of recent estimates of daily cannabis consumption in Canada (203).

Five main hypotheses could account for the THC-related changes we observed. First, it may be that SOM interneurons were not being generated at the developmental time points they normally would be, resulting in a reduction in the overall number of

interneurons available. Second, GABA signaling could have been enhanced by alcohol exposure in the prenatal period, a time period when GABA signalling can be excitatory, and this could have selectively reduced interneuron numbers through apoptosis. Third, the timing of the "GABA switch" could have been altered by prenatal alcohol exposure, changing the developmental trajectory and the incorporation of interneurons into developing circuits. Fourth, because CB1 receptors are important for axon guidance, activation of CB1 receptors *in utero* could result in the migration of interneurons being off-target, although this is complicated by the finding that even interneurons transplanted *in utero* migrate correctly (20). Finally, if the excitatory inputs to interneurons are not present because of changes in CB1 receptor density, this could also lead to improper cell migration and development.

Repeated THC exposure during the prenatal period can cause a downregulation of CB1 receptors, leading to a loss of inhibition of vesicle release though a $G_{i/o}$ dependent pathway (1,70). While many cells aren't considered "synaptically active" until the late second trimester, which is near the end of our exposure paradigm, circuit establishment is known to require GABA input (204,205). This increased GABA input could lead to excitotoxicity and cell death of principal cells as well as interneurons, as runaway excitation amplifies. Excitotoxicity is also thought to happen with prenatal ethanol exposure, and is supported by a co-morbidity of FASD and epilepsy (206). While we have revealed a role for THC in altering SOM interneuron density, it is also clear that prenatal ethanol exposure can also produce excitotoxicity (206).

The GABA switch is a biphasic process that begins when an animal passes through the birth canal (134). During this process, KCC2 chloride receptors are upregulated (134). Before this upregulation, the intracellular concentration of chloride is so high that when

the existing chloride channels open, the ions exit the cell along its concentration gradient, causing interneurons to have an excitatory effect *in utero* (134). However, it has long been known that the switch is delayed by chronic blockade of $GABA_A$ receptors and accelerated by increased $GABA_A$ receptor activation (207). Scheyer *et al.* have shown that THC exposure during lactation, after the first part of the GABA switch has begun, causes a delay in the duration of the GABA switch (208).

Canonically, there is strong evidence that CCK interneurons express CB1 receptors during adulthood, and some evidence that SOM interneurons do as well, but it is thought that all interneurons express CB1 during development for neuronal migration (2). While hippocampal excitatory neurons are born *in situ*, all interneurons are born in either the CGE or MGE and must migrate (18). Specifically, SOM interneurons are MGE derived (18). Thus, downregulation of CB1 receptors could mean that interneurons cannot migrate to the hippocampus successfully. Follow-up studies may be able to elucidate this. This could explain the decrease in dorsal versus the increase in ventral density in the CA1; the dorsal hippocampus contains stronger neocortical inputs whereas the ventral hippocampus contains stronger amygdalar inputs.

One further hypothesis also involves the CB1 receptor's involvement in axonal guidance. Work by Fishell's group has shown that cortical SOM interneurons require long-range thalamic inputs to mature correctly (209). Perhaps this is also the case in the hippocampus, where CA1 SOM interneurons require innervation by Schaffer Collaterals to develop appropriately, and the DG requires perforant path inputs to function correctly (121). Therefore, if there is a deficit in the axonal guidance of these inputs, the development of these cells may be impaired.

4.5.2 Neuropeptide Y

In the CA1, the general trend observed suggests that there is a decrease in NPY interneurons with either THC or EtOH alone, but this deficit is not seen with combined exposure. This is surprising, given the presynaptic-postsynaptic synergy of CB1 and $GABA_A$ receptors. A possible explanation for this is that while NPY interneurons are impacted by prenatal alcohol and cannabis exposure alone, combined exposure causes such a deficit that the amount of NPY is upregulated. This would mirror work in perinatal sevoflurane research, where both isoflurane and sevoflurane caused a decrease in NPY levels, and that exogenous NPY administration could rescue the phenotype. Reductions in NPY could impact hippocampal excitability. Thus, it is important to determine if there is a relationship between prenatal cannabis exposure and the development of epilepsy. There is a paucity of literature in this area, possibly because cannabidiol (CBD) has been shown to have antiepileptic effects in adult animals after the "GABA switch" has occurred (210).

There was a difference in trends between male and female animals in the dentate gyrus, although in both cases the effect is stronger in the dorsal subregion. In female animals, there are lower densities of NPY interneurons in almost every drug-exposed group relative to control. An important follow-up study would assess the impact of prenatal drug exposure on neurogenesis, and if changes in neurogenesis correlate with a decreased NPY innervation. In males there seems to be less of an effect in the combined exposure group compared with either drug individually, suggesting once again that in males, NPY may be upregulated as a protective mechanism. This sex difference would make sense given that in prenatal alcohol research, male animals are often found to show larger deficits than female animals; a greater amount of NPY interneurons may be

indicative of an attempt by the brain to ameliorate a larger deficit (211,212). Examination of NPY interneuron density at earlier developmental periods would help determine if this is the case. One possible confounding factor is that there is a difference between overall NPY protein levels and the number of cells that can be counted as NPY positive. More research is needed to follow up on why these differences in cell densities may occur.

4.6 Conclusions

This study assessed prenatal cannabis and alcohol exposure, as well as a combination of the two, to determine how they impacted somatostatin and neuropeptide Y-positive interneurons. In somatostatin interneurons, we did not find significant changes in the dentate gyrus subfield, but there were specific changes in the CA1 subfield. Only the group exposed to THC alone showed reductions in somatostatin-positive neurons in the dorsal CA1 subfield. Conversely, this was accompanied by a significant increase in somatostatin-positive neurons in the ventral CA1 subfield. In neuropeptide Y interneurons, there were sex-specific trends that suggest males may upregulate neuropeptide Y in response to combined prenatal ethanol and cannabis exposure. Most of the effect in CA1 is THC related. This research aims to discover how prenatal teratogen exposure can affect the hippocampal circuits thought to be important for learning and memory processes, in the hopes that this and subsequent research will both enhance our understanding of learning and memory mechanisms, as well as provide insight into new therapies that may help to improve the condition of those affected.

CHAPTER 5

Prenatal THC exposure is correlated with changes in microglia morphology in the rat hippocampus.

5.1 Abstract

This study aimed to investigate the effects of prenatal exposure to THC on microglia morphology in the hippocampus of adult rats. The results of a circularity analysis showed that prenatal THC exposure did have an effect on morphology, and this was compounded with sex and regional effects. A Sholl analysis further supported the hypothesis and indicated that the phenotype observed was that of increased ramification without the presence of a hyper-ramified-like phenotype. This research shows that microglia can be altered long after insult in utero, yet before any obvious damage is seen. Regional and sex differences in results point to diverse subpopulations of cells, even within the hippocampus.

5.2 Introduction

There is evidence that cannabis has anti-inflammatory effects, but what about in utero? A 2019 systematic review and meta-analysis found the global rate of cannabis use during pregnancy to be about 2%, with two American studies echoing the number (115,213,214). This means that cannabis use is as prevalent as alcohol use during pregnancy (215). And yet, there are many more studies on fetal alcohol spectrum disorder than there are on prenatal cannabis exposure. The studies that have been

published in humans to date suggest a correlation with learning difficulties, attention deficit hyperactive disorder (ADHD), and other psychiatric disorders (216).

The most abundant G-protein coupled receptor (GPCR) in the brain is the CB1 receptor, which is targeted by THC, the psychoactive component of cannabis (217,218). They have been implicated in cell migration, differentiation, and adult neurogenesis (22,219). More recently, they have been found to exist in microglia and astrocytes, solidifying their role as a mediator of inflammation (220). CB1 signaling has been shown to suppress the release of inflammatory cytokines such as TNFα and IL-6 in a mouse model of multiple sclerosis (221).

The CB1 receptor's endogenous ligands are the fatty acids anandamide and 2-arachidonoylglycerol glycerol (222). Their signalling is retrograde across the synapse, where endocannabinoids (eCBs) are released post-synaptically and then act on the presynaptic neuron. CB1 receptors are $G_{i/o}$ coupled, and so their activation causes a signal cascade that leads to the suppression of neurotransmitter release (222). Knockout of the CB1 receptor has been shown to increase the susceptibility of mice to a chronic social defeat paradigm, and is correlated with increased glucocorticoid levels, and thus are implicated in social stress (223).

Our previous work suggests that there are long-term cellular changes in interneurons with prenatal THC exposure, and the work of others in the field suggests that prenatal cannabis exposure decreases the density of CB1 receptors (200,224). These results and others suggest that indeed, prenatal cannabis exposure inhibits cell migration, wiring, and density. At adolescent time points, microglia perform trogocytosis, pruning the brain of unused synapses (225). Thus, if microglia are affected by prenatal cannabis

exposure, there could also be changes in synaptic pruning. One study by VanRyzen *et al.* showed that in the basal lateral amygdala, the eCB 2-AG acts as a phagocytic signal in adolescence, causing microglia to phagocytose otherwise healthy cells, and shaping the development of sex differences in play aggression (27).

Due to the expansive effects of the eCB system, parsing out the effects of THC exposure on the developing brain will require a global effort. Its effects on microglia could be direct or indirect. For example, is the CB1 receptor in late gestation, when neurons are coming online, causing excitotoxicity with acute activation because the KCC2 receptor has not yet been upregulated, and thus GABAergic signaling is excitatory? Are microglia affected by an early apoptotic insult? Or, are interneurons not migrating correctly from a loss of CB1 receptors from repeated exposure, and is this miswiring causing inflammation? Or are the CB1 receptors on the microglia themselves being acted on around the time of microglial infiltration to the brain, causing changes in the expression of regulatory genes?

It is now known that microglia form distinct subpopulations in different brain regions (226). One such region is the hippocampus, an area both central to learning and memory and affected by acute THC exposure (121). Further, it is a region that contains a high density of CB1 receptors. Therefore, we have chosen to examine hippocampal microglia in this study. Because adult neurogenesis occurs in the dentate gyrus but not the cornu ammonis region of the hippocampus, both the CA1 and DG were assessed. We chose to further constrain our study to the molecular layers of each region, where microglia are well-spaced for analysis.

Microglia research has increased exponentially in the last decade. We are now far from the M1 M2 hypothesis of microglial activation, and now recognize the diverse and numerous ways that microglia can exist regarding morphology and cytokine profile (226). Further, the microglia are now considered to be one third of the tripartite synapse (226). They, and astrocytes participate in the endocannabinoid system (227). However, just as studies of diverse human populations can tell us a lot about a society, so too can population studies of microglial characteristics tell us about the brain. At the most basic level, form tends to dictate function and so in the case of prenatal THC exposure, we assessed if morphological changes would be observed in adulthood, far after the teratogenic insult. Here, we assess microglial circularity and the tree characteristics as determined by Sholl analysis on a large scale throughout the rat hippocampus to determine the effects of prenatal THC exposure on inflammatory-like morphological characteristics.

5.3 Materials and Methods

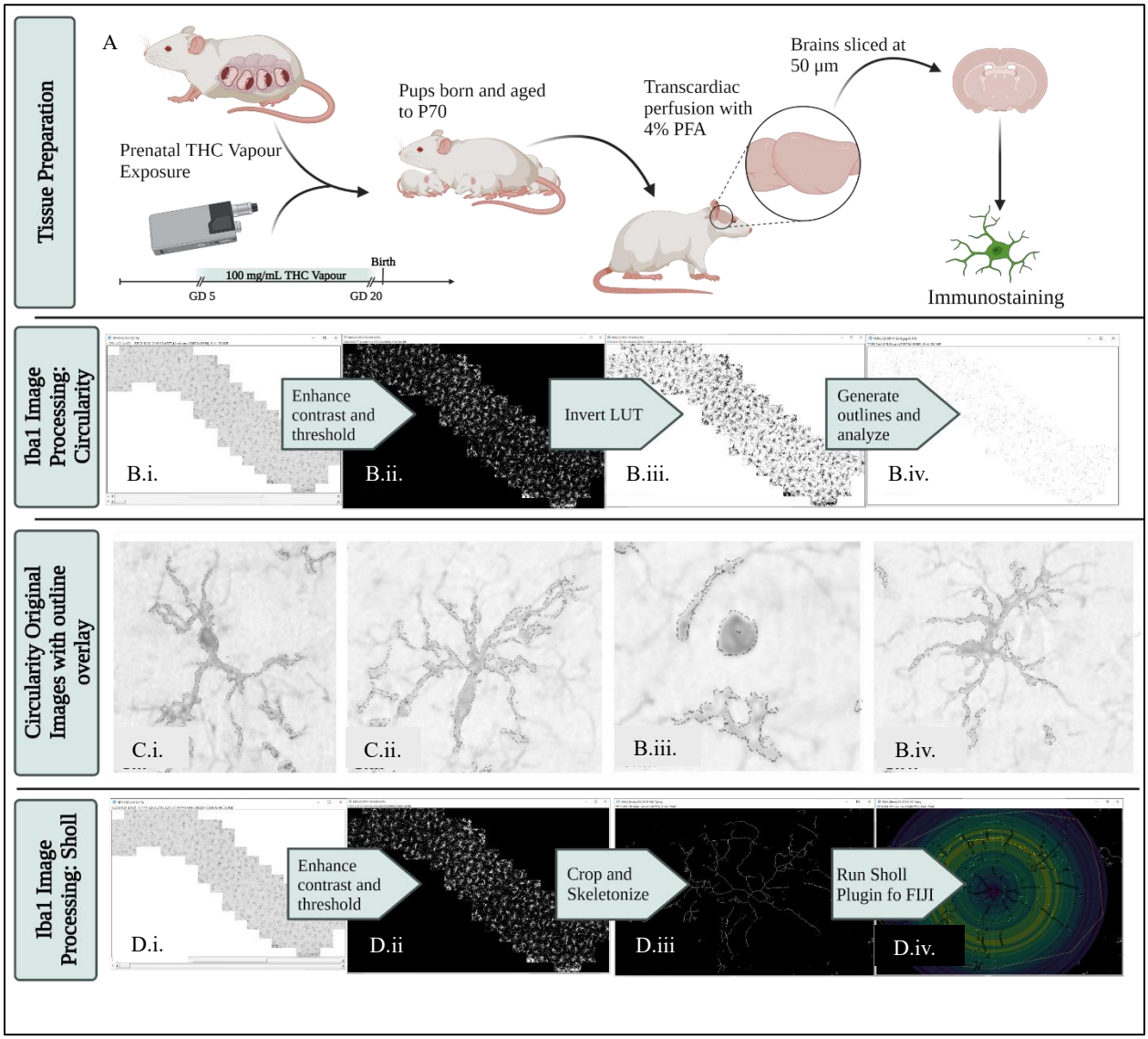

Figure 5.1 *Animal generation and image processing methods. A. Rats were either exposed to THC or propylene glycol vehicle at an airflow of 2mL/min. Between PD60-70, the adult offspring were deeply anesthetized with lethal ketamine (67 mg/mL) and xylazine (6.7 mg/mL) and underwent transcardiac perfusion. Brains were collected and post-fixed in 4% paraformaldehyde for 24 hours. Brains were sliced at 50 µm for histology. B. Image preparation steps for circularity analysis C. Overlay of Iba1 cells and the outline generated during analysis showing efficacy of the protocol D. Sholl analysis preparation and output. Created with Biorender.*

5.3.1 Animal Generation

Female Sprague-Dawley rats (n=24) were assigned to receive 1 of 2 experimental conditions THC or vehicle (VEH; propylene glycol, Sigma-Aldrich; see Figure 5.1). Pregnancy was confirmed in all dams by the presence of a seminal plug, and this was designated as gestational day (GD) 0. Pregnant rats were exposed to their assigned drug exposure condition once daily from GD 5 to GD 20 in a vapor inhalation chamber (La Jolla Alcohol Research Incorporated, La Jolla, CA). Subjects were either exposed to THC (100 mg/mL; NIDA Drug Supply Program) or the VEH (propylene glycol; Sigma-Aldrich) at an airflow rate of 2 L/min; THC and VEH were administered in single 6-second puffs every 5 min for a 30-min period (7 puffs total). An additional 10 minutes of airflow was administered before opening the chambers to remove any residual vaporized drug. Dams gave birth on GD 22, and litters were culled on postnatal day (PD) 2. One male and one female pup from each dam were used in this study (Figure 5.1). All animals used in this study had previously been tested in an open field (PD 31-34); measuring activity levels in the open field is not expected to be a confound (Breit et al., 2019).

5.3.2 Tissue Preparation

Between PD 60-70, the adult offspring were deeply anesthetized with a lethal ketamine (67 mg/mL) and xylazine (6.7 mg/mL) dose (0.001 mL/g) and transcardially perfused with cold saline followed by 4% paraformaldehyde (PFA) in a phosphate buffer. Brains were extracted and post-fixed in 4% PFA for 24 hours. Brains were sectioned using a Leica vibratome into 50 μM slices. Immunohistochemistry was performed using a 1 in 6 series of tissue. A 3-minute incubation in 1% sodium borohydride in PBS was used for

antigen retrieval. Wako rabbit anti-Iba1 antibody (#019-1947) was used at 1:1000 in 3% normal goat serum (NGS) and 0.5 % Triton X-100 in PBS (0.5% PBST) for 48 hours at 4 °C with shaking. Biotinylated goat anti-rabbit secondary antibody (ThermoFisher # 31804) was used at 1:500 in 3% NGS and 0.5% PBST for 2 hours at room temperature with shaking. Amplification was performed with Vectastain ABC Elite avidin-biotin peroxidase complex and 3,3'-Diaminobenzidine was used to visualize the labeled cells (Vector laboratories Burlingame, CA). ABC and DAB were prepared as per supplier instructions.

5.3.3 Microscopy and Analysis

Images for area analysis were taken using an Olympus brightfield BX51TF microscope (MBF Bioscience, Williston, VT, USA) and StereoInvestigator software version 11.03 (MBF Bioscience, Williston, VT, USA). Analysis was performed using FIJI-Image J (Version 1.52p, National Institutes of Health, USA). To allow a large number of Iba1+ cells to be analyzed, stitched image stacks at 100x were taken spanning the entire suprapyramidal blade of the Stratum Granulare of the dentate gyrus subfield and the entire Stratum Radiatum of the CA1 subfield. A 0.5 μm step size was used to acquire the stack images. Although the brains were sliced at 50 μm, post-mounting tissue shrinkage caused the slices to be approximately 20 μm on average. Due to the large number of images stitched together by the software, small variations in Focus Adjustment (a step in the Slide Scanning Workflow in StereoInvestigator) could cause large variations in focus across the entire. The Focus Adjustment step is necessary to extrapolate micrometer slopes across the slide as mounted in the tray, or account for any irregularities in slice thickness. For this reason, a stack of 20 images was taken for each

image, and the final analysis included 15. This means that we included approximately 20 μm of brain tissue after accounting for tissue shrinkage. A limitation of this selection is that some microglia may have had processes that stretched out of the acquired area, however, any out-of-focus images bias the macro towards measuring increased circularity and we believe that this choice maximized the robustness of our measurements.

The final dataset is comprised of over 650 gigabytes of compressed .jpx image files. These files were moved to an analysis computer using an external hard drive and one brain was uncompressed at a time using Microfile+ (https://www.mbfbioscience.com/products/microfileplus). Uncompressed images were between ~10 and 40 gigabytes each. Images were analyzed using our FIJI macro that loaded the images in greyscale, selected the correct channel, selected the correct slices, enhanced the contrast such that 1% of the pixels were saturated, ran a 2% threshold using the Default settings with the output background set to black, Z-projected using "Maximum Intensity", inverted the LUT, ran the "Open" command, then ran the "Analyze Particles" command with "Area" and "Shape Descriptors" set and gaited to collect particles with an area of 10 to 500 μm2. The output of the macro was a .jpeg of the outlines acquired by the macro, and an Excel file with the same name as the image file. Due to the image size, the macro was not batched. The scale was set manually by the researcher on opening FIJI. All outlines are labeled with a number corresponding to the results spreadsheet. We determined that the smallest particle likely to be a cell had an area of 30 μm2 and the largest had an area of 500 μm2. Larger than this and the outline generally depicted two or more cells. Figure 5.1 shows the overlay of some greyscale

images with the resulting outlines. The benefit of using this method of analysis was that 50-400 cells were able to be analyzed per image, so that the sample size would be able to overcome any error incurred in the analysis. The images were opened with channels due to the use of BioFormats Importer (228), a FIJI plug-in necessary to load images of this size. The macro was developed and tested relative to all three resulting channels, the second of which was deemed to work the best. The threshold output was set to black and then inverted later because the "Maximum Projection" step works the most accurately with light cells on a dark background.

To investigate whether circularity changes were due to longer microglial processes or bushier ones, a Sholl analysis was performed. For this analysis, the same decompressed images were run through a preparation macro. Briefly, this macro selected channel 2, removed the first 6 images in a stack, enhanced the image contrast such that 1% of all pixels were saturated (and experimentally determined value), then the image was thresholded to 2% of the histogram value, and then saved to the original folder as an image stack with "Binary3D" added to the name. For Sholl analysis, these binary image stacks were opened and the polygon select tool was used to select a complete appearing cell. This image was then cropped to increase the speed of the subsequent processing steps. The Skeletonize (2D/3D) FIJI plugin was used to create a skeleton of a given cell. A projection was then created using the "Max Intensity" method. A second polygon was then traced around this projection and added to the ROI manager. The Sholl plug-in was then used on default settings to analyze the image. The output was two Excel sheets of measurements and a plot of a linear fit model of N versus distance. Five cells per image were selected at random and analyzed by researchers blinded to the condition. Analysis

sessions always consisted of all five cells in an image getting analyzed to prevent cells from being selected more than once.

An omnibus ANOVA was run in SPSS to see if there were any significant effects of sex or dorsal/ventral location, and a Students 2-tailed t-test was run on the final groups. Figures were made in R Studio and Biorender.

5.4 Results

5.4.1 Circularity Analysis

Data is presented as both a heat map (Figures 5.2-5.3) and a bar graph (Figures 5.2-5.3). Heatmaps are presented to help illustrate the distribution of the 19,454 cell circularities analyzed. A white dotted line indicates the median in each heat map, to show if there is any shift in group means.

The omnibus ANOVA showed a significant effect of layer ($p < 0.001$), sex ($p = 0.007$), dorsal or ventral location ($p = 0.005$), and exposure group ($p < 0.001$). A two-way interaction between sex and exposure group was also found ($p = 0.001$) as well as a three-way interaction between dorsal/ventral location, layer, and exposure group ($p < 0.001$). Due to these effects and interactions, student's two-tailed t-tests were performed in the two exposure groups separated by layer, dorsal/ventral location, and sex. Levene's test was used to assess if the variances were equal between groups. If the variances were not equal, an adjusted p-value was used. The largest change in p-value between the adjusted and non-adjusted tests was 0.006, and in no case did it change whether the null hypothesis was rejected.

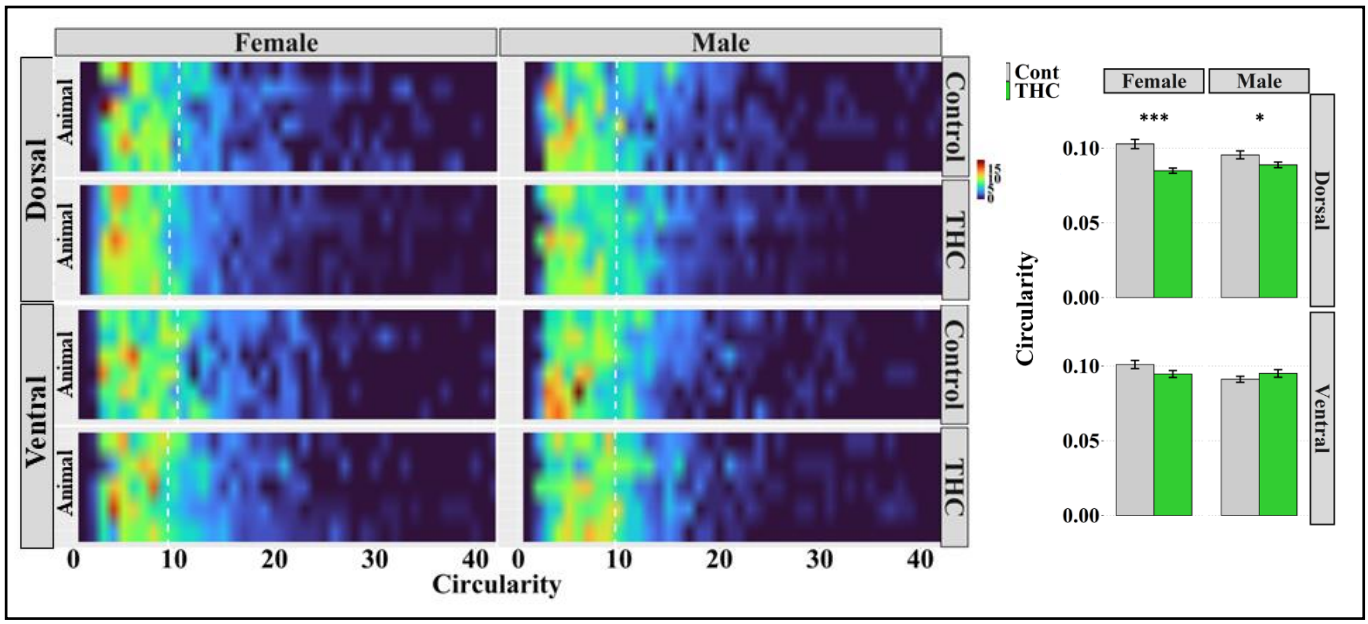

Figure 5.2 *Iba1 circularity in the stratum moleculare. On the left each row of the heatmap represents one animal. Each of the circularity measurements were bucketed from 1 – 100 so that the frequency of the dataset could be visualized. X axis cut off at 40 as nearly all measurements fall below that line. Dotted white line represents the mean for the group with all measurements from all animals averaged. This same mean is represented in the bar graphs on the right for easy interpretation.*

In the stratum moleculare no changes in circularity were observed in either males or females in the ventral hippocampus. In the dorsal hippocampus, there was a decrease in circularity in both the females ($p < 0.001$, Cohen's D = 0.246, lower = 0.157, upper = 0.335) and males ($p = 0.04$, Cohen's D = 0.095, lower = 0.007, upper = 0.182) (Figures 5.2, 5.4). This indicates that there is a correlation between an increase in ramified and decreases in amoeboid morphology in female rats and males prenatally exposed to THC but the effect size is small.

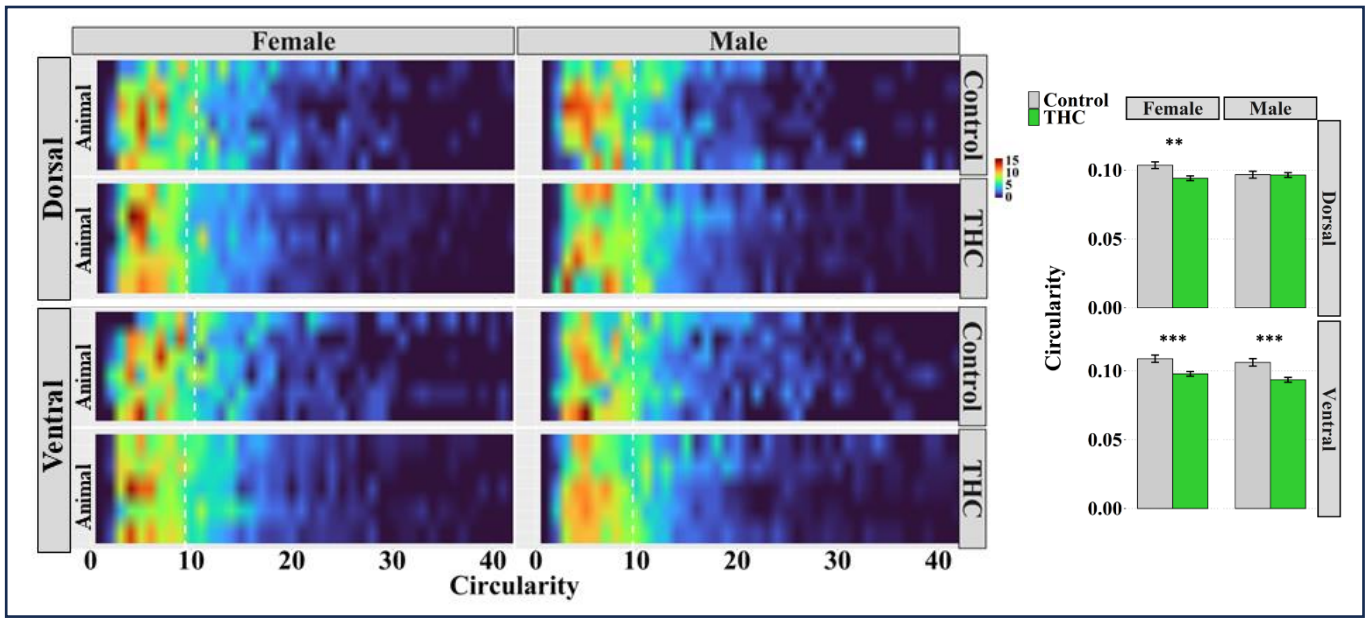

Figure 5.3 *Iba1 circularity in the stratum radiatum. On the left each row of the heatmap represents one animal. Each of the circularity measurements were bucketed from 1 – 100 so that the frequency of the dataset could be visualized. X axis cut off at 40 as nearly all measurements fall below that line. Dotted white line represents the mean for the group with all measurements from all animals averaged. This same mean is represented in the bar graphs on the right for easy interpretation.*

In the stratum radiatum, there is a significant decrease in circularity in the dorsal hippocampus in female animals only ($p = 0.001$, Cohen's $D = 0.122$, lower = 0.048, upper = 0.196), with a small effect size. In the ventral stratum radiatum, there is a significant decrease in circularity in both the male ($p < 0.001$, Cohen's $D = 0.157$, lower = 0.081, upper = 0.233) and female ($p < 0.001$, Cohen's $D = 0.142$, lower = 0.066, upper = 0.218) groups (Figures 5.3, 5.5). In both cases, the effect size is small.

5.4.2 Sholl Analysis

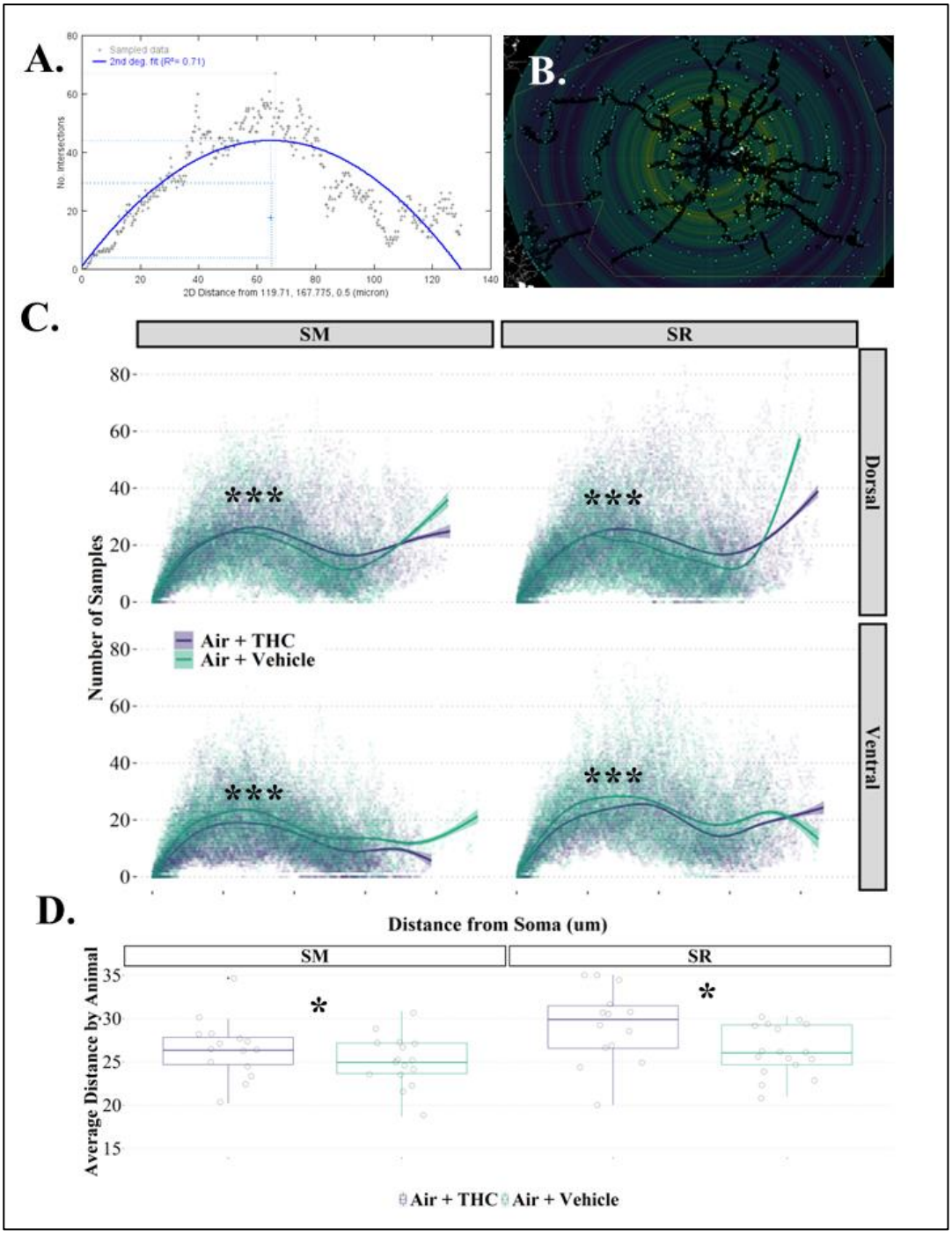

Figure 5.4 *Iba1 Sholl analysis. A. Representative length versus distance output for a singe cell showing a normal distribution B. Representative visual output of Sholl analysis plugin C. Smoothed conditional means plot over raw datapoints. D. Mean distance point crossing away from the soma averaged by animal (sexes pooled).*

The sholl analysis showed that THC-exposed animals had on average, more branching further away from the soma ($p>0.001$) (Figure 5.4 c). Because the output variables, frequency and distance from the soma, are both scalar variables, with distance as a covariate of frequency, and because these two scales are informed by dorsal-ventral location, hippocampal region, sex, and condition, a Poisson regression was performed. This regression showed a significant effect of treatment, region, and dorsal-ventral location on the scalar variables (all $p>0.001$). The output of the combined raw data contained ~170,000 observations, creating concern regarding spurious correlations. And so, a second analysis was performed (Figure 5.4 d). Briefly, 300 buckets, each representing 1 μm were created per region per layer per animal. Each of those buckets was used first to gather the data into a computable size. After, the sum of observations falling within one bucket was divided by the sum of all observations in that bucket and then multiplied by 100, to yield a percent of line crosses at a given distance relative to the whole, per animal. An index was then created by multiplying the frequency of one bucket by its percentage. These normalized values were then averaged and plotted in 5.4 d. A univariate general linear model ANOVA was then used to assess if the effect remained, even when measurements were condensed to individual animals. It was found that the effect of treatment was retained ($p = 0.014$) as was the effect of region ($p = 0.014$). However, the effect of the dorsal-ventral location was not seen.

5.5 Discussion

The present study aimed to investigate the effects of prenatal THC exposure on microglial morphology in the hippocampus of adult rats. The results of the circularity analysis showed significant effects of treatment, sex, region, and dorsal-ventral location,

while the Sholl analysis data showed significant effects of treatment, region, and had some evidence of differences between the dorsal and ventral hippocampus. The disagreement in these results could be due to cell morphology changes that the analyses were differentially sensitive to. A follow-up study should be conducted to assess if there are differences in more specific morphologies, such as rod-shaped microglia.

This study identified morphological differences in microglia with prenatal THC exposure. Interestingly, many microglial studies assay morphologic and functional changes either around the time of acute injury, or during neurodegeneration (229,230). Literature assessing the hyper-ramified phenotype often does not assess past 30 days following the stressor, likely due to cell turnover (231). This research highlights that microglia may be dysregulated far before any age-related phenotype is observed, and recasts microglia as not just passive cells that clear debris, but drivers of neuronal functionality. As for diversity, the three-way interaction observed in the circularity analysis between dorsal-ventral location, treatment, and layer, supports the findings that discrete subpopulations of microglia support different brain regions. Even with the most conservative statistical analysis, we have shown that microglia react to prenatal THC exposure in a region dependent manner. And even without the Sholl's support for sex differences, regional differences in microglia inevitably feed into sex differences in between brain regions. For example, in fetal alcohol spectrum disorder research, there is a clear sex difference in deficit between the more dorsal, neocortical-connected hippocampus with the ventral, amygdalar-connected hippocampus (232).

One hypothesis for why these morphological differences is seen in prenatal THC exposure is that there may also be a dysregulation in the endogenous cannabinoid 2-AG.

Since it has been shown that prenatal cannabinoid exposure decreases CB1 receptors, it is possible that endocannabinoid production is upregulated to compensate for this (75). And since it has been shown that endocannabinoids also signal microglia, a lasting change in eCB levels could lead to the lasting change in microglial morphology.

The changes in microglia morphology seen here suggest that these cells have a more surveiling-like phenotype. The Sholl analysis was necessary to parse out this phenotype from a hyper-ramified phenotype. Hyper-ramified microglia have a decreased circularity, as they retract their processes on the way to becoming amoeboid (226). And while this morphology is considered to be transient, and therefore unlikely to be observed in adult animals with a prenatal exposure, it was necessary to exclude. The Sholl analysis demonstrates that the microglia are not just less round, but also that their processes are longer, and branch farther from the soma. If 2-AG levels are indeed increased, then this hyper-extended phenotype may be a symptom a of long-term low-grade presence of aberrant signalling molecules. In other words, the microglia are stretched along a gradient, looking for the source of phagocytic signal but never reaching the phagocytic threshold.

5.6 Conclusions

The results of this study provide evidence of morphological changes in microglia associated with prenatal exposure to THC. The circularity analysis revealed significant effects of treatment, sex, region, and dorsal-ventral location. The Sholl analysis further supported the finding that prenatal THC exposure affects microglial morphology, although the same regional differences were not observed. The discrepancy in these results may be due to the differential sensitivities of these tests, and more detailed

follow up studies should be conducted to this end. This research highlights that microglia can be altered far after an insult, and before any obvious cognitive or neurodegenerative changes have occurred. Three-way interactions between microglia and location suggest there are distinct subpopulations of cells within the hippocampus. The morphological differences seen warrant a follow up study of microglia density, or could be due to 2-AG signalling alterations. Overall, this study provides insight into the effect of prenatal THC exposure in the hippocampus.

CHAPTER 6

Hippocampal synaptic plasticity and synaptic marker deficits in a rat model of prenatal THC exposure

6.1 Abstract

This study investigated the effects of prenatal THC exposure on synaptic plasticity and synaptic receptor co-localization in a rat exposure model. Dams did not show behavioural differences when assessed in an open field, nor was their grooming or rearing altered. Male but not female offspring showed earlier eye opening in THC compared with control animals. A classic 900 pulse at 1 Hz paradigm did not show sex differences when assessed in cage controls, however a second paradigm, 6000 pulses at 10 Hz showed sex differences in the amount of LTD, as well as how they respond to MPEP and AM251. In prenatally exposed animals, there were no changes observed in paired-pulse ratio or input-output curves, however there was an increase in the number of dendritic spines in both males and females pre-stimulus. However, females showed differences in three spine morphologies while males showed differences only in stubby spines. As THC is thought to alter CB1 receptors, and because some LTD was shown to be CB1 dependent, a study of CB1 receptor co-localization with the inhibitory marker gephyrin was performed. This study showed significant increases in the dorsal hippocampus of both male and female animals. Male animals also had smaller clusters of CB1 receptors with drug exposure. These findings suggest that prenatal THC exposure leads to dysregulation of the endocannabinoid system in the rat hippocampus by

altering CB1 receptor levels, and this in turn correlates with an increase in dendritic spines and a deficiency of hippocampal LTD.

6.2 Introduction

Cannabis is among one of the most prevalent drugs used around the world, especially by those of reproductive age (233). Yet there are few studies that assess how cannabis affects the developing brain. With legalization of cannabis for recreational use in North America, it is further important that the unintended effects of this drug be studied. The combination of legalization and lack of research into harms of cannabis use in pregnancy may support the assumption that some have that cannabis is natural and therefore safe. This may cause some people to see it as a suitable treatment for morning sickness, since it is approved for nausea treatment in cancer care (234). And while it is true that fatal overdoses from cannabis use have never been reported, human studies are emerging which show that *in utero* exposure to THC, the psychoactive component of cannabis, is correlated with negative psychiatric outcomes and premature birth (235–237). Approximately 2% of pregnant people report using cannabis, a number that is comparable to alcohol (213). It is also important to note that the THC content in cannabis products has increased fourfold between 1995 and 2019 (238).

THC acts on four main receptors in the brain. They are the cannabinoid type 1 (CB1) receptor, the cannabinoid type 2 (CB2) receptor, and the orphan g protein receptor GPR55, and the newly discovered GPR18 (239). Until recently, it was thought that the CB1 receptor was the isoform found in the central nervous system, and the CB2 receptor was the isoform found in the peripheral nervous system (240). It is now known that the CB2 receptor is very much also in the brain, with studies suggesting that it is implicated

in neuroinflammation (241). THC is not the only cannabinoid in cannabis, cannabidiol (CBD) has been shown to both act as an inverse partial agonist, and more recently to potentiate the effects of THC under some conditions. Cannabis also contains numerous phytocannabinoids and terpenes which may alter the effects of THC (242). For the purpose of this study, we used purified THC, to minimize as any possible confounds. The endocannabinoid system is a retrograde signalling system, meaning that eCBs produced post-synaptically travel backwards across the synapse and act pre-synaptically (243). In this way the eCB system allows post-synaptic cells to modulate incoming signals. The majority of CB1 receptors are found on inhibitory, or GABAergic interneurons, although some are found on glutamatergic cells as well as microglia and astrocytes (222,244). Astrocytes can detect spillover of calcium from a synapse, and activate MAGL or DAGL, depending upon the context (245). Because the CB1 (and CB2) receptor is $G_{i/o}$ coupled, activation of the CB1 receptor causes a signal cascade that decreases intracellular cyclic AMP (cAMP) levels and prevents neurotransmitter release at the synapse (222). In the case of interneurons, this means that GABA is not released, and so acute activation of the CB1 receptor increases excitability of principle neurons, and in the case of glutamatergic – glutamatergic CB1 signalling, receptor activation leads to a decrease of excitability. This ability to modulate synaptic strength is an important feature of synaptic plasticity.

The area of the brain earliest known for long-term synaptic plasticity is the hippocampus (246). The hippocampus is a brain region central to learning and memory (247). Because the hippocampus is a unidirectional circuit, a stimulating electrode can be placed in one location and monosynaptic connections can be assayed with a

recording electrode (121). Recent studies have shown that long-term depression (LTD), has an endocannabinoid component (6). Typical induction protocols for LTD are around 1 Hz, with 900 pulses at 1 Hz being common in the literature (248). However, recent r-TMS studies have shown that a 10Hz frequency can induce plasticity (249). Parallel to this, our lab has recently shown that an induction protocol of 6000 pulses at 10 Hz induces an isoform of LTD that is endocannabinoid dependent (6). More specifically, in LTD the firing causes an amount of calcium into the cell such that phosphatases rather than kinases are activated, leading to endocytosis of AMPA receptors, or on a larger scale, the pruning of the synapse altogether (250). However, LTD can also occur across a broader population of synapses (251). The protocol that studies this second type of LTD is relatively novel, with this the first study that we are aware of that uses adult female animals.

Since adult cannabis exposure affects learning and memory, a process that the hippocampus is central to, here we study synaptic plasticity in the hippocampus of rats prenatally exposed to THC.

Two types of LTD were assayed, as well as the proportion of excitatory and inhibitory synaptic markers that co-localized with cannabinoid receptors, in order to study how synaptic plasticity and the balance of excitation to inhibition are altered in prenatal THC exposure. We assayed the changes in receptor co-localization between gephyrin and CB1, as well as Psd95 and CB1. Gephyrin is a marker of inhibitory synapses while pSD95 is a marker of excitatory synapses, and so assaying the relative ratio can elucidate some of the mechanisms of prenatal cannabis exposure. Lastly, we assayed dendritic spine density and morphology.

6.3 Methods

Litters of vehicle and THC treated animals were generated at the University of Victoria. Animals used to study the characteristics of the two LTD types were purchased from Charles River. All protocols adhered to CCAC guidelines. All animals were housed on a 12/12 light dark cycle in a temperature and humidity-controlled room. Animals were housed in cages of 2 or 3, and had access to food and water ad libitum, and were also provided with a red plastic hut. For prenatal exposure, pregnancy of nulliparous dams was confirmed with a plug check, and this day was designated as gestational day (GD) 0. From GD 5-20, dams were exposed to 100 mg/mL THC vapor or a 70/30 vegetable glycerol/propylene glycol vehicle control, with an additional 10% of polyethylene glycol 400 (PEG400) for solubility. THC was never used more than 48 hours after preparation from solid THC resin. Dams were placed in the vape chamber for 35 minutes per day, with the last 5 running only air. The vape chamber was designed and built by La Jolla Alcohol Research, and the model used was the Victoria model. This model allowed dams to be placed into individual boxes, each supplied with their own vape cartridge and air flow monitor. THC was vapourised in a baby beast brother 2 cartridge, with 5 second bursts given every 3 minutes. On GD 15, dams were placed in an open field for 5 minutes, 15 minutes after the end of the vape session. A 16 square grid was drawn on the bottom of the field. Researchers assessed the total number of seconds the animals spent grooming as well as the number of times the animal groomed itself, the total number of seconds the animals reared, as well as the number of times the animals reared, the total time the animals climbed the walls as well as the number of times the animals climbed the walls, the total time spent in the centre 4 boxes as well as the number of times the

animals crossed into the centre of the area, and the total number of times the animals crossed the gridlines in the arena.

Pups were assessed visually for eye opening, and then left to age up for experimentation. Pups were separated into groups destined for histology and electrophysiology. Between post-natal day (PND) 28 and 30, all electrophysiology animals were put through a novel location recognition task as described previously. Briefly, animals were allowed to habituate to a behaviour area for 5 minutes on day 1, on day 2 the habituation was repeated, and then one hour later the animals were introduced to two identical objects. One day later the animals were re-introduced to the behaviour arena with the same two

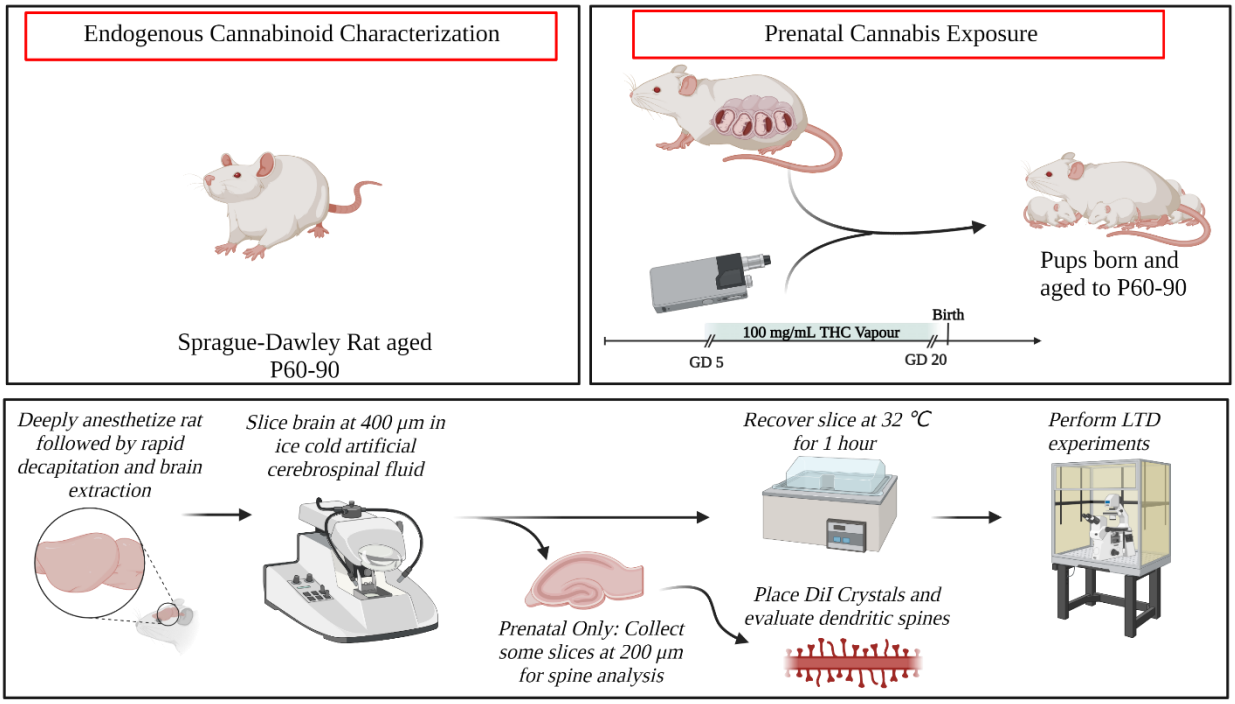

Figure 6.1*: Pregnant rats were exposed to 100 mg/mL THC or propylene glycol vehicle at an airflow rate of 2mL/min. Endogenous characterization animals received no drug and no vehicle. Between PD 60-90, the adult offspring were deeply anesthetized with isoflurane and underwent rapid decapitation. Brains were sliced at 400 µm for electrophysiology and then at 200 µm for DiI analysis. Created with Biorender.*

objects, however one object had been moved. The interaction with the object in the novel location versus familiar location is the outcome measure.

Between PND 60-90, electrophysiology experiments were performed (Figure 6.1). The protocol is modified from Fontiane et al., with the addition of ascorbic acid and pyruvate to the artificial cerebrospinal fluid (aCSF) composed of (in mM) 125 NaCl, 2.5 KCl, 1.25 NaH_2PO_4, 25 $NaHCO_3$, 2 $CaCl_2$, 1.3 $MgCl_2$, and 1.4 dextrose bubbled continuously with carbogen (95% O_2/5% CO_2; 295–305 mOsm; pH 7.2). Animals were deeply anesthetized with isoflurane before being rapidly decapitated and having their brains extracted into ice-cold aCSF bubbling with carbogen. Brians were sliced at 400 μm on the compresstome before being allowed to recover at 32 °C for one hour. For the DiI study, dorsal slices were collected at 200 μm and immediately fixed in 1% PFA for 1 hour at room temperature. DiI crystals were then placed under a dissecting microscope with a dissection needle then allowed to incubate for 24 hours in the fridge then another 24 hours on slide after being mounted (252). For the ephys experiments, after one-hour slices were allowed to equilibrate to room temperature. After equilibration, slices were placed in recording chambers suspended under microscopes (Olympus, BX50WI, Olympus, Center Valley, PA, USA). Glass recording electrodes 1-4 mΩ and bipolar stimulating electrodes were placed in the medial perforant path (MPP) of the dentate gyrus for recording. Square wave pulses at 5 seconds apart (0.12 ms) were used to find a signal before a 15 second pulse interval was used for recording baseline. For recording an Axon Multiclamp 700 B amplifier, digitized by an Axon Digidata 1550, and recorded using Clampex 10.5 software (Molecular Devices, San Jose, CA, USA) was used. Once signals were acquired, the stimulating voltage was increased stepwise until the signal no

longer increased in size. This signal had to be at least 0.7 mV to be included in the dataset. After the maximum signal was found, the voltage was decreased until 70% of maximum amplitude was reached. At least 5 minutes of stable baseline occurred before the paired pulse and input/output curve were generated. Preconditioning recordings were run after this test to ensure that the act of conducting these tests would not interfere with the induction of LTD. In the case of a drug study, 5 mines of stable preconditioning were acquired after paired pulse and input/output testing, then stability had to be maintained for a total of 20 minutes before the induction protocol. In the prenatal study, no drugs were used and a minimum of 20 minutes of stable pre-conditioning were recorded before stimulus. One of two stimuli, either 900 pulses at 1 Hz or 6000 pulses at 10 Hz were applied. One hour of post-conditioning were recorded. For the prenatal study, slices were either categorized into a success (LTD was induced) or a failure. Slices with LTD were used in an analysis of the magnitude while all other slices were included in failure testing. In all LTD experiments, there had to be a fibre volley visible at the end of the 60 minutes, in order to differentiate between depressed and dead slices. All slices had to have a baseline fEPSP slope of less than 0.5, and the post conditioning response had to have a slope of less than 1.5 in the last 10 minutes.

On PND 70, histology animals were euthanized by perfusion. Animals were deeply anesthetized with isoflurane then perfused with first ice-cold heparinized PBS then with 4% paraformaldehyde (PFA) in PBS. Brains were extracted and allowed to post fix in PFA for 24 hours. After fixation, brains were placed in 30% sucrose until they sank (~3 days) before being stored in PBS with 1% sodium azide. Brains were sliced at 50 μm on a Leica 1200VT vibratome (Leica) and collected in 12 well plates. A triple label of CB1,

gephyrin, and PSD95 was performed as follows; tissue was blocked in PBS containing 0.5% Triton X-100 (0.5 PBST) containing 3% normal goat serum (NGS) and 3% normal donkey serum (NGS). Following blocking, slices were incubated in antibody (AbCam α-PSD95 ab18258, SYSY α-gephyrin 147 111, and Nittobo α-CB1 AB 2571593) at 4 °C for 48 hours with shaking in blocking buffer. The slices were then washed in PBS before incubation in the dark with secondary antibody for 2 hours at room temperature with shaking. Slices were then washed before incubating in 1:20,000 Hoechst in PBS for 20 minutes and mounted with FluromountG. Images were taken with an oil immersion 60x confocal microscope (Olympus BX61WI) where saturated pixels were used to determine the laser power. All images for one slice were acquired in a single imaging session. Images were analysed in FIJI imageJ using one of 6 macros. Macros were recorded by the researcher but the expansion of macro functionality was done with the help of ChatGPT (253). Macro 1 co-localized gephyrin and CB1 puncta, macro 2 co-localized PSD95 and CB1 puncta, macro 3 analysed CB1 puncta alone, macro 4 analysed large gephyrin puncta, macro 5 analysed small gephyrin puncta, and macro 6 assessed if there were any holes or blood vessels in the images so that an area adjustment could be performed. DiI analysis was performed by a researcher blind to conditions. Images were loaded into Neurolucida 360 where the spine analysis module was used in semi-guided mode to trace dendrites then detect and classify synapses. Researchers used standard settings then increased the limits of detection of spines until all spines were captured. From there 3D meshes were exported to Neurolucida Explorer where the spines were analysed and an excel file of characteristics created. All spines assessed were on second order branches or farther away from the cell soma. A 30-70 μm segment was used for each observation. Three to five dendritic segments from at least 3 cells were analysed

per slice. One to two slices per animals were used. A Hoechst counterstain was used to make sure that cells selected were in the molecular layer of the dentate gyrus. Any dendritic segments showing varicosities or which were not spiny were excluded.

All statistics were run in SPSS software and graphs were made in Microsoft Excel and R Studio.

6.4 Results

6.4.1 Dam behaviour is not affected by THC exposure paradigm

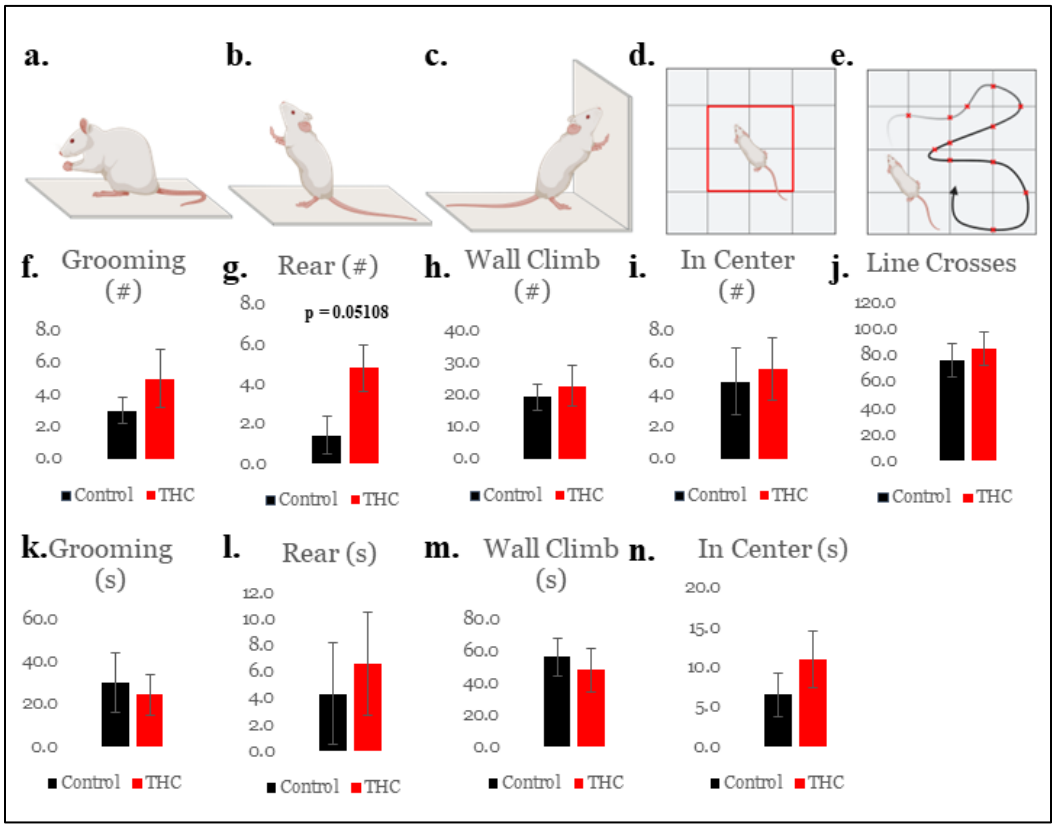

Figure 6.2 *Dams exposed to THC showed no behavioural deficits of locomotion or open field behaviours. a, f, k grooming; b, g, l, rearing; c, h, m, wall climbing; d, I, n, anxiety-like behaviour; e, j locomotion. Created with Biorender.*

Dam behaviour was not affected by THC exposure in the behaviour paradigms tested (**Figure 6.1**). There was no significant effect in the number of times the animals groomed themselves or total time grooming (Figure 6.2 a, f, k). Similarly, there was no significant effect in the number of times the animals climbed the wall or the total

number of seconds the animals spent climbing the wall (Figure 6.2 c, h, m). There was no significant difference between THC and vehicle animals in the amount of time the animal spent in the centre of the arena or the number of times the animals crossed into the centre (Figure 6.2 d, i, n). There was no change in locomotion as measured by total line crosses (Figure 6.2 e, j). There was a trend towards significance in the total number of times the animals reared away from the wall ($p = 0.05108$, independent samples t-test, Figure 6.2 b,g), but no significance in the total number of seconds spent rearing away from the wall (Figure 6..2 l). Of note, there was an n of 5 animals per group, so the power of the experiment was low.

6.4.2 THC exposed pups had earlier eye opening but no changes in memory behaviour

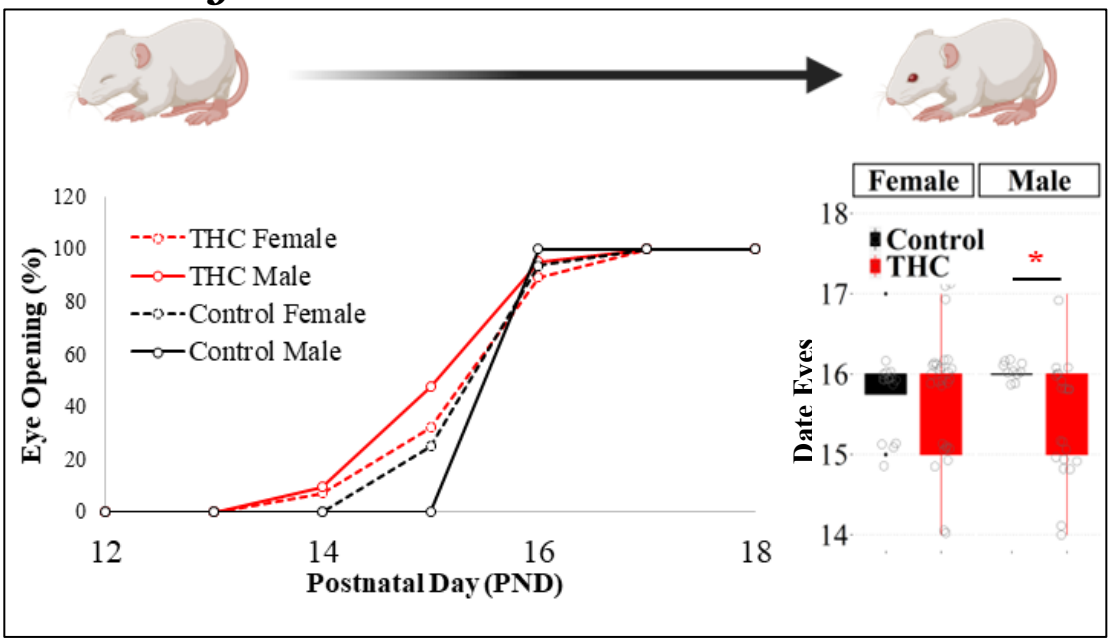

Figure 6.3 *Male animals exposed to THC in utero opened their eyes earlier than cage control animals. Created with Biorender.*

The dates of pup eye opening were significantly earlier in THC exposed males compared with cage control males (Levene's adjusted p = 0.004, t independent samples t-test, Figure 6.3). There was no significant change between female animals exposed prenatally to THC relative to cage controls. Of the four THC exposed litters used in this study, three of them were born on GD21, with the last being born on GD 22. During adolescence there was no change in the amount of time spent investigating an object in a novel location relative to a familiar condition in either male or female animals (Figure 6.4). For this study a litter n of 3

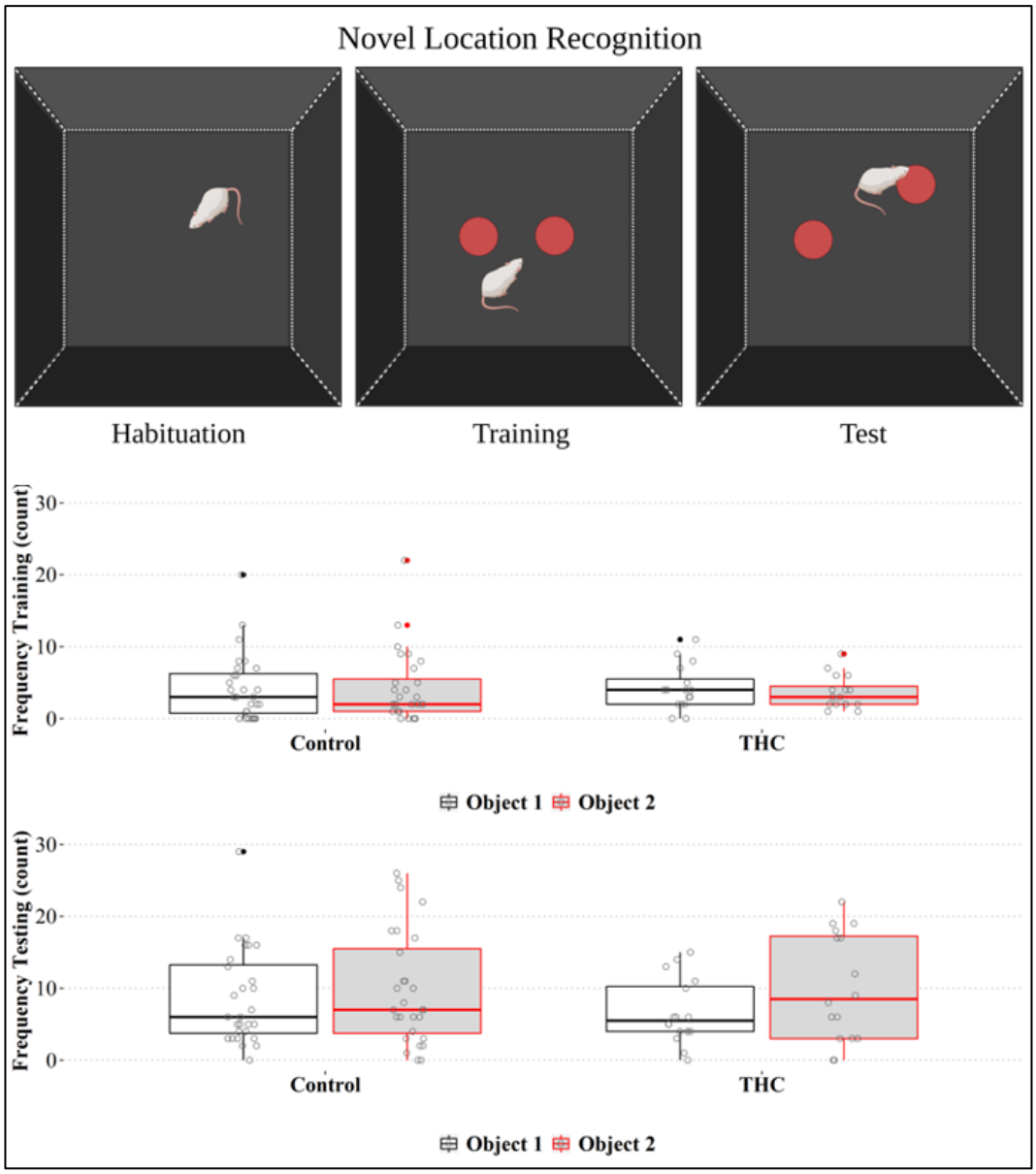

Figure 6.4 *No change in novel location recognition in either male or female rats with prenatal exposure to THC. Created with Biorender.*

and an animal n of 10-16 was used per sex per group. No significant sex effects were found and so the data was pooled.

6.4.3 There are sex differences in the endocannabinoid component of the 10 Hz but not 1 Hz LTD paradigms

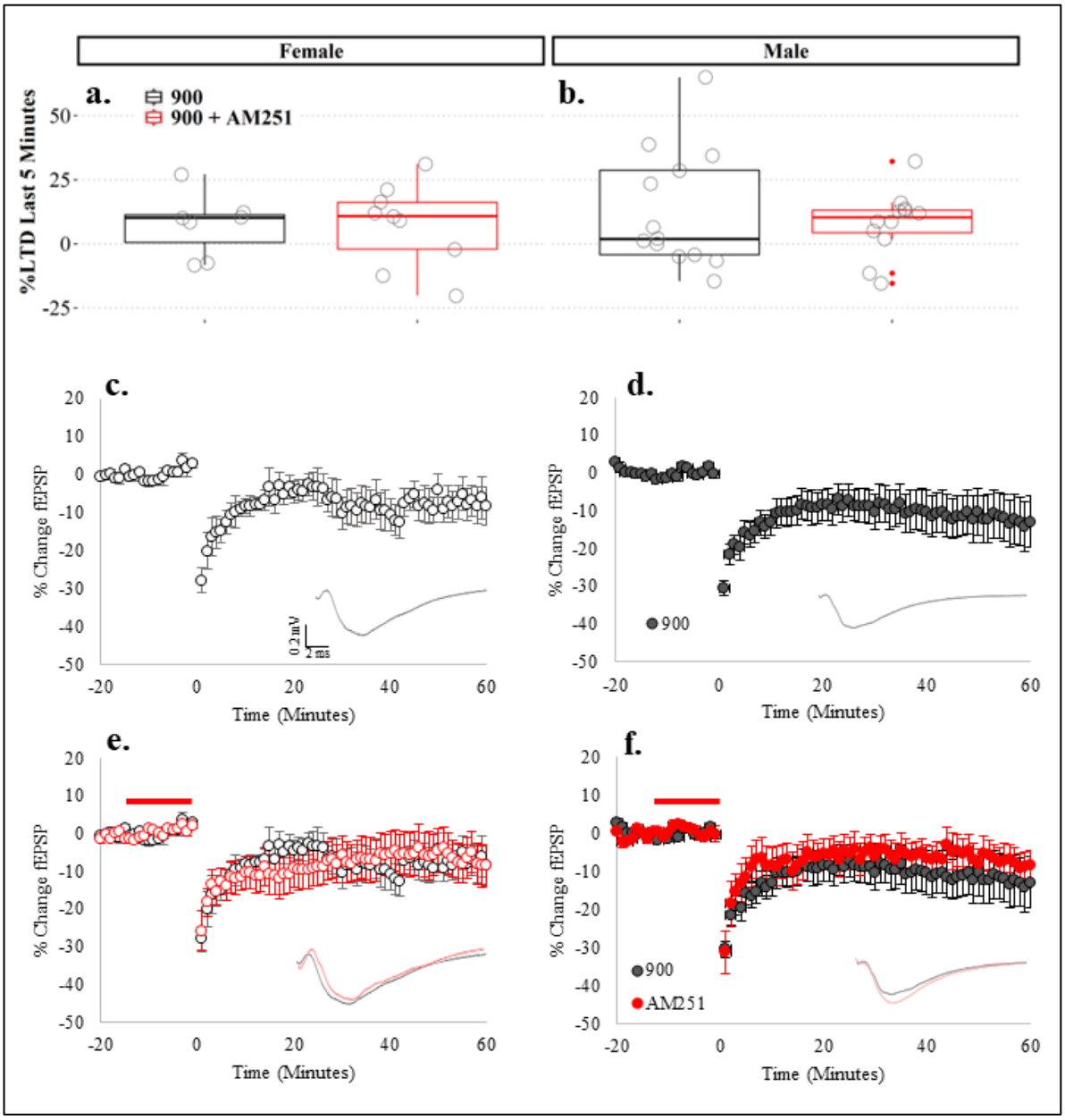

Figure 6.5 *900 x 1 Hz LTD is not eCB dependent in either male (b, d, f) or female (a, c, e) animals*

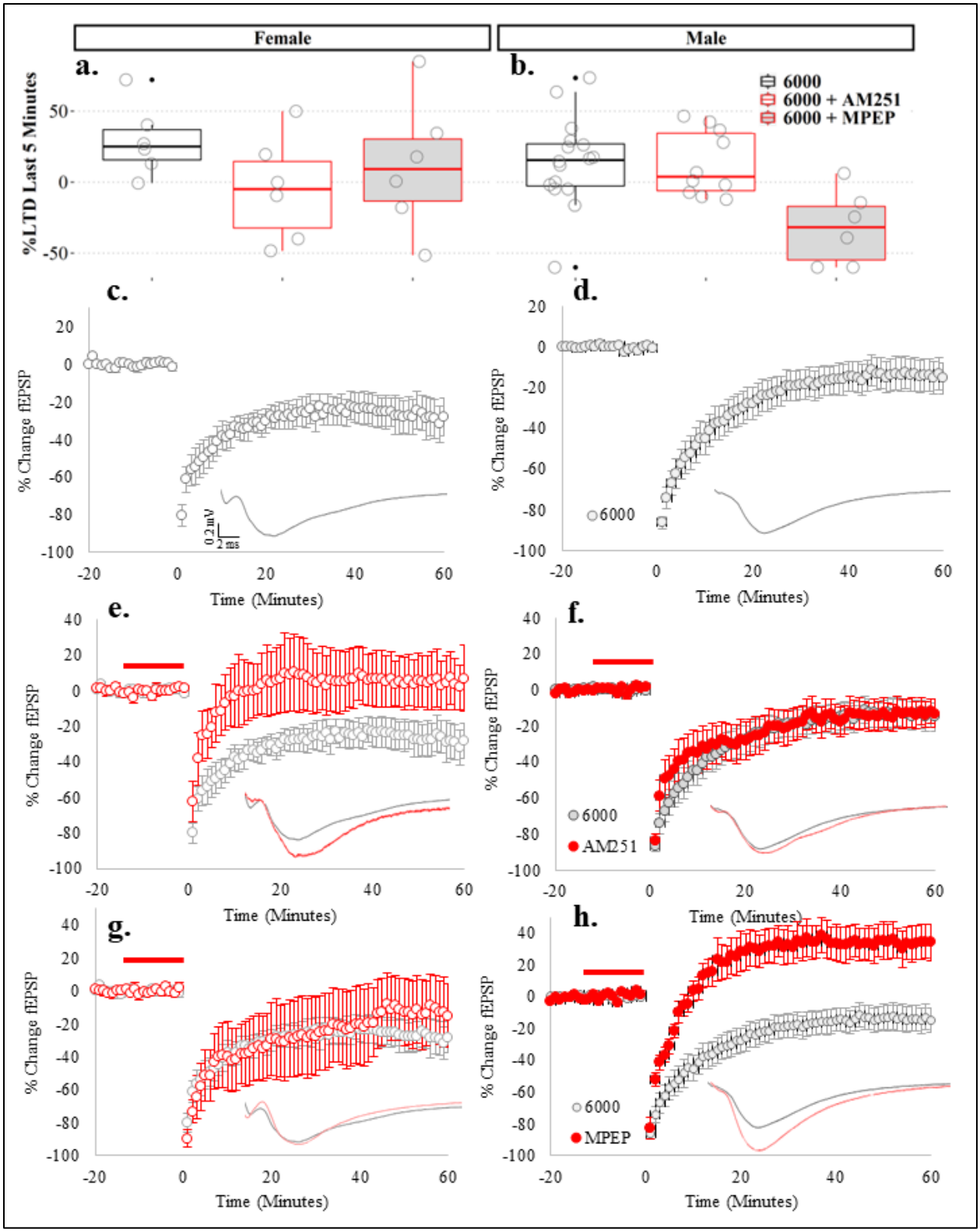

Figure 6.6 *6000 x 10 Hz LTD is eCB dependent in females (a, c, e, g) and mGluR dependent in males (b, d, f, h)*

6.4.3.1 1 Hz

In the 1 Hz protocol in males, an animal n of 9 and a slice n of 13 was used to assess LTD. With slices that did not depress included in the dataset, 13.12% LTD was observed (Figure 6.5 d). With bath application of the CB1 inverse agonist AM251, there was no significant change in the amount of observed LTD (slice n = 11, animal n = 6, average LTD = 8.10%, Figure 6.5 b, f). In female animals, only 7.56% of LTD was observed in the 1 Hz paradigm (slice n = 7, animal n = 4, Figure 6.5 c). With the application of AM251, there was similarly no difference in the amount of LTD (7.35%, slice n = 9, animal n = 9 Figure 6.5 a, c).

6.4.3.2 10 Hz

The 10 Hz protocol was endocannabinoid dependent in females but not males (Figure 6.6). Females showed 37.20% LTD with no drug applied (slice n = 6, animal n = 5), and this shrank to -4.78% ($p = 0.046$, Levene's = variance equal, independent samples t-test, slice n = 6, animal n = 6, Figure 6.6 a, c, e) when AM251 was applied for the last 15 minutes of pre-conditioning and during protocol. Males showed 14.01% LTD (slice n = 16, animal n = 10), and 12.93% LTD with AM251 (slice n = 10, animal n = 7, Figure 6.6 b, d, f). Because metabotropic glutamate receptors also communicate with the eCB system, an experiment with a bath application of MPEP was also performed. In females there was no significant change in the amount of LTD, at 12.07% (slice n = 6, animal n = 4, Figure 6.6 a, g), but in males the application of MPEP blocked LTD to reveal LTP ($p = 0.007$, Levene's correction applied, independent samples t-test, slice n = 7, animal n = 4, Figure 6.6 b, h).

6.4.4 THC exposed males showed a decrease in the amount of LTD but all THC exposed animals showed a decrease in the efficacy of LTD induction

6.4.4.1 Slice characteristics

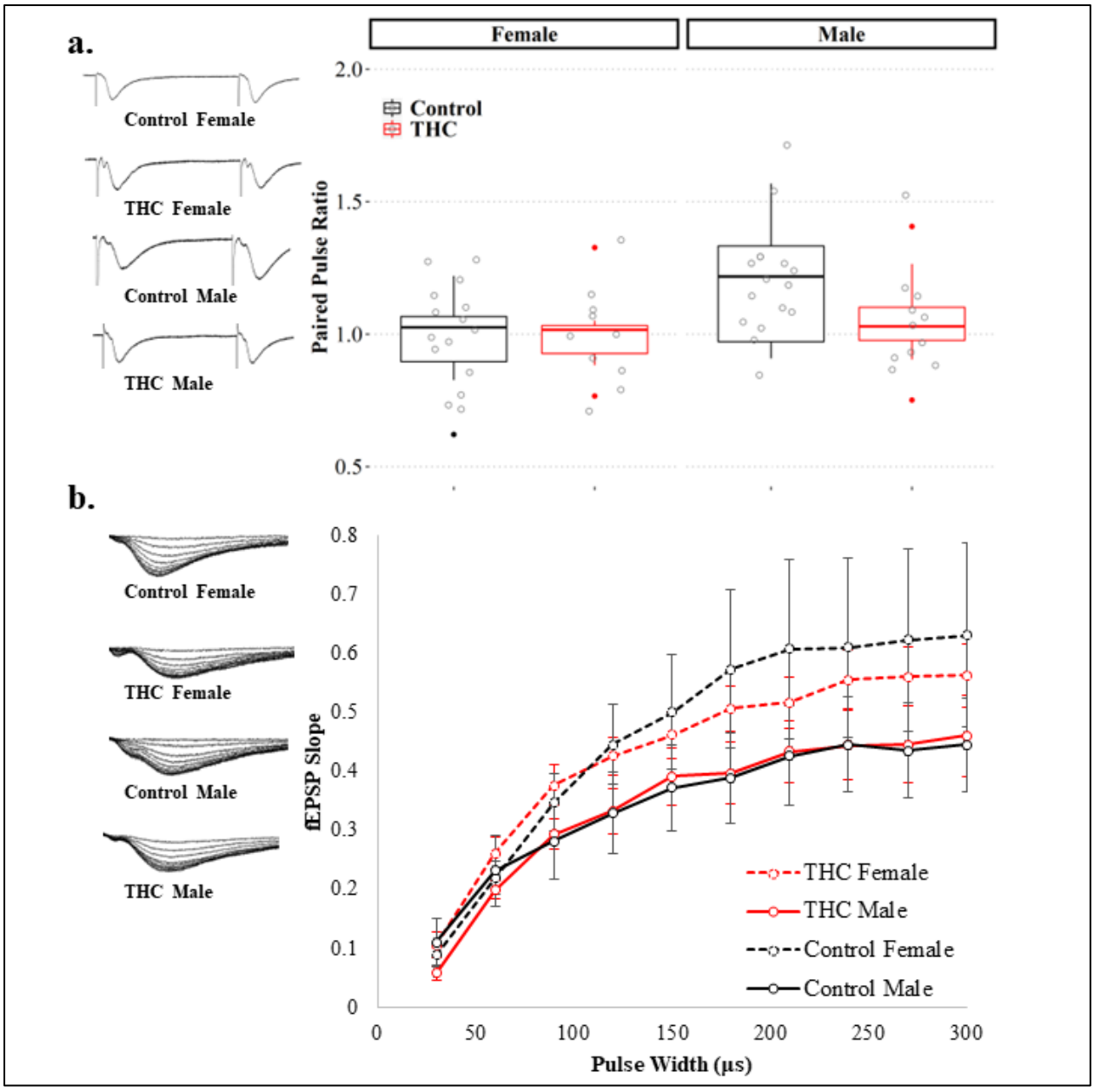

Figure 6.7 *Paired-pulse and input/output ratios are not affected by prenatal THC exposure. A. paired-pulse representative traces and graph b. input/output representative traces and graph. Two-tailed t-test performed in SPSS.*

In the paired-pulse ratio measurements, there was a significant effect of sex ($p = 0.013$, Figure 6.7 a). In the males, there was a trend towards a decrease ($p = 0.067$), from the control to the prenatal THC exposed group but it did not meet the threshold of significance (Figure 6.7 a). There were no significant differences observed in the input output curves between any groups (Figure 6.7 b).

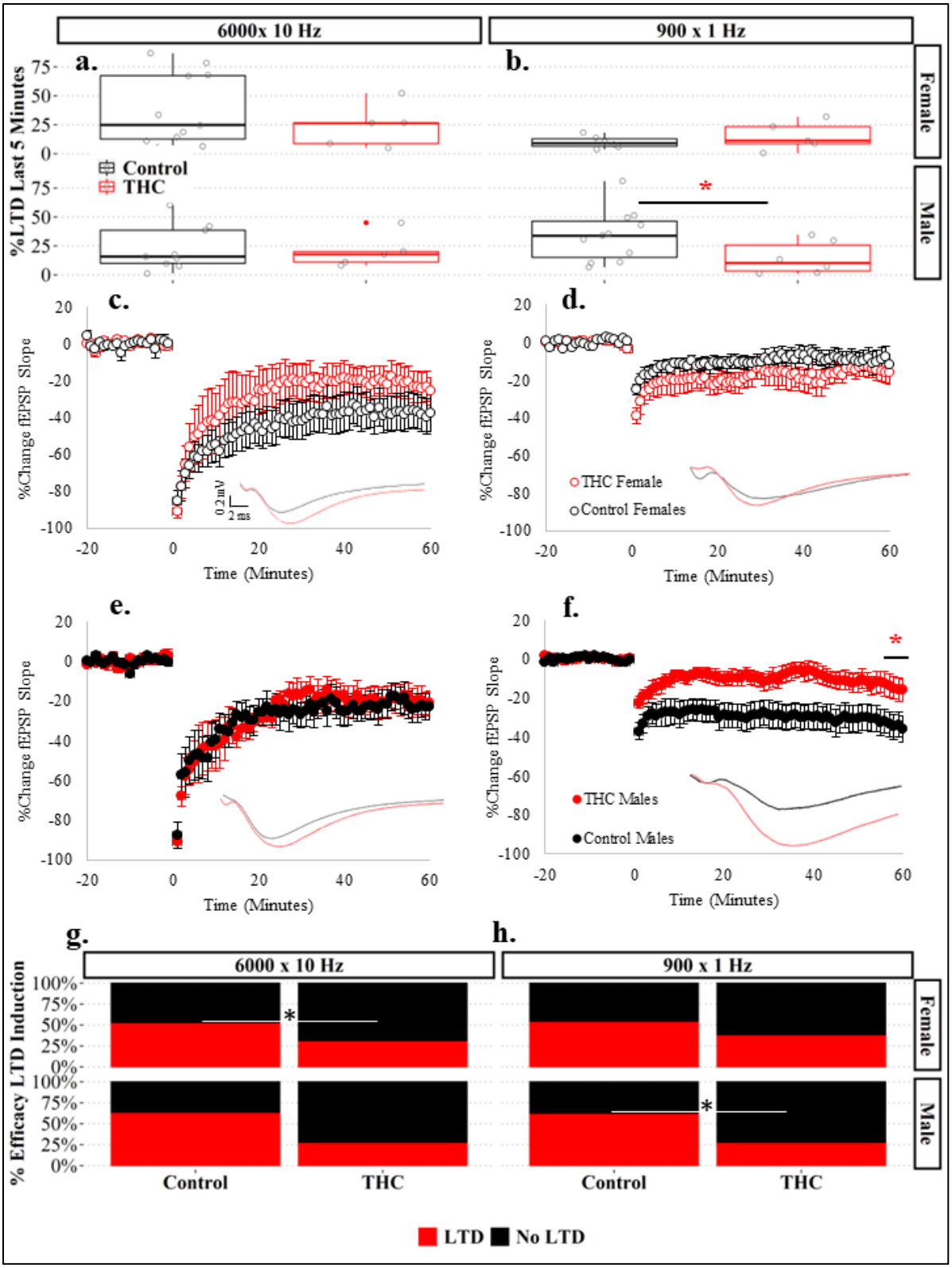

Figure 6.8 *900 x 1Hz and 6000 x 10 Hz LTD in prenatal THC exposed animals. a, c, e, g trend towards deficit in females (c, open circles) but not the males (e, closed circles) in the 6000 x 10 Hz paradigm however females show deficit in slice LTD induction success rate (g). b, d, f, h deficit in males (f) but not females (d) in the 900 x 1 Hz protocol where males also show a deficit in slice success rate (h).*

6.4.4.2 10 Hz

Because male and female animals responded to the drug differentially, they were assessed separately here. In this experiment, the ability to induce LTD and the magnitude of LTD were assessed separately. Females showed no differences in the amount 6000 x 10 Hz LTD in vehicle exposed (36.62%, slice n = 11, animal n = 8) relative to THC exposed (23.81%, slice n = 5, animal n = 3, Figure 6.8 a, c). The animal n for the THC exposed animals was 5, however, only slices from three animals depressed. There was a significant difference in the efficacy of LTD induction in these females ($p = 0.030$, Figure 6.8 a, g). Males showed no change in the amount of LTD in the control group (23.07%, slice n = 9, animal n = 5), compared with the prenatally exposed group (20.40%, slice n = 5, animal n = 4, Figure 6.8 e). There was no significant decrease in the efficacy of LTD induction in the males (Figure 6.8 g).

6.4.4.3 1 Hz

In the 900 x 1 Hz LTD experiment there were no significant differences between the control females (9.98%, slice n = 6, animal n = 6) compared with THC exposed females (15.12%, slice n = 5, animal n = 4, Figure 6.7 b, d) as well as no change between the efficacy of LTD induction (Figure 6.7 h). In the males however showed a significant decrease in the amount of LTD ($p = 0.049$) in controls (33.85%, slice n = 11, animal n = 9), compared with THC exposed (14.65%, slice n = 6, animal n = 5, Figure 6.7 b, f). There was also a significant decrease in the efficacy of LTD induction in the males ($p = 0.05$, Figure 6.7 h).

6.4.5 Prenatal THC exposed animals showed a difference in cannabinoid receptor size, cannabinoid receptor localization, and the ratio of large to small gephyrin clusters in a sex dependent manner.

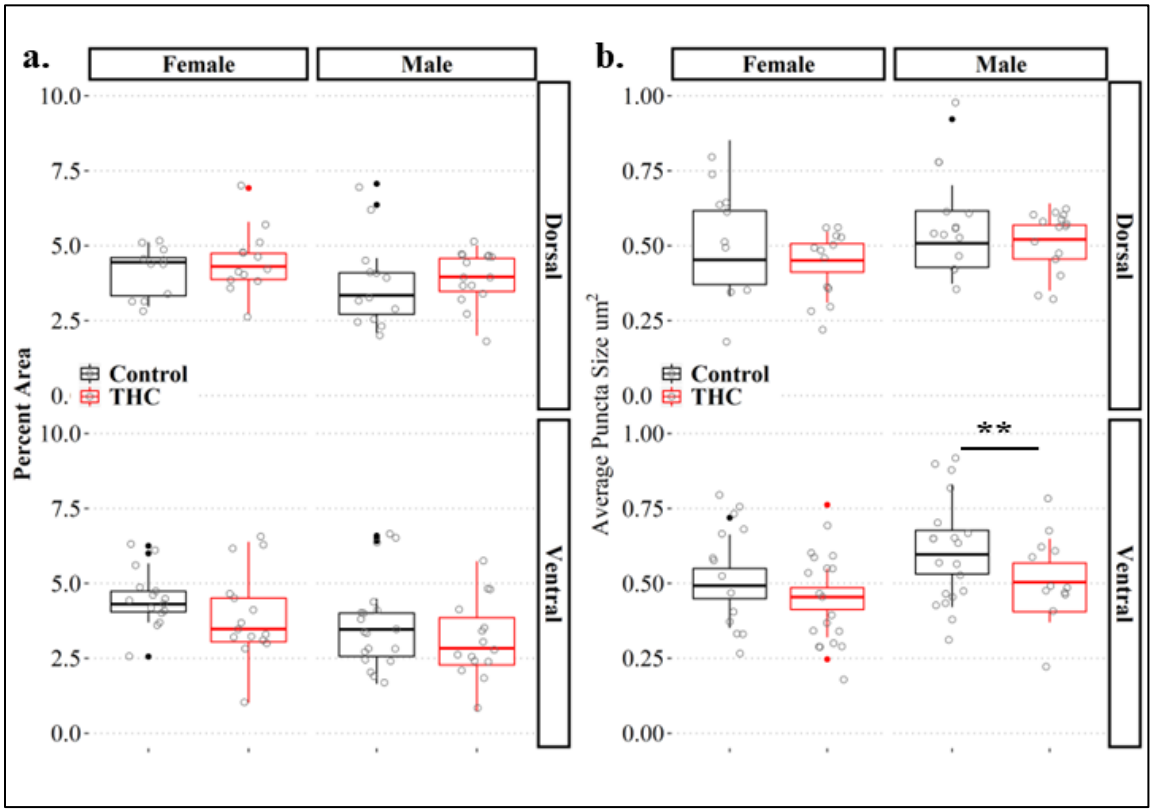

Figure 6.9 CB1 receptor area and size. Average puncta size is decreased in the ventral hippocampus of male animals.

CB1 receptor density (as measured by percent area) was not altered across any of the groups (Figure 6.8 a). However, in the average puncta size was decreased in a region and sex dependant manner (Figure 6.8 b). In males prenatally exposed to THC, there was a significant reduction ($p = 0.009$) in CB1 puncta size compared with the control group (Figure 6.8 b). Interestingly, in general control male animals had larger CB1 puncta clusters relative to THC male animals ($p = 0.007$).

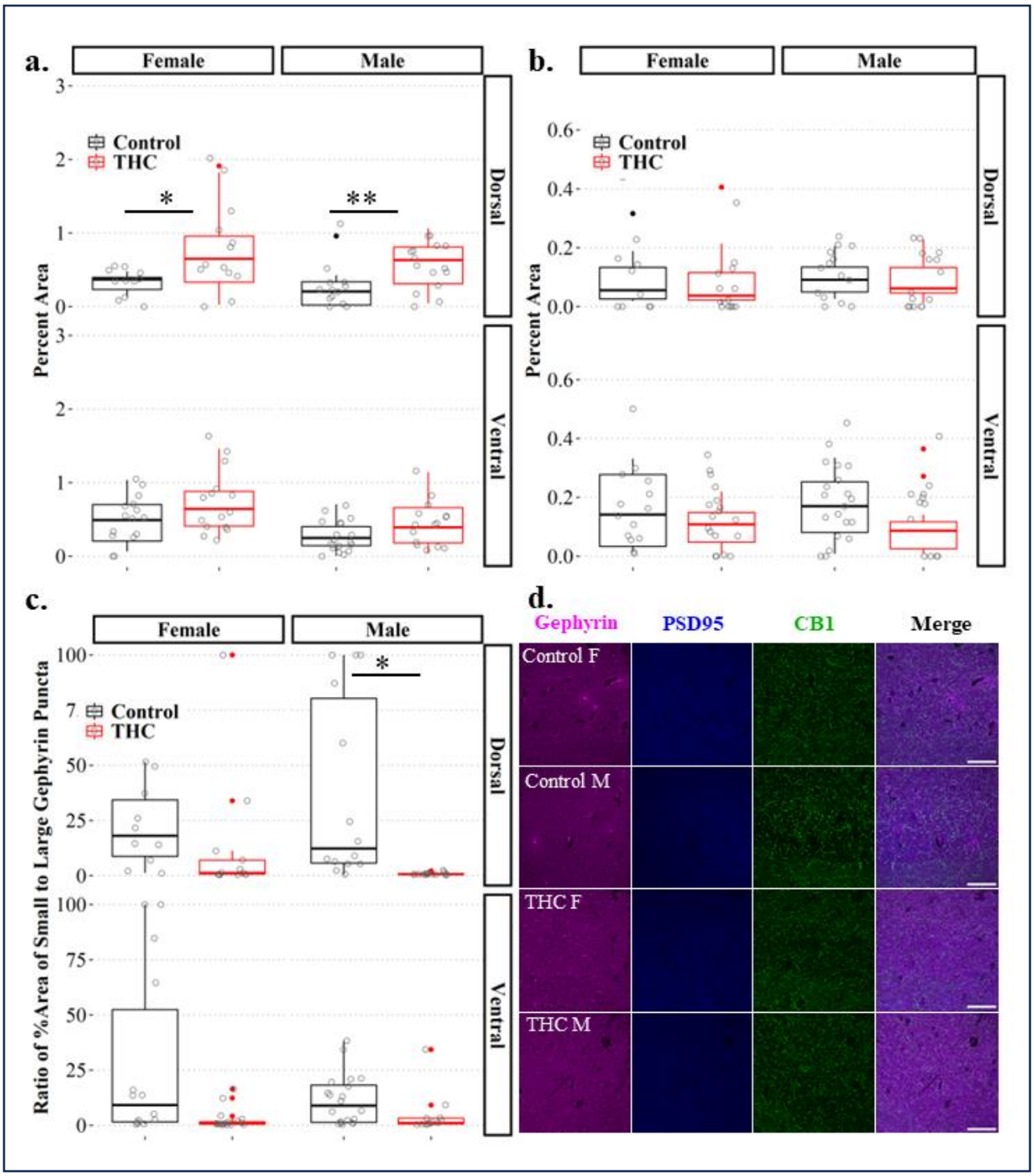

Figure 6.10 Co-localization of CB1 with gephyrin and PSD95. A. increase in the co-localization of CB1 with gephyrin in the dorsal but not ventral hippocampus of male and female animals. b. no change in the co-localization of PSD95 with CB1. c. Ratio of area covered by small or large gephyrin puncta.

When comparing receptor co-localisation between CB1 and gephyrin, a significant increase was observed in prenatal THC animals in both females ($p = 0.016$), and males ($p = 0.002$) compared with control animals in the dorsal dentate gyrus (Figure 6.9 a). A similar trend was observed ventrally, however did not meet the statistical threshold (female $p = 0.077$, male $p = 0.079$). There were no significant differences observed in receptor co-localization between PSD95 and CB1 in any cases. The relative ratio of large to small gephyrin clusters was found to be decreased in the dorsal dentate gyrus of males ($p = 0.041$), with a similar, non-significant trend observed in the ventral dentate gyrus of females ($p = 0.057$, Figure 6.9 c).

6.4.6 Prenatal THC exposed animals show an increase in dendritic spines

An omnibus ANOVA revealed a significant effect of treatment ($p<0.001$) as well as sex ($p = 0.005$). As such male and female animals were analysed separately. Both male and female animals showed a significant increase in the density of dendritic spines (male $p < 0.001$, female $p = 0.009$). However, when assessing the different spine morphologies, only females showed a decrease in the density of mushroom ($p = 0.013$) and filipodia ($p = 0.023$). Both males and females showed an increase in the density of stubby spines (male $p > 0.001$, female $p = 0.003$).

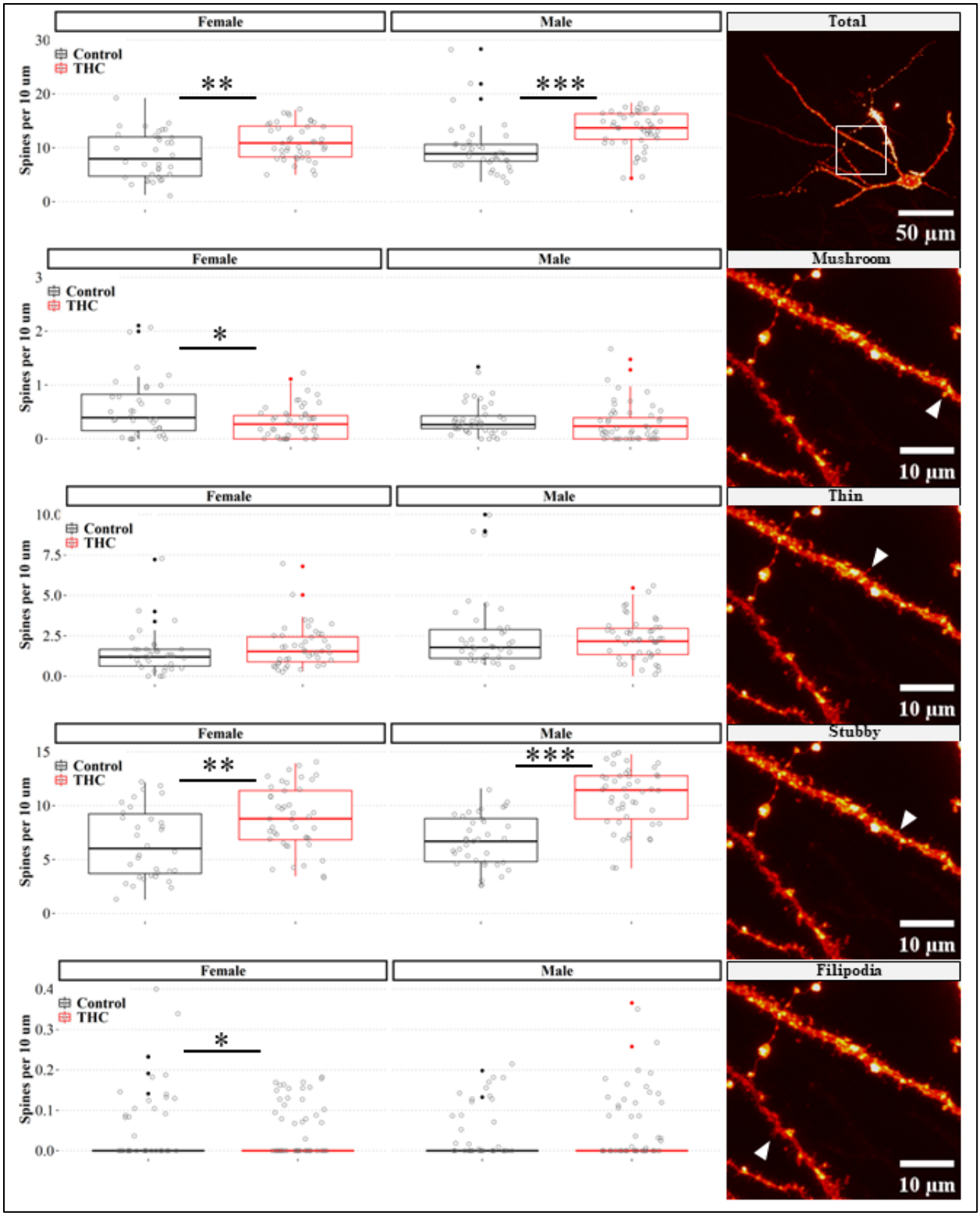

Figure 6.11 *Dendritic spines are altered with prenatal THC exposure. Increase observed in spine density in male and female animals, predominantly from an increase in stubby spines. Females also show a decrease in filipodia and mushroom spines.*

6.5 Discussion

This study investigated synaptic plasticity and receptor co-localization in a rat model of prenatal THC exposure. These results are sex and region dependent, and some underlying differences in male and female brains were elucidated. This prenatal THC exposure paradigm was designed to approximately reflect a population who smokes one joint per day (254). Interestingly, no obvious behavioural deficits in the dams were observed. However, only hypolocomotion, one of the four elements of the cannabinoid tetrad, was studied. The other three are analgesia, catalepsy, and hypothermia, which were not assessed to minimize maternal stress (255). Interestingly, the male pups opened their eyes significantly earlier. This is likely due to the premature birth that was observed. This premature birth is like what is seen in human studies of prenatal cannabis exposure, and the sex differences seen follow the trend where male animals are affected more strongly by teratogens than female animals (237,256).

The endocannabinoid component of 900 x 1 Hz LTD was first studied in our lab by Dr. Christine Fontaine (6). Her study found that there was an eCB component of this LTD type while this study did not. Interestingly, her study used adolescent males (~p20s) while this study assessed adult male and female animals (6). This suggests the possibility that the strategy used to induce this type of depression may change over the course of the lifespan. Similarly, males did not show a direct effect of antagonizing the CB1 receptor on LTD. MPEP, which caused potentiation in males during the 6000 x 10 Hz protocol, is a negative allosteric modulator of the metabotropic glutamate receptor 5 (mGluR5), meaning that MPEP binds to the receptor at a separate cite than endogenous ligands and causes a conformational change that decreases receptor affinity for its

substrate (257). Therefore, MPEP is expected to decrease the mGluR's affinity for glutamate. This receptor subclass is often found post-synaptically on excitatory and inhibitory neurons, as well as presynaptically on excitatory neurons (258). Under normal conditions mGluR activation would be theorized to cause depression by stimulating the production of endocannabinoids, which would travel in retrograde across the synapse, activating CB1 receptors and thus decreasing transmitter release. However, that is only if excitatory cells are considered. Given that these results (Figure 6.9 a and b) support the literature in that more cannabinoid receptors are involved with inhibitory synapse relative or excitatory synapses, a different model must be considered. In general, the same mGluR signalling pathway applies, where postsynaptic receptor activation leads to the suppression of presynaptic neurotransmitter release. The difference is that the neurotransmitter whose release is being suppressed is GABA. So, more GABA release at inhibitory synapses would lead to a suppression of that release though CB1 receptors on the presynaptic terminal. Similarly on excitatory CB1 containing synapses, mGluR activation by glutamate would lead to a negative feedback loop where less glutamate is released. An important point to consider with the former inhibitory synapses, is that they generally do not release glutamate. And yet mGluR1/5 receptors are found there. This indicates that it likely acts as a coincidence detector of glutamate spill over from neighbouring synapses. However, none of this explains how mGluR activation prevents the induction of LTD, and indeed causes potentiation. It could be that the feedback loop that exists on excitatory synapses is the form primarily affected, and that it works in a way that is independent of CB1 receptors. More interestingly, these differential effects could be the product of differential activation of the CB1 receptor under different ligand concentrations. The CB1 receptor has been

shown to have ligand bias with agonists of different affinities, and couple with different G protein effectors so it is possible that the effect of MPEP is from decreasing the level of endogenous cannabinoids such that the very low ligand concentration is leading to a homeostatic mechanism of upregulation.

The female animals showed a 6000 x 10 Hz LTD that trended towards showing an endocannabinoid dependent phenotype. The fact that there was no trend with MPEP application suggests that in females, the mechanism of LTD in the 6000 x 10 Hz protocol is from the production of eCBs from high intracellular calcium concentrations instead of from the mGluR receptor. This could explain the trend towards a decrease shown in female animals prenatally exposed to THC. Female animals showed increased variability relative to male animals, an effect likely caused by the oestrous cycle. Interestingly, the female animals showed a decreased efficacy of LTD induction in THC exposed animals relative to controls.

Male animals exposed to THC showed a significant decrease in the 900 x 1 HZ LTD, and a decrease in the efficacy of inducing this LTD.

Endocannabinoid induced inhibitory LTD (iLTD) is known to be correlated with a decrease in CB1 receptor cluster bouton size. In the ventral hippocampus of males, a decrease in CB1 size was observed in males prenatally exposed to THC. Further in both male and female animals there was an increase in the co-localization of CB1 receptors with gephyrin. This supports the hypothesis that chronic THC exposure during development causes increased excitation, mediated by interneurons prior to the turning of the GABA switch. The classic dogma that “neurons that fire together wire together” suggests that an increased amount of excitatory connection via the property of GABA as

excitatory during development did indeed lead to an increased amount of interneuron wiring in this model (259). The increased ratio of larger GABAergic boutons, as indicated by larger gephyrin clusters, related to smaller ones, also supports this hypothesis (260).

As for dendritic spines, an increase in spines is sensical relative to what is already known in the field; being that children exposed to THC prenatally show symptoms of ADHD and autism, and that in ADHD and autistic brains show an increase in dendritic spines (216,261,262). The fact that the type of spine that is increased in the stubby subtype is also interesting. While dendritic spines are plastic, the head to neck ratio determines much of their physiological characteristics, and stubby spines are not as selective regarding which signals get propagated compared with mushroom spines (263). This finding suggests that the increase in spines with lower signal fidelity could be a mechanism of alteration.

Together these data show that the endocannabinoid system is dysregulated after prenatal THC exposure caused by an increase in the number of excitatory synapses, and that these receptor changes are correlated with deficits in synaptic plasticity.

6.6 Conclusions

In conclusion, the results of this study demonstrate sex and region- dependent effects of prenatal THC exposure on synaptic plasticity and receptor co-localization. Despite no apparent behavioural deficits in the dams, premature birth was observed, with pre-mature eye opening in male pups. The 900 x 1 Hz LTD study did not show an endocannabinoid-dependant component in either male or female animals, however

most previous studies assayed adolescent animals while here we assayed adults, suggesting potential developmental differences in the strategy for inducing this form of depression. In the 6000 x 10 Hz experiment, females but not males' results suggested an endocannabinoid component. The involvement of mGluRs was explored, and it was observed that mGluR1/5 activation led to potentiation instead of depression, possibly through a CB1 autonomous mechanism. Prenatal THC exposure resulted in decreased 1 Hz LTD and decreased efficacy of 10 Hz LTD induction, while female showed deficits only in the induction of 10 Hz LTD, but not its magnitude. Furthermore, THC exposed males exhibited a reduction in CB1 puncta size in a region-specific manner, and both sexes showed an increase of CB1 gephyrin co-localization in a region-dependent manner. This study suggests that the endocannabinoid system is dysregulated even in adulthood following prenatal THC exposure, and this dysregulation has consequences for synaptic plasticity.

CHAPTER 7

Conclusions

7.1 Synthesis of results

In this dissertation, I examined the overarching effects of prenatal cannabis exposure on the developing hippocampus, with special interest paid to the inhibitory aspect of this brain region. In chapter 2, I highlighted the lack of studies in prenatal cannabis exposure in the hippocampus. The rest of my dissertation has been spent trying to fill those research gaps using a combination of field electrophysiology, immunohistochemistry, and behavioural assays.

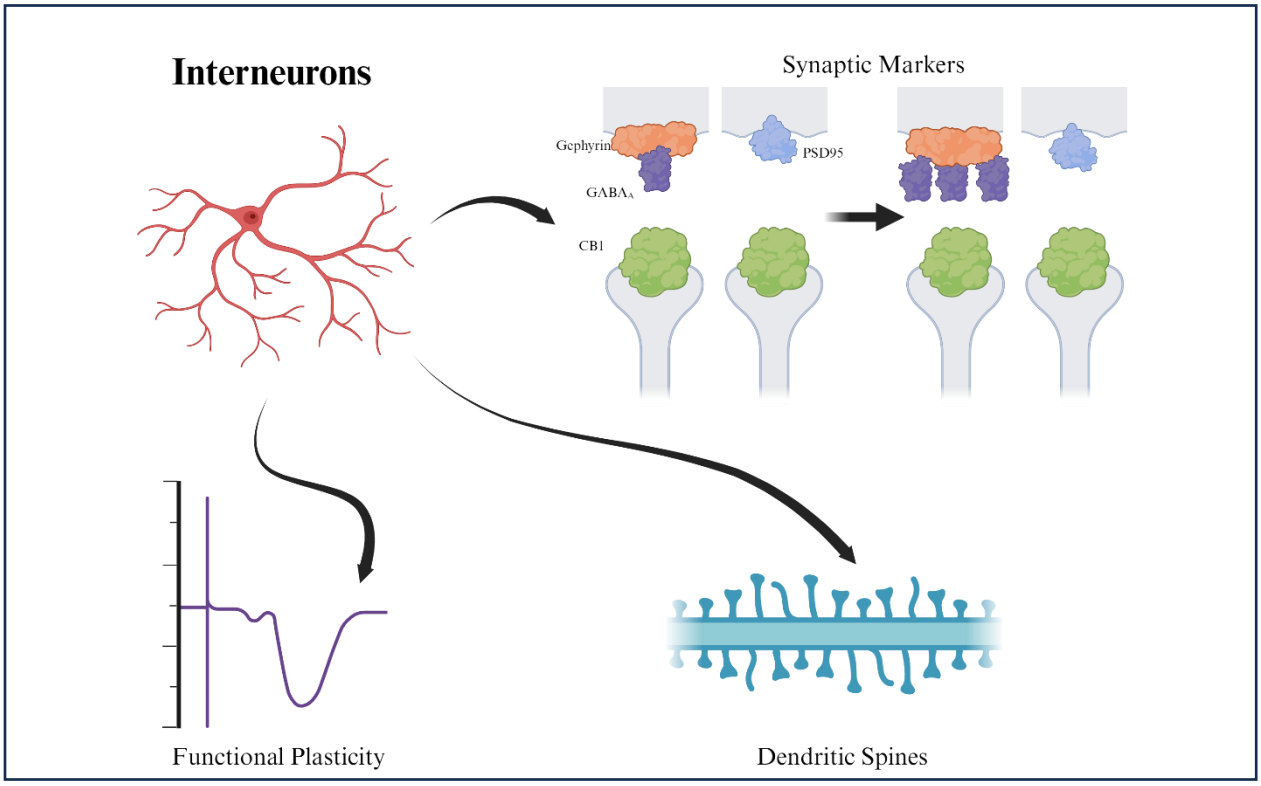

Figure 7.1 *Interneurons densities do not change appreciably during adulthood, and so likely are a driving effector of changes in synaptic markers, functional plasticity, and dendritic spine density.*

Prenatal THC exposure was found to lead to a reduction in the number of inhibitory interneurons in a region and sex-specific manner, highlighting the importance of studying sex differences in the brain. Inhibitory interneurons play an important role in the maintenance of the inhibitory/ excitatory balance of the brain, and so alterations of their numbers are likely to disrupt that balance. The change in E/I balance was further investigated in chapter 6, where functional differences in slice recordings were contrasted with co-localization of CB1 with inhibitory and excitatory markers. Because the endocannabinoid system is so intertwined with neuroinflammation, microglia were also assayed and found to be altered.

All of these findings revolve around the CB1 receptor, and what happens when it is activated exogenously during development. The decrease of interneurons in the dorsal but no change or increase in the ventral suggest that the CB1 receptor's role in cell migration is impacted by prenatal cannabis exposure. The microglia studies suggest that aberrant CB1 receptor activation could lead to excitotoxicity- leaving microglia in the adult brain with the lasting changes of experiencing inflammatory insult. It could also indicate that the altered CB1 receptors lead to altered eCB levels, affecting the signalling to microglia. The synaptic plasticity and receptor studies indicate that the combination of the prenatal GABA switch, and downregulation of CB1 receptors around the time when the brain is wiring up are indeed what is happening, and that extra GABAergic connections are created, altering the E/I balance in the brain and inhibiting synaptic plasticity. Further, these results suggest that more functional GABAA receptor clusters exist in animals prenatally exposed to THC. Given that receptors density, functional plasticity, and dendritic spines have all been shown to be changeable, much more so

than interneuron cell densities, it is likely that the early effects of prenatal THC exposure act on interneurons which then impact these other measures. Together these results show that prenatal THC exposure has long lasting consequences in the hippocampus that persist into adulthood.

7.2 Limitations

The interneuron studies were limited by the nature of the study design, specifically in that they are snapshots of what is happening in the adult brain and do not yield causative results. The microglia study was limited by the lack of western blot results to fully characterize the phenotype, and by the fact that cell density is not known. Some electrophysiology experiments are limited by low slice numbers. The model of prenatal THC exposure only exposes animals to a known quantity of THC but does not assess how much THC is metabolized. The maternal behaviour study should be run separately to animal generation so that the full cannabinoid tetrad can be performed. The receptor studies are limited by the variable nature of puncta analysis, although I think thresholding relative to the images own histogram was helpful with this. This work would benefit from a control genetic models where the CB1 receptor could be modulated independently of THC administration, to confirm that the results seen are not a result of any binding with the CB2 receptor or other off-target effects.

7.3 Future Directions

The questions answered in these studies have opened the door to many new questions. In no particular order future studies should assess the cannabinoid tetrad in pregnant dams, the amount of THC metabolites in the pregnant dams, the amount of endogenous cannabinoids in the offspring, the survival of interneurons across the lifespan, interneuron migration, the impacts on adult neurogenesis, the inflammatory profiles of microglia, microglia's ability to respond to immune challenge, the specific characteristics of interneurons using patch clamping, the reason for the MPEP potentiation should be further investigated. Finally, drug studies of treatments such as anti-epileptics should be done to assess if postnatal intervention can ameliorate the phenotype.

References

1. Tortoriello G, Morris C V, Alpar A, Fuzik J, Shirran SL, Calvigioni D, et al. Miswiring the brain: Delta(9)-tetrahydrocannabinol disrupts cortical development by inducing an SCG10/stathmin-2 degradation pathway. EMBO J. 2014 Apr;33(7):668–85.

2. Saez TMM, Bessone IF, Rodriguez MS, Alloatti M, Otero MG, Cromberg LE, et al. Kinesin-1-mediated axonal transport of CB1 receptors is required for cannabinoid-dependent axonal growth and guidance. Dev Camb. 2020 Apr 1;147(8).

3. Amaya F, Shimosato G, Kawasaki Y, Hashimoto S, Tanaka Y, Ji RR, et al. Induction of CB1 cannabinoid receptor by inflammation in primary afferent neurons facilitates antihyperalgesic effect of peripheral CB1 agonist. PAIN. 2006 Sep;124(1–2):175–83.

4. De Meij J, Alfanek Z, Morel L, Decoeur F, Leyrolle Q, Picard K, et al. Microglial Cannabinoid Type 1 Receptor Regulates Brain Inflammation in a Sex-Specific Manner. Cannabis Cannabinoid Res. 2021 Dec;6(6):488–507.

5. Monday HR, Bourdenx M, Jordan BA, Castillo PE. CB1-receptor-mediated inhibitory LTD triggers presynaptic remodeling via protein synthesis and ubiquitination. Westbrook GL, Schuman EM, editors. eLife. 2020 Sep 9;9:e54812.

6. Fontaine CJ, Gräfe EL, Pinar C, Bonilla-Del Río I, Grandes P, Christie BR. Endocannabinoid receptors contribute significantly to multiple forms of long-term depression in the rat dentate gyrus. Learn Mem. 2020 Sep;27(9):380–9.

7. Andersen P, Morris R, Amaral D, Bliss T, O'Keefe J. The Hippocampus Book. Oxford: Oxford University Press; 2007. 832 p.

8. Petersen RP, Moradpour F, Eadie BD, Shin JD, Kannangara TS, Delaney KR, et al. Electrophysiological identification of medial and lateral perforant path inputs to the dentate gyrus. Neuroscience. 2013 Nov;252:154–68.

9. Hunsaker MR, Mooy GG, Swift JS, Kesner RP. Dissociations of the medial and lateral perforant path projections into dorsal DG, CA3, and CA1 for spatial and nonspatial (visual object) information processing. Behav Neurosci. 2007 Aug;121(4):742–50.

10. Cassel JC, Duconseille E, Jeltsch H, Will B. THE FIMBRIA-FORNIX/CINGULAR BUNDLE PATHWAYS: A REVIEW OF NEUROCHEMICAL AND BEHAVIOURAL APPROACHES USING LESIONS AND TRANSPLANTATION TECHNIQUES. Prog Neurobiol. 1997 Apr 1;51(6):663–716.

11. Vann SD. Dismantling the Papez circuit for memory in rats. Eichenbaum H, editor. eLife. 2013 Jun 25;2:e00736.

12. Lu HC, Mackie K. Review of the Endocannabinoid System. Biol Psychiatry Cogn Neurosci Neuroimaging. 2021 Jun;6(6):607–15.

13. Tsuboi K, Okamoto Y, Ikematsu N, Inoue M, Shimizu Y, Uyama T, et al. Enzymatic formation of N-acylethanolamines from N-acylethanolamine plasmalogen through N-acylphosphatidylethanolamine-hydrolyzing phospholipase D-dependent and -independent pathways. Biochim Biophys Acta. 2011 Oct;1811(10):565–77.

14. Yin A qi, Wang F, Zhang X. Integrating endocannabinoid signaling in the regulation of anxiety and depression. Acta Pharmacol Sin. 2019 Mar;40(3):336–41.

15. Schurman LD, Carper MC, Moncayo LV, Ogasawara D, Richardson K, Yu L, et al. Diacylglycerol Lipase-Alpha Regulates Hippocampal-Dependent Learning and Memory Processes in Mice. J Neurosci Off J Soc Neurosci. 2019 Jul;39(30):5949–65.

16. Shin M, Ware TB, Hsu KL. DAGL-Beta Functions as a PUFA-Specific Triacylglycerol Lipase in Macrophages. Cell Chem Biol. 2020 Mar 19;27(3):314-321.e5.

17. Pandey R, Mousawy K, Nagarkatti M, Nagarkatti P. Endocannabinoids and immune regulation. Pharmacol Res Off J Ital Pharmacol Soc. 2009 Aug;60(2):85–92.

18. Pelkey KA, Chittajallu R, Craig MT, Tricoire L, Wester JC, McBain CJ. Hippocampal GABAergic Inhibitory Interneurons. Physiol Rev. 2017 Oct 1;97(4):1619–747.

19. Fishell G. Perspectives on the developmental origins of cortical interneuron diversity. Novartis Found Symp. 2007;288:21–35; discussion 35-44, 96–8.

20. Wichterle H, Turnbull DH, Nery S, Fishell G, Alvarez-Buylla A. In utero fate mapping reveals distinct migratory pathways and fates of neurons born in the mammalian basal forebrain. Dev Camb Engl. 2001;128(19):3759–71.

21. Mańko M, Bienvenu TC, Dalezios Y, Capogna M. Neurogliaform cells of amygdala: a source of slow phasic inhibition in the basolateral complex. J Physiol. 2012 Nov 15;590(Pt 22):5611–27.

22. Song ZH, Zhong M. CB1 Cannabinoid Receptor-Mediated Cell Migration. J Pharmacol Exp Ther. 2000 Jul 1;294(1):204–9.

23. Kawamura Y, Fukaya M, Maejima T, Yoshida T, Miura E, Watanabe M, et al. The CB1 cannabinoid receptor is the major cannabinoid receptor at excitatory presynaptic sites in the hippocampus and cerebellum. J Neurosci. 2006 Mar;26(11):2991–3001.

24. Tay TL, Savage JC, Hui CW, Bisht K, Tremblay MÈ. Microglia across the lifespan: from origin to function in brain development, plasticity and cognition. J Physiol. 2017;595(6):1929–45.

25. Grabon W, Rheims S, Smith J, Bodennec J, Belmeguenai A, Bezin L. CB2 receptor in the CNS: From immune and neuronal modulation to behavior. Neurosci Biobehav Rev. 2023 Jul 1;150:105226.

26. Toguri JT, Lehmann C, Laprairie RB, Szczesniak AM, Zhou J, Denovan-Wright EM, et al. Anti-inflammatory effects of cannabinoid CB2 receptor activation in endotoxin-induced uveitis. Br J Pharmacol. 2014;171(6):1448–61.

27. VanRyzin JW, Marquardt AE, Argue KJ, Vecchiarelli HA, Ashton SE, Arambula SE, et al. Microglial Phagocytosis of Newborn Cells Is Induced by Endocannabinoids and Sculpts Sex Differences in Juvenile Rat Social Play. Neuron. 2019 Apr;102(2):435-449.e6.

28. Nagarkatti P, Pandey R, Rieder SA, Hegde VL, Nagarkatti M. Cannabinoids as novel anti-inflammatory drugs. Future Med Chem. 2009 Oct;1(7):1333–49.

29. Christie BR, Abraham WC. Priming of associative long-term depression in the dentate gyrus by θ frequency synaptic activity. Neuron. 1992 Jul 1;9(1):79–84.

30. Foy MR. Long-term Depression (Hippocampus). In: Smelser NJ, Baltes PB, editors. International Encyclopedia of the Social & Behavioral Sciences [Internet]. Oxford: Pergamon; 2001 [cited 2023 May 28]. p. 9074–8. Available from: https://www.sciencedirect.com/science/article/pii/B0080430767034380

31. Reyes-García SE, Escobar ML. Calcineurin Participation in Hebbian and Homeostatic Plasticity Associated With Extinction. Front Cell Neurosci [Internet]. 2021 [cited 2023 May 28];15. Available from: https://www.frontiersin.org/articles/10.3389/fncel.2021.685838

32. Huse M, Kuriyan J. The Conformational Plasticity of Protein Kinases. Cell. 2002 May 3;109(3):275–82.

33. Ashby MC, De La Rue SA, Ralph GS, Uney J, Collingridge GL, Henley JM. Removal of AMPA Receptors (AMPARs) from Synapses Is Preceded by Transient Endocytosis of Extrasynaptic AMPARs. J Neurosci. 2004 Jun 2;24(22):5172–6.

34. Terry-McElrath YM, Patrick ME. Simultaneous Alcohol and Marijuana Use Among Young Adult Drinkers: Age-Specific Changes in Prevalence from 1977 to 2016. Alcohol-Clin Exp Res. 2018 Nov;42(11):2224–33.

35. Dunson DB, Colombo B, Baird DD. Changes with age in the level and duration of fertility in the menstrual cycle. Hum Reprod. 2002 May;17(5):1399–403.

36. Finer LB, Zolna MR. Shifts in intended and unintended pregnancies in the United States, 2001-2008. Am J Public Health. 2014 Feb;104 Suppl(Suppl 1):S43-8.

37. Chasnoff IJ, Landress HJ, Barrett ME. The Prevalence of Illicit-Drug or Alcohol Use during Pregnancy and Discrepancies in Mandatory Reporting in Pinellas County, Florida. N Engl J Med. 1990 Apr;322(17):1202–6.

38. Jackson KM, Sher KJ, Schulenberg JE. Conjoint developmental trajectories of young adult substance use. Alcohol Clin Exp Res. 2008;32(5):723–37.

39. Subbaraman MS, Kerr WC. Simultaneous versus concurrent use of alcohol and cannabis in the National Alcohol Survey. Alcohol Clin Exp Res. 2015 May;39(5):872–9.

40. Goldschmidt L, Richardson GA, Cornelius MD, Day NL. Prenatal marijuana and alcohol exposure and academic achievement at age 10. Neurotoxicol Teratol. 2004;26(4):521–32.

41. Government of Canada. Canadian Tobacco, Alcohol and Drugs Survey (CTADS): summary of results for 2017. 2017.

42. Goodfellow MJ, Lindquist DH. Significant Long-Term, But Not Short-Term, Hippocampal-Dependent Memory Impairment in Adult Rats Exposed to Alcohol in Early Postnatal Life. Dev Psychobiol. 2014 Sep;56(6):1316–26.

43. Livy DJ, Miller EK, Maier SE, West JR. Fetal alcohol exposure and temporal vulnerability: effects of binge-like alcohol exposure on the developing rat hippocampus. Neurotoxicol Teratol. 2003;25(4):447–58.

44. Kafaee Razavi M, Ebrahimpour S, Tehranipour M, Behnam Rasouli M. The investigation of the long-term effects of aquatic extraction of Cannabis sativa on spatial memory consolidation in Rats. Arak Med Univ J. 2010;13(2):125–33.

45. Wright NE, Maple KE, Lisdahl KM, Preedy VR. Effects of cannabis use on neurocognition in adolescents and emerging adults. In: Handbook of cannabis and related pathologies: Biology, pharmacology, diagnosis, and treatment. Elsevier Academic Press; 2017. p. 151–9.

46. May PA, Blankenship J, Marais AS, Gossage JP, Kalberg WO, Joubert B, et al. Maternal alcohol consumption producing fetal alcohol spectrum disorders (FASD): Quantity, frequency, and timing of drinking. Drug Alcohol Depend. 2013 Dec;133(2):502–12.

47. Riley EP, Infante MA, Warren KR, Court A, Diego S, Warren KR. Fetal Alcohol Spectrum Disorders: An Overview. 2011 Jun;21(2):73–80.

48. Renwick JH, Asker RL. Ethanol-sensitive times for the human conceptus. Early Hum Dev. 1983 Jul;8(2):99–111.

49. Brocardo PS, Gil-Mohapel J, Wortman R, Noonan A, McGinnis E, Patten AR, et al. The Effects of Ethanol Exposure During Distinct Periods of Brain Development on Oxidative Stress in the Adult Rat Brain. Alcohol Clin Exp Res. 2017 Jan;41(1):26–37.

50. Kleiber ML, Mantha K, Stringer RL, Singh SM. Neurodevelopmental alcohol exposure elicits long-term changes to gene expression that alter distinct molecular pathways dependent on timing of exposure. J Neurodev Disord. 2013 Mar;5.

51. Maier SE, Miller JA, Blackwell JM, West JR. Fetal alcohol exposure and temporal vulnerability: Regional differences in cell loss as a function of the timing of binge-like alcohol exposure during brain development. Alcohol-Clin Exp Res. 1999 Apr;23(4):726–34.

52. Hamilton GF, Murawski NJ, St.cyr SA, Jablonski SA, Schiffino FL, Stanton ME, et al. Neonatal alcohol exposure disrupts hippocampal neurogenesis and contextual fear conditioning in adult rats. Brain Res. 2011;1412:88–101.

53. Ikonomidou C, Bittigau P, Ishimaru MJ, Wozniak DF, Koch C, Genz K, et al. Ethanol-induced apoptotic neurodegeneration and fetal alcohol syndrome. Science. 2000 Feb;287(5455):1056–60.

54. Redila VA, Olson AK, Swann SE, Mohades G, Webber AJ, Weinberg J, et al. Hippocampal cell proliferation is reduced following prenatal ethanol exposure but can be rescued with voluntary exercise. HIPPOCAMPUS. 2006;16(3):305–11.

55. Bonthius DJ, West JR. Alcohol-induced neuronal loss in developing rats: increased brain damage with binge exposure. Alcohol Clin Exp Res. 1990 Feb;14(1):107–18.

56. Guerri C, Bazinet A, Riley EP. Foetal Alcohol Spectrum Disorders and alterations in brain and behaviour. Alcohol Alcohol Oxf Oxfs. 44(2):108–14.

57. Patten AR, Fontaine CJ, Christie BR. A comparison of the different animal models of fetal alcohol spectrum disorders and their use in studying complex behaviors. Front Pediatr. 2014 Jan;2(September):93.

58. Olney JW, Wozniak DF, Jevtovic-Todorovic V, Farber NB, Bittigau P, Ikonomidou C. Glutamate and GABA receptor dysfunction in the fetal alcohol syndrome. Neurotox Res. 2002;4(4):315.

59. Akerman CJ, Cline HT. Refining the roles of GABAergic signaling during neural circuit formation. Trends Neurosci. 2007;30(8):382–9.

60. Varaschin RK, Allen NA, Rosenberg MJ, Valenzuela CF, Savage DD. Prenatal Alcohol Exposure Increases Histamine H-3 Receptor-Mediated Inhibition of Glutamatergic Neurotransmission in Rat Dentate Gyrus. Alcohol-Clin Exp Res. 2018 Feb;42(2):295–305.

61. Vargish GA, Pelkey KA, Yuan X, Chittajallu R, Collins D, Fang C, et al. Persistent inhibitory circuit defects and disrupted social behaviour following in utero exogenous cannabinoid exposure. Mol Psychiatry. 2017;22(1):56–67.

62. Grotenhermen F. Pharmacokinetics and Pharmacodynamics of Cannabinoids. Clin Pharmacokinet. 2003;42(4):327–60.

63. Huizink AC, Mulder EJH. Maternal smoking, drinking or cannabis use during pregnancy and neurobehavioral and cognitive functioning in human offspring. Neurosci Biobehav Rev. 2006;30(1):24–41.

64. Fernández-Ruiz J, Berrendero F, Hernández ML, Ramos JA. The endogenous cannabinoid system and brain development. Trends Neurosci. 2000 Jan;23(1):14–20.

65. Harkany T, Guzmán M, Galve-Roperh I, Berghuis P, Devi LA, Mackie K. The emerging functions of endocannabinoid signaling during CNS development. Trends Pharmacol Sci. 2007 Feb;28(2):83–92.

66. Galiègue S, Mary S, Marchand J, Dussossoy D, Carrière D, Carayon P, et al. Expression of central and peripheral cannabinoid receptors in human immune tissues and leukocyte subpopulations. Eur J Biochem. 1995 Aug;232(1):54–61.

67. Roche M, Finn DP. Brain CB2 Receptors: Implications for Neuropsychiatric Disorders. Pharm Basel Switz. 2010 Aug;3(8):2517–53.

68. Martín-Sánchez A, Warnault V, Montagud-Romero S, Pastor A, Mondragón N, Torre RD La, et al. Alcohol-induced conditioned place preference is modulated by CB2 cannabinoid receptors and modifies levels of endocannabinoids in the mesocorticolimbic system. Pharmacol Biochem Behav. 2019;183:22–31.

69. Basavarajappa BS, Joshi V, Shivakumar M, Subbanna S. Distinct functions of endogenous cannabinoid system in alcohol abuse disorders. Br J Pharmacol. 2019;176(17):3085–109.

70. Scheyer AF, Melis M, Trezza V, Manzoni OJJ. Consequences of Perinatal Cannabis Exposure. Trends Neurosci. 2019;42(12):871–84.

71. Berrendero F, Sepe N, Ramos JA, Di Marzo V, Fernandez-Ruiz JJ. Analysis of cannabinoid receptor binding and mRNA expression and endogenous cannabinoid contents in the developing rat brain during late gestation and early postnatal period. SYNAPSE. 1999 Sep;33(3):181–91.

72. Mulder J, Aguado T, Keimpema E, Barabas K, Ballester Rosado CJ, Nguyen L, et al. Endocannabinoid signaling controls pyramidal cell specification and long-range axon patterning. Proc Natl Acad Sci. 2008 Jun;105(25):8760–5.

73. Berghuis P, Rajnicek AM, Morozov YM, Ross RA, Mulder J, Urban GM, et al. Hardwiring the Brain: Endocannabinoids Shape Neuronal Connectivity. Science. 2007 May;316(5828):1212–6.

74. Berghuis P, Dobszay MB, Wang X, Spano S, Ledda F, Sousa KM, et al. Endocannabinoids regulate interneuron migration and morphogenesis by transactivating the TrkB receptor. Proc Natl Acad Sci. 2005 Dec;102(52):19115–20.

75. de Salas-Quiroga A, García-Rincón D, Gómez-Domínguez D, Valero M, Simón-Sánchez S, Paraíso-Luna J, et al. Long-term hippocampal interneuronopathy drives sex-dimorphic spatial memory impairment induced by prenatal THC exposure. Neuropsychopharmacology. 2020;

76. Praag H Van, Schinder AF, Christie BR, Toni N, Palmer TD, Gage FH. Functional neurogenesis in the adult hippocampus. 2002;415(February).

77. Clelland CD, Choi M, Romberg C, Clemenson GD, Fragniere A, Tyers P, et al. A Functional Role for Adult Hippocampal Neurogenesis in Spatial Pattern Separation. Science. 2009;325(5937):210–3.

78. Snyder JS. Recalibrating the Relevance of Adult Neurogenesis . Vol. 42, Trends in Neurosciences . LONDON : Elsevier Ltd ; 2019. p. 164–78.

79. Green CR, Mihic AM, Nikkel SM, Stade BC, Rasmussen C, Munoz DP, et al. Executive function deficits in children with fetal alcohol spectrum disorders (FASD) measured using the Cambridge Neuropsychological Tests Automated Battery (CANTAB). J Child Psychol Psychiatry. 2009;50(6):688–97.

80. Mouro FM, Kofalvi A, Andre LA, Baqi Y, Muller CE, Ribeiro JA, et al. Memory deficits induced by chronic cannabinoid exposure are prevented by adenosine A2AR receptor antagonism. Neuropharmacology. 2019 Sep;155:10–21.

81. Breit KR, Zamudio B, Thomas JD. The effects of alcohol and cannabinoid exposure during the brain growth spurt on behavioral development in rats. Birth Defects Res. 2019 Jul;111(12):760–74.

82. Janisse JJ, Bailey BA, Ager J, Sokol RJ. Alcohol, tobacco, cocaine, and marijuana use: relative contributions to preterm delivery and fetal growth restriction. Subst Abuse. 2014;35(1):60–7.

83. Boa-Amponsem O, Zhang C, Mukhopadhyay S, Ardrey I, Cole GJ. Ethanol and cannabinoids interact to alter behavior in a zebrafish fetal alcohol spectrum disorder model. BIRTH DEFECTS Res. 2019 Jul;111(12, SI):775–88.

84. Fish EW, Murdaugh LB, Zhang C, Boschen KE, Boa-Amponsem O, Mendoza-Romero HN, et al. Cannabinoids Exacerbate Alcohol Teratogenesis by a CB1-Hedgehog Interaction. Sci Rep. 2019;9(1):16057.

85. Moher D, Liberati A, Tetzlaff J, Altman DG, Group TP. Preferred Reporting Items for Systematic Reviews and Meta-Analyses: The PRISMA Statement. PLOS Med. 2009;6(7):1–6.

86. Christie BR, Cameron HA. Neurogenesis in the adult hippocampus. Hippocampus. 2006 Jan;16(3):199–207.

87. Cameron HA, Mckay RDG. Adult neurogenesis produces a large pool of new granule cells in the dentate gyrus. J Comp Neurol. 2001;435:406–17.

88. Gerdes J, Schwab U, Lemke H, Stein H. Production of a mouse monoclonal antibody reactive with a human nuclear antigen associated with cell proliferation. Int J Cancer. 1983 Jan 15;31(1):13–20.

89. Kronenberg G, Reuter K, Steiner B, Brandt MD, Jessberger S, Yamaguchi M, et al. Subpopulations of proliferating cells of the adult hippocampus respond differently to physiologic neurogenic stimuli. J Comp Neurol. 2003 Dec;467(4):455–63.

90. Elibol-Can B, Dursun I, Telkes I, Kilic E, Canan S, Jakubowska-Dogru E. Examination of age-dependent effects of fetal ethanol exposure on behavior, hippocampal cell counts, and doublecortin immunoreactivity in rats. Dev Neurobiol. 2014 May;74(5):498–513.

91. Gil-Mohapel J, Boehme F, Patten A, Cox A, Kainer L, Giles E, et al. Altered adult hippocampal neuronal maturation in a rat model of fetal alcohol syndrome. Brain Res. 2011 Apr;1384:29–41.

92. Gil-Mohapel J, Titterness AK, Patten AR, Taylor S, Ratzlaff A, Ratzlaff T, et al. Prenatal ethanol exposure differentially affects hippocampal neurogenesis in the adolescent and aged brain. Neuroscience. 2014 Jul;273:174–88.

93. Olateju OI, Spocter MA, Patzke N, Ihunwo AO, Manger PR. Hippocampal neurogenesis in the C57BL/6J mice at early adulthood following prenatal alcohol exposure. Metab Brain Dis. 2018 Apr;33(2):397–410.

94. van Praag H, Christie BR, Sejnowski TJ, Gage FH. Running enhances neurogenesis, learning, and long-term potentiation in mice. Proc Natl Acad Sci. 1999 Nov;96(23):13427–31.

95. Klintsova AY, Helfer JL, Calizo LH, Dong WK, Goodlett CR, Greenough WT. Persistent impairment of hippocampal neurogenesis in young adult rats following early postnatal alcohol exposure. Alcohol Clin Exp Res. 2007 Dec;31(12):2073–82.

96. Sliwowska JH, Barker JM, Barha CK, Lan N, Weinberg J, Galea LAM. Stress-induced suppression of hippocampal neurogenesis in adult male rats is altered by prenatal ethanol exposure. Stress Int J Biol STRESS. 2010 Jul;13(4):302–14.

97. Uban KA, Sliwowska JH, Lieblich S, Ellis LA, Yu WK, Weinberg J, et al. Prenatal alcohol exposure reduces the proportion of newly produced neurons and glia in the dentate gyrus of the hippocampus in female rats. Horm Behav. 2010 Nov;58(5):835–43.

98. Bird CW, Taylor DH, Pinkowski NJ, Chavez GJ, Valenzuela CF. Long-term Reductions in the Population of GABAergic Interneurons in the Mouse Hippocampus following Developmental Ethanol Exposure. Neuroscience. 2018 Jul;383:60–73.

99. Lu J, Jiao Z, Yu Y, Zhang C, He X, Li Q, et al. Programming for increased expression of hippocampal GAD67 mediated the hypersensitivity of the hypothalamic-pituitary-adrenal axis in male offspring rats with prenatal ethanol exposure. CELL DEATH Dis. 2018 May;9.

100. Vargish GA, Pelkey KA, Yuan X, Chittajallu R, Collins D, Fang C, et al. Persistent inhibitory circuit defects and disrupted social behaviour following in utero exogenous cannabinoid exposure. Mol PSYCHIATRY. 2017 Jan;22(1):56–67.

101. Hamilton GF, Murawski NJ, St Cyr SA, Jablonski SA, Schiffino FL, Stanton ME, et al. Neonatal alcohol exposure disrupts hippocampal neurogenesis and contextual fear conditioning in adult rats. BRAIN Res. 2011 Sep;1412:88–101.

102. Lu J, Jiao Z, Yu Y, Zhang C, He X, Li Q, et al. Programming for increased expression of hippocampal GAD67 mediated the hypersensitivity of the hypothalamic-pituitary-adrenal axis in male offspring rats with prenatal ethanol exposure. Cell Death Dis. 2018;

103. Kempermann G, Jessberger S, Steiner B, Kronenberg G. Milestones of neuronal development in the adult hippocampus. Trends Neurosci. 2004;27(8):447–52.

104. Kee N, Sivalingam S, Boonstra R, Wojtowicz JM. The utility of Ki-67 and BrdU as proliferative markers of adult neurogenesis. J Neurosci Methods. 2002;115(1):97–105.

105. Bonthius DJ, West JR. Permanent neuronal deficits in rats exposed to alcohol during the brain growth spurt. Teratology. 1991 Aug;44(2):147–63.

106. Khaspekov L, Brenz Verca M, Frumkina L, Marsicano D, Hermann H, Heinzmann U, et al. P.5.028 CB1 cannabinoid receptor-mediatedprotection against excitotoxic damage of hippocampal neurons in vitro: Histological and ultrastructural analysis. Eur Neuropsychopharmacol. 2005 Apr 2;15(2):S216.

107. Han J, Kesner P, Metna-Laurent M, Duan T, Xu L, Georges F, et al. Acute cannabinoids impair working memory through astroglial CB1 receptor modulation of hippocampal LTD. Cell. 2012 Mar;148(5):1039–50.

108. Sheng M, Kim E. The postsynaptic organization of synapses. Cold Spring Harb Perspect Biol. 2011;

109. Chevaleyre V, Castillo PE. Endocannabinoid-mediated metaplasticity in the hippocampus. Neuron. 2004 Sep;43(6):871–81.

110. Selvam R, Yeh ML, Levine ES. Endogenous cannabinoids mediate the effect of BDNF at CA1 inhibitory synapses in the hippocampus. SYNAPSE. 2019 Feb;73(2).

111. Losonczy A, Biro AA, Nusser Z. Persistently active cannabinoid receptors mute a subpopulation of hippocampal interneurons. Proc Natl Acad Sci U S A. 2004 Feb;101(5):1362–7.

112. Huang CC, Lo SW, Hsu KS. Presynaptic mechanisms underlying cannabinoid inhibition of excitatory synaptic transmission in rat striatal neurons. J Physiol. 2001 May;532(Pt 3):731–48.

113. Fish EW, Murdaugh LB, Zhang C, Boschen KE, Boa-Amponsem O, Mendoza-Romero HN, et al. Cannabinoids Exacerbate Alcohol Teratogenesis by a CB1-Hedgehog Interaction. Sci Rep. 2019;9(1):16057.

114. Hayatbakhsh MR, Flenady VJ, Gibbons KS, Kingsbury AM, Hurrion E, Mamun AA, et al. Birth outcomes associated with cannabis use before and during pregnancy. Pediatr Res. 2012;

115. Young-Wolff KC, Sarovar V, Tucker LY, Conway A, Alexeeff S, Weisner C, et al. Self-reported Daily, Weekly, and Monthly Cannabis Use among Women before and during Pregnancy. JAMA Netw Open. 2019 Jul 3;2(7):e196471–e196471.

116. Breit KR, Rodriguez CG, Lei A, Thomas JD. Combined vapor exposure to THC and alcohol in pregnant rats: Maternal outcomes and pharmacokinetic effects. Neurotoxicol Teratol. 2020 Nov 1;82:106930.

117. Li Y, Shen M, Stockton ME, Zhao X. Hippocampal deficits in neurodevelopmental disorders. Neurobiol Learn Mem. 2019 Nov 1;165.

118. Christie BR, Franks KM, Seamans JK, Saga K, Sejnowski TJ. Synaptic plasticity in morphologically identified CA1 stratum radiatum interneurons and giant projection cells. Hippocampus. 2000 Jan 1;10(6):673–83.

119. Fontaine CJ, Patten AR, Sickmann HM, Helfer JL, Christie BR. Effects of pre-natal alcohol exposure on hippocampal synaptic plasticity: Sex, age and methodological considerations. Neurosci Biobehav Rev. 2016 May;64:12–34.

120. Hill MN, Froc DJ, Fox CJ, Gorzalka BB, Christie BR. Prolonged cannabinoid treatment results in spatial working memory deficits and impaired long-term potentiation in the CA1 region of the hippocampus in vivo. Eur J Neurosci. 2004 Aug;20(3):859–63.

121. Andersen P, Morris R, Amaral D, Bliss T, O'Keefe J. The Hippocampus Book. Oxford: Oxford University Press; 2007. 832 p.

122. Jessberger S, Clark RE, Broadbent NJ, Clemenson GD, Consiglio A, Lie DC, et al. Dentate gyrus-specific knockdown of adult neurogenesis impairs spatial and object recognition memory in adult rats. Learn Mem. 2009;

123. Eadie BDBDBD, Cushman J, Kannangara TSTS, Fanselow MSMS, Christie BRBR. NMDA receptor hypofunction in the dentate gyrus and impaired context discrimination in adult Fmr1 knockout mice. Hippocampus. 2012 Feb;22(2):241–54.

124. Bartsch T, Döhring J, Rohr A, Jansen O, Deuschl G. CA1 neurons in the human hippocampus are critical for autobiographical memory, mental time travel, and autonoetic consciousness. Proc Natl Acad Sci U S A. 2011 Oct 18;108(42):17562–7.

125. Okuyama T, Kitamura T, Roy DS, Itohara S, Tonegawa S. Ventral CA1 neurons store social memory. Science. 2016 Sep 30;353(6307):1536–41.

126. Reid HMOHMO, Lysenko-Martin MR, Snowden TMTM, Thomas JDJD, Christie BRBR, Lysenko-Martin MR, et al. A Systematic Review of the Effects of Perinatal Alcohol Exposure and Perinatal Marijuana Exposure on Adult Neurogenesis in the Dentate Gyrus. Alcohol Clin Exp Res. 2020 May 14;44(6):acer.14332.

127. Sadrian B, Wilson DA, Saito M. Long-lasting neural circuit dysfunction following developmental ethanol exposure. Brain Sciences. 2013.

128. Vargish GA, Pelkey KA, Yuan X, Chittajallu R, Collins D, Fang C, et al. Persistent inhibitory circuit defects and disrupted social behaviour following in utero exogenous cannabinoid exposure. Mol PSYCHIATRY. 2017 Jan;22(1):56–67.

129. Mackie K. Mechanisms of CB1 receptor signaling: endocannabinoid modulation of synaptic strength. Int J Obes. 2006 Apr;30(1):S19–23.

130. Sim-Selley LJ. Regulation of Cannabinoid CB1 Receptors in the Central Nervous System by Chronic Cannabinoids. Vol. 15, Critical Reviews in Neurobiology. Begel House Inc.; 2003. p. 91–119.

131. Cabral GA. Cannabinoid receptors in microglia of the central nervous system: immune functional relevance. J Leukoc Biol. 2005;

132. Kawamura Y, Fukaya M, Maejima T, Yoshida T, Miura E, Watanabe M, et al. The CB1 cannabinoid receptor is the major cannabinoid receptor at excitatory presynaptic sites in the hippocampus and cerebellum. J Neurosci. 2006;

133. Han J, Kesner P, Metna-Laurent M, Duan T, Xu L, Georges F, et al. Acute cannabinoids impair working memory through astroglial CB1 receptor modulation of hippocampal LTD. Cell. 2012 Mar;148(5):1039–50.

134. Leonzino M, Busnelli M, Antonucci F, Verderio C, Mazzanti M, Chini B. The Timing of the Excitatory-to-Inhibitory GABA Switch Is Regulated by the Oxytocin Receptor via KCC2. Cell Rep. 2016;

135. Ognjanovski N, Schaeffer S, Wu J, Mofakham S, Maruyama D, Zochowski M, et al. Parvalbumin-expressing interneurons coordinate hippocampal network dynamics required for memory consolidation. Nat Commun. 2017 Apr 6;8(1):1–14.

136. Murray AJ, Sauer JF, Riedel G, McClure C, Ansel L, Cheyne L, et al. Parvalbumin-positive CA1 interneurons are required for spatial working but not for reference memory. Nat Neurosci. 2011 Mar 30;14(3):297–9.

137. Deng X, Gu L, Sui N, Guo J, Liang J. Parvalbumin interneuron in the ventral hippocampus functions as a discriminator in social memory. Proc Natl Acad Sci U S A. 2019 Aug 13;116(33):16583–92.

138. Reha RK, Dias BG, Nelson CA, Kaufer D, Werker JF, Kolbh B, et al. Critical period regulation acrossmultiple timescales. Vol. 117, Proceedings of the National Academy of Sciences of the United States of America. National Academy of Sciences; 2020. p. 23242–51.

139. Espinoza C, Guzman SJ, Zhang X, Jonas P. Parvalbumin + interneurons obey unique connectivity rules and establish a powerful lateral-inhibition microcircuit in dentate gyrus. Nat Commun. 2018;

140. Czeh B, Simon M, van der Hart MG, Schmelting B, Hesselink MB, Fuchs E. Chronic Stress Decreases the Number of Parvalbumin-Immunoreactive Interneurons in the Hippocampus: Prevention by Treatment with a Substance P Receptor (NK1) Antagonist. Neuropsychopharmacology. 2005 Jan 1;30(1):67–79.

141. Konradi C, Yang CK, Zimmerman EI, Lohmann KM, Gresch P, Pantazopoulos H, et al. Hippocampal interneurons are abnormal in schizophrenia. Schizophr Res. 2011 Sep 1;131(1–3):165–73.

142. Bernstein HHG, Johnson M, Perry RH, LeBeau FENN, Dobrowolny H, Bogerts B, et al. Partial loss of parvalbumin-containing hippocampal interneurons in dementia with Lewy bodies. Neuropathology. 2011 Feb 1;31(1):1–10.

143. Fuchs EC, Zivkovic AR, Cunningham MO, Middleton S, LeBeau FEN, Bannerman DMM, et al. Recruitment of Parvalbumin-Positive Interneurons Determines Hippocampal Function and Associated Behavior. Neuron. 2007;

144. Song J, Sun J, Moss J, Wen Z, Sun GJ, Hsu D, et al. Parvalbumin interneurons mediate neuronal circuitry–neurogenesis coupling in the adult hippocampus. Nat Neurosci. 2013 Dec 10;16(12):1728–30.

145. Meconi A, Wortman RC, Wright DK, Neale KJ, Clarkson M, Shultz SR, et al. Repeated mild traumatic brain injury can cause acute neurologic impairment without overt structural damage in juvenile rats. 2018;1–24.

146. Palkovits M. The rat brain in stereotaxic coordinates. Neuropeptides. 1983;

147. Computing RF for S. R Core Team. R: A Language and Environment for Statistical Computing. 2018.

148. Stull J. SPSS for Windows. Teach Sociol. 1994;

149. Lu J, Jiao Z, Yu Y, Zhang C, He X, Li Q, et al. Programming for increased expression of hippocampal GAD67 mediated the hypersensitivity of the hypothalamic-pituitary-adrenal axis in male offspring rats with prenatal ethanol exposure. Cell Death Dis. 2018 May;9.

150. Bell SH, Stade B, Reynolds JN, Rasmussen C, Andrew G, Hwang PA, et al. The remarkably high prevalence of epilepsy and seizure history in fetal alcohol spectrum disorders. Alcohol Clin Exp Res. 2010;

151. Huang S, Kirkwood A. Endocannabinoid Signaling Contributes to Experience-Induced Increase of Synaptic Release Sites From Parvalbumin Interneurons in Mouse Visual Cortex. Front Cell Neurosci. 2020 Sep 30;14:304.

152. Finnegan L. Substance Abuse in Canada: Licit and Illicit Drug Use during Pregnancy: Maternal, Neonatal and Early Childhood Consequences. 2013.

153. Fukui Y, Sakata-Haga H. Intrauterine environment-genome interaction and children's development (1): Ethanol: a teratogen in developing brain. J Toxicol Sci. 2009;34 Suppl 2:SP273-P278.

154. Mattson SN, Bernes GA, Doyle LR. Fetal Alcohol Spectrum Disorders: A Review of the Neurobehavioral Deficits Associated With Prenatal Alcohol Exposure. Alcohol Clin Exp Res. 2019 Jun 1;43(6):1046–62.

155. Oesterheld JR, Kofoed L, Tervo R, Fogas B, Wilson A, Fiechtner H. Effectiveness of methylphenidate in Native American children with fetal alcohol syndrome and attention deficit/hyperactivity disorder: a controlled pilot study. J Child Adolesc Psychopharmacol. 1998;8(1):39–48.

156. May PA, Gossage JP, Kalberg WO, Robinson LK, Buckley D, Manning M, et al. Prevalence and epidemiologic characteristics of FASD from various research methods with an emphasis on recent in-school studies. Dev Disabil Res Rev. 2009/09/05 ed. 2009;15(3):176–92.

157. Kathleen R. Stratton Frederick C. Battaglia, CJH. Fetal Alcohol Syndrome: Diagnosis, Epidemiology, Prevention, and Treatment. Washington, D.C.: NATIONAL ACADEMY PRESS; 1996.

158. Popova S, Lange S, Probst C, Gmel G, Rehm J. Global prevalence of alcohol use and binge drinking during pregnancy, and fetal alcohol spectrum disorder. Biochem Cell Biol. 2018;96(2):237–40.

159. Burd L. Drinking at the end of pregnancy: why don't we see it? Pediatr Res 2020 882. 2020 Mar 14;88(2):142–142.

160. Popova S, Dozet D, Akhand Laboni S, Brower K, Temple V. Why do women consume alcohol during pregnancy or while breastfeeding? Drug Alcohol Rev. 2022 May 1;41(4):759–77.

161. CDC. National Center on Birth Defects and Developmental Disabilites. 2021 [cited 2021 Nov 26]. Basics about FASDs | CDC. Available from: https://www.cdc.gov/ncbddd/fasd/facts.html

162. Jirikowic T, Carmichael Olson H. Fetal alcohol spectrum disorders. In: The Curated Reference Collection in Neuroscience and Biobehavioral Psychology. 2016.

163. Chasnoff IJ, Landress HJ, Barrett ME. The Prevalence of Illicit-Drug or Alcohol Use during Pregnancy and Discrepancies in Mandatory Reporting in Pinellas County, Florida. N Engl J Med. 1990 Apr;322(17):1202–6.

164. Sweeney MM, Rass O, DiClemente C, Schacht RL, Vo HT, Fishman MJ, et al. Working memory training for adolescents with cannabis use disorders: A randomized controlled trial. J Child Adolesc Subst Abuse. 2018;27(4):211–26.

165. Khemiri L, Brynte C, Stunkel A, Klingberg T, Jayaram-Lindström N. Working Memory Training in Alcohol Use Disorder: A Randomized Controlled Trial. Alcohol Clin Exp Res. 2019 Jan 1;43(1):135–46.

166. Reid HMO, Lysenko-Martin MR, Snowden TM, Thomas JD, Christie BR. A Systematic Review of the Effects of Perinatal Alcohol Exposure and Perinatal Marijuana Exposure on Adult Neurogenesis in the Dentate Gyrus. Vol. 44, Alcoholism: Clinical and Experimental Research. Blackwell Publishing Ltd; 2020. p. 1164–74.

167. Sawchuk SD, Reid HMO, Neale KJ, Shin J, Christie BR. Effects of Ethanol on Synaptic Plasticity and NMDA Currents in the Juvenile Rat Dentate Gyrus. Brain Plast Amst Neth. 2020 Oct 2;6(1):123–36.

168. Hill MN, Titterness AK, Morrish AC, Carrier EJ, Lee TTY, Gil-Mohapel J, et al. Endogenous cannabinoid signaling is required for voluntary exercise-induced enhancement of progenitor cell proliferation in the hippocampus. Hippocampus. 2010;20(4).

169. Titterness AK., Christie BR. Prenatal ethanol exposure enhances NMDAR-dependent long-term potentiation in the adolescent female dentate gyrus. Hippocampus. 2012 Jan;22(1):69–81.

170. Titterness A, Christie B. Long-term depression in vivo: Effects of gender, diet and prenatal ethanol exposure. Alcohol Clin Exp Res. 2007;31.

171. Peñasco S, Rico-Barrio I, Puente N, Fontaine CJ, Ramos A, Reguero L, et al. Intermittent ethanol exposure during adolescence impairs cannabinoid type 1 receptor-dependent long-term depression and recognition memory in adult mice. Neuropsychopharmacology. 2020;45(2).

172. Bonilla-Del Río I, Puente N, Peñasco S, Rico I, Gutiérrez-Rodríguez A, Elezgarai I, et al. Adolescent ethanol intake alters cannabinoid type-1 receptor localization in astrocytes of the adult mouse hippocampus. Addict Biol. 2019 Nov;24(2):182–92.

173. Peñasco S, Rico-Barrio I, Puente N, Gómez-Urquijo SMSM, Fontaine CJCJ, Egaña-Huguet J, et al. Endocannabinoid long-term depression revealed at medial perforant path excitatory synapses in the dentate gyrus. Neuropharmacology. 2019 Jul;153(Apr):32–40.

174. Chung H, Park K, Jang HJ, Kohl MM, Kwag J. Dissociation of somatostatin and parvalbumin interneurons circuit dysfunctions underlying hippocampal theta and gamma oscillations impaired by amyloid beta oligomers in vivo. BRAIN Struct Funct. 2020;

175. Schmid LC, Mittag M, Poll S, Steffen J, Wagner J, Geis HR, et al. Dysfunction of Somatostatin-Positive Interneurons Associated with Memory Deficits in an Alzheimer's Disease Model. NEURON. 2016 Oct;92(1):114–25.

176. Antonoudiou P, Tan YL, Kontou G, Louise Upton A, Mann EO. Parvalbumin and somatostatin interneurons contribute to the generation of hippocampal gamma oscillations. J Neurosci. 2020 Sep 30;40(40):7668–87.

177. Flossmann T, Kaas T, Rahmati V, Kiebel SJ, Witte OW, Holthoff K, et al. Somatostatin Interneurons Promote Neuronal Synchrony in the Neonatal Hippocampus. Cell Rep. 2019 Mar 19;26(12):3173-3182.e5.

178. Zou S, Kumar U. Colocalization of cannabinoid receptor 1 with somatostatin and neuronal nitric oxide synthase in rat brain hippocampus. BRAIN Res. 2015 Oct;1622:114–26.

179. Abbas AI, Sundiang MJM, Henoch B, Morton MP, Bolkan SS, Park AJ, et al. Somatostatin Interneurons Facilitate Hippocampal-Prefrontal Synchrony and Prefrontal Spatial Encoding. Neuron. 2018 Nov 21;100(4):926-939.e3.

180. Zheng J, Li HL, Tian N, Liu F, Wang L, Yin Y, et al. Interneuron Accumulation of Phosphorylated tau Impairs Adult Hippocampal Neurogenesis by Suppressing GABAergic Transmission **Needs Erratum. CELL STEM CELL. 2020 Mar;26(3):331+.

181. Godin EA, Dehart DB, Parnell SE, O'Leary-Moore SK, Sulik KK. Ventromedian forebrain dysgenesis follows early prenatal ethanol exposure in mice. Neurotoxicol Teratol. 2011;33(2):231–9.

182. Friend LN, Williamson RC, Merrill CB, Newton ST, Christensen MT, Petersen J, et al. Hippocampal Stratum Oriens Somatostatin-Positive Cells Undergo CB1-Dependent Long-Term Potentiation and Express Endocannabinoid Biosynthetic Enzymes. MOLECULES. 2019 Apr;24(7).

183. Andrade JP, Fernando PM, Madeira MD, Paula-Barbosa MM, Cadete-Leite A, Zimmer J. Effects of chronic alcohol consumption and withdrawal on the somatostatin-immunoreactive neurons of the rat hippocampal dentate hilus. Hippocampus. 1992;2(1):65–71.

184. Adrian TE, Allen JM, Bloom SR, Ghatei MA, Rossor MN, Roberts GW, et al. Neuropeptide Y distribution in human brain. Nature. 1983 Dec;306(5943):584–6.

185. dos Santos V V, Santos DB, Lach G, Rodrigues ALS, Farina M, De Lima TCM, et al. Neuropeptide Y (NPY) prevents depressive-like behavior, spatial memory deficits and oxidative stress following amyloid-β (Aβ1–40) administration in mice. Behav Brain Res. 2013;244:107–15.

186. Angelucci F, Fiore M, Cozzari C, Aloe L. Prenatal ethanol effects on NGF level, NPY and ChAT immunoreactivity in mouse entorhinal cortex: A preliminary study. Neurotoxicol Teratol. 1999;21(4):415–25.

187. Schmeltzer SN, Herman JP, Sah R. Neuropeptide Y (NPY) and posttraumatic stress disorder (PTSD): A translational update. Vol. 284, Experimental Neurology. Academic Press Inc.; 2016. p. 196–210.

188. Alviña K, Jodeiri Farshbaf M, Mondal AK. Long term effects of stress on hippocampal function: Emphasis on early life stress paradigms and potential involvement of neuropeptide Y. J Neurosci Res. 2021;99(1):57–66.

189. Yao Y, Hu Y, Yang J, Zhang C, He Y, Qi H, et al. Inhibition of neuronal nitric oxide synthase protects against hippocampal neuronal injuries by increasing neuropeptide Y expression in temporal lobe epilepsy mice. Free Radic Biol Med. 2022;188:45–61.

190. Decressac M, Wright B, David B, Tyers P, Jaber M, Barker RA, et al. Exogenous neuropeptide Y promotes in vivo hippocampal neurogenesis. Hippocampus. 2011 Mar;21(3):233–8.

191. Mirchandani-Duque M, Barbancho MA, López-Salas A, Alvarez-Contino JE, García-Casares N, Fuxe K, et al. Galanin and Neuropeptide Y Interaction Enhances Proliferation of Granule Precursor Cells and Expression of Neuroprotective Factors in the Rat Hippocampus with Consequent Augmented Spatial Memory. Biomedicines. 2022;10(6).

192. Hadad-Ophir O, Albrecht A, Stork O, Richter-Levin G. Amygdala activation and GABAergic gene expression in hippocampal sub-regions at the interplay of stress and spatial learning. Front Behav Neurosci. 2014;8:3.

193. Remmers CL, Castillon CCM, Armstrong JN, Contractor A. Recruitment of parvalbumin and somatostatin interneuron inputs to adult born dentate granule neurons. Sci Rep. 2020;10(1):17522.

194. Briones BA, Pisano TJ, Pitcher MN, Haye AE, Diethorn EJ, Engel EA, et al. Adult-born granule cell mossy fibers preferentially target parvalbumin-positive interneurons surrounded by perineuronal nets. Hippocampus. 2021 Apr;31(4):375–88.

195. Tanaka M, Yamada S, Watanabe Y. The Role of Neuropeptide Y in the Nucleus Accumbens. Int J Mol Sci. 2021;22(14).

196. Brothers SP, Wahlestedt C. Therapeutic potential of neuropeptide Y (NPY) receptor ligands. EMBO Mol Med. 2010;2(11):429–39.

197. Oláh S, Füle M, Komlósi G, Varga C, Báldi R, Barzó P, et al. Regulation of cortical microcircuits by unitary GABA-mediated volume transmission. Nature. 2009 Oct;461(7268):1278–81.

198. Karagiannis A, Gallopin T, Dávid C, Battaglia D, Geoffroy H, Rossier J, et al. Classification of NPY-expressing neocortical interneurons. J Neurosci. 2009;

199. Breit KR, Zamudio B, Thomas JD. The effects of alcohol and cannabinoid exposure during the brain growth spurt on behavioral development in rats. Birth Defects Res. 2019 Jul 15;111(12):760–74.

200. Reid HMO, Snowden TM, Shkolnikov I, Breit KR, Rodriguez C, Thomas JD, et al. Prenatal alcohol and cannabis exposure can have opposing and region-specific effects on parvalbumin interneuron numbers in the hippocampus. Alcohol Clin Exp Res. 2021;00:1–10.

201. Spohr HL, Steinhausen -Chr. H. Follow-up studies of children with fetal alcohol syndrome. Neuropediatrics. 1987 Mar 19;18(1):13–7.

202. Grabenauer M, Wilson J. Differences in Cannabis Impairment and its Measurement Due to Route of Administration Final Summary Overview. 2020;

203. Sikorski C, Leos-Toro C, Hammond D. Cannabis Consumption, Purchasing and Sources among Young Canadians: The Cannabis Purchase and Consumption Tool (CPCT). https://doi.org/101080/1082608420211879142. 2021;56(4):449–57.

204. Luhmann HJ, Sinning A, Yang JW, Reyes-Puerta V, Stüttgen MC, Kirischuk S, et al. Spontaneous neuronal activity in developing neocortical networks: From single cells to large-scale interactions. Front Neural Circuits. 2016 May 24;10(MAY):40.

205. Arama J, Abitbol K, Goffin D, Fuchs C, Sihra TS, Thomson AM, et al. GABAA receptor activity shapes the formation of inhibitory synapses between developing medium spiny neurons. Front Cell Neurosci. 2015 Aug 6;9(AUGUST):290.

206. Wozniak JR, Riley EP, Charness ME. Diagnosis, epidemiology, assessment, pathophysiology, and management of fetal alcohol spectrum disorders. Lancet Neurol. 2019 Aug 1;18(8):760.

207. Ganguly K, Schinder AF, Wong ST, Poo M ming. GABA itself promotes the developmental switch of neuronal GABAergic responses from excitation to inhibition. Cell. 2001 May 18;105(4):521–32.

208. Scheyer AF, Borsoi M, Pelissier-Alicot AL, Manzoni OJJ. Perinatal THC exposure via lactation induces lasting alterations to social behavior and prefrontal cortex function in rats at adulthood. Neuropsychopharmacol Off Publ Am Coll Neuropsychopharmacol. 2020 Oct;45(11):1826–33.

209. Tuncdemir SN, Wamsley B, Stam FJ, Osakada F, Goulding M, Callaway EM, et al. Early somatostatin interneuron connectivity mediates the maturation of deep layer cortical circuits. Neuron. 2016 Feb 3;89(3):521.

210. Daha SK, Sharma P, Sah PK, Karn A, Poudel A, Pokhrel B. Effects of prenatal cannabis use on fetal and neonatal development and its association with neuropsychiatric disorders: A systematic review. Neurol Psychiatry Brain Res. 2020;38:20–6.

211. Grafe EL, Wade MMM, Hodson CE, Thomas JD, Christie BR. Postnatal Choline Supplementation Rescues Deficits in Synaptic Plasticity Following Prenatal Ethanol Exposure. Nutrients. 2022;14(10).

212. Bake S, Pinson MR, Pandey S, Chambers JP, Mota R, Fairchild AE, et al. Prenatal alcohol-induced sex differences in immune, metabolic and neurobehavioral outcomes in adult rats. Brain Behav Immun. 2021;98:86–100.

213. Ko JY, Farr SL, Tong VT, Creanga AA, Callaghan WM. Prevalence and patterns of marijuana use among pregnant and nonpregnant women of reproductive age. Am J Obstet Gynecol. 2015 Aug;213(2):201.e1-201.e10.

214. Brown QL, Sarvet AL, Shmulewitz D, Martins SS, Wall MM, Hasin DS. Trends in marijuana use among pregnant and nonpregnant reproductive-aged women, 2002-2014. Vol. 317, JAMA - Journal of the American Medical Association. American Medical Association; 2017. p. 207–9.

215. Denny CH, Acero CS, Naimi TS, Kim SY. Consumption of Alcohol Beverages and Binge Drinking Among Pregnant Women Aged 18–44 Years — United States, 2015–2017. Morb Mortal Wkly Rep. 2019 Apr 26;68(16):365–8.

216. Baranger DAA, Paul SE, Colbert SMC, Karcher NR, Johnson EC, Hatoum AS, et al. Association of Mental Health Burden With Prenatal Cannabis Exposure From Childhood to Early Adolescence: Longitudinal Findings From the Adolescent Brain Cognitive Development (ABCD) Study. JAMA Pediatr. 2022 Dec 1;176(12):1261–5.

217. Krishna Kumar K, Shalev-Benami M, Robertson MJ, Hu H, Banister SD, Hollingsworth SA, et al. Structure of a Signaling Cannabinoid Receptor 1-G Protein Complex. Cell. 2019 Jan 24;176(3):448-458.e12.

218. Wilkinson JD, Whalley BJ, Baker D, Pryce G, Constanti A, Gibbons S, et al. Medicinal cannabis: is Δ9–tetrahydrocannabinol necessary for all its effects? J Pharm Pharmacol. 2003 Dec 1;55(12):1687–94.

219. Prenderville JA, Kelly AM, Downer EJ. The role of cannabinoids in adult neurogenesis. Br J Pharmacol. 2015 Aug;172(16):3950–63.

220. Abate G, Uberti D, Tambaro S. Potential and Limits of Cannabinoids in Alzheimer's Disease Therapy. Biology. 2021 Jun;10(6):542.

221. Jean-Gilles L, Braitch M, Latif ML, Aram J, Fahey AJ, Edwards LJ, et al. Effects of pro-inflammatory cytokines on cannabinoid CB 1 and CB 2 receptors in immune cells. Acta Physiol Oxf Engl. 2015 May;214(1):63–74.

222. Busquets-Garcia A, Bains J, Marsicano G. CB1 Receptor Signaling in the Brain: Extracting Specificity from Ubiquity. NEUROPSYCHOPHARMACOLOGY. 2018 Jan;43(1):4–20.

223. Beins EC, Beiert T, Jenniches I, Hansen JN, Leidmaa E, Schrickel JW, et al. Cannabinoid receptor 1 signalling modulates stress susceptibility and microglial responses to chronic social defeat stress. Transl Psychiatry. 2021 Mar 15;11(1):1–15.

224. de Salas-Quiroga A, Diaz-Alonso J, Garcia-Rincon D, Remmers F, Vega D, Gomez-Canas M, et al. Prenatal exposure to cannabinoids evokes long-lasting functional alterations by targeting CB1 receptors on developing cortical neurons. Proc Natl Acad Sci U S A. 2015 Nov;112(44):13693–8.

225. Lim TK, Ruthazer ES. Microglial trogocytosis and the complement system regulate axonal pruning in vivo. VijayRaghavan K, Mason CA, Aizenman C, Gross CT, Sierra A, editors. eLife. 2021 Mar 16;10:e62167.

226. Stratoulias V, Venero JL, Tremblay MÈ, Joseph B. Microglial subtypes: diversity within the microglial community. EMBO J. 2019 Sep 2;38(17):e101997.

227. Scheyer A, Yasmin F, Naskar S, Patel S. Endocannabinoids at the synapse and beyond: implications for neuropsychiatric disease pathophysiology and treatment. Neuropsychopharmacology. 2023 Jan;48(1):37–53.

228. Linkert M, Rueden CT, Allan C, Burel JM, Moore W, Patterson A, et al. Metadata matters: access to image data in the real world. J Cell Biol. 2010 May 31;189(5):777–82.

229. Hansen DV, Hanson JE, Sheng M. Microglia in Alzheimer's disease. J Cell Biol. 2018 Feb 5;217(2):459–72.

230. Dong R, Huang R, Wang J, Liu H, Xu Z. Effects of Microglial Activation and Polarization on Brain Injury After Stroke. Front Neurol [Internet]. 2021 [cited 2023 May 28];12. Available from: https://www.frontiersin.org/articles/10.3389/fneur.2021.620948

231. Vidal-Itriago A, Radford RAW, Aramideh JA, Maurel C, Scherer NM, Don EK, et al. Microglia morphophysiological diversity and its implications for the CNS. Front Immunol [Internet]. 2022 [cited 2023 May 28];13. Available from: https://www.frontiersin.org/articles/10.3389/fimmu.2022.997786

232. Flannigan K, Poole N, Cook J, Unsworth K. Sex-related differences among individuals assessed for fetal alcohol spectrum disorder in Canada. Alcohol Clin Exp Res. 2023 Mar;47(3):613–23.

233. Lim CCW, Sun T, Leung J, Chung JYC, Gartner C, Connor J, et al. Prevalence of Adolescent Cannabis Vaping: A Systematic Review and Meta-analysis of US and Canadian Studies. JAMA Pediatr. 2022 Jan 1;176(1):42–51.

234. Young-Wolff KC, Sarovar V, Tucker LY, Avalos LA, Conway A, Armstrong MA, et al. Association of Nausea and Vomiting in Pregnancy With Prenatal Marijuana Use. JAMA Intern Med. 2018 Oct 1;178(10):1423–4.

235. Paul SE, Hatoum AS, Fine JD, Johnson EC, Hansen I, Karcher NR, et al. Associations Between Prenatal Cannabis Exposure and Childhood Outcomes: Results From the ABCD Study. JAMA Psychiatry. 2021 Jan 1;78(1):64–76.

236. Powell D, Pacula RL, Jacobson M. Do medical marijuana laws reduce addictions and deaths related to pain killers? J Health Econ. 2018 Mar 1;58:29–42.

237. Duko B, Dachew BA, Pereira G, Alati R. The effect of prenatal cannabis exposure on offspring preterm birth: a cumulative meta-analysis. Addiction. 2023;118(4):607–19.

238. United Nations publication. World Drug Report 2021 [Internet]. The United Nations Office on Drugs and Crime; 2021. Report No.: No. E. 21. Available from: chrome-extension://efaidnbmnnnibpcajpcglclefindmkaj/https://www.unodc.org/res/wdr2021/field/WDR21_Booklet_1.pdf

239. Guerrero-Alba R, Barragán-Iglesias P, González-Hernández A, Valdez-Moráles EE, Granados-Soto V, Condés-Lara M, et al. Some Prospective Alternatives for Treating Pain: The Endocannabinoid System and Its Putative Receptors GPR18 and GPR55. Front Pharmacol [Internet]. 2019 [cited 2023 May 28];9. Available from: https://www.frontiersin.org/articles/10.3389/fphar.2018.01496

240. Shahbazi F, Grandi V, Banerjee A, Trant JF. Cannabinoids and Cannabinoid Receptors: The Story so Far. iScience. 2020 Jun 20;23(7):101301.

241. Jordan CJ, Xi ZX. Progress in brain cannabinoid CB2 receptor research: From genes to behavior. Neurosci Biobehav Rev. 2019 Mar 1;98:208–20.

242. Namdar D, Voet H, Ajjampura V, Nadarajan S, Mayzlish-Gati E, Mazuz M, et al. Terpenoids and Phytocannabinoids Co-Produced in Cannabis Sativa Strains Show Specific Interaction for Cell Cytotoxic Activity. Molecules. 2019 Aug 21;24(17):3031.

243. Cristino L, Bisogno T, Di Marzo V. Cannabinoids and the expanded endocannabinoid system in neurological disorders. Nat Rev Neurol. 2020 Jan;16(1):9–29.

244. Katona I, Sperlagh B, Sik A, Kafalvi A, Vizi ES, Mackie K, et al. Presynaptically located CB1 cannabinoid receptors regulate GABA release from axon terminals of specific hippocampal interneurons. J Neurosci. 1999 Jun;19(11):4544–58.

245. Liu X, Chen Y, Vickstrom CR, Li Y, Viader A, Cravatt BF, et al. Coordinated regulation of endocannabinoid-mediated retrograde synaptic suppression in the cerebellum by neuronal and astrocytic monoacylglycerol lipase. Sci Rep. 2016 Oct 24;6(1):35829.

246. Farmer J, Zhao X, van Praag H, Wodtke K, Gage FH, Christie BR. Effects of voluntary exercise on synaptic plasticity and gene expression in the dentate gyrus of adult male sprague–dawley rats in vivo. Neuroscience. 2004 Jan 1;124(1):71–9.

247. Wong TP, Howland JG, Robillard JM, Ge Y, Yu W, Titterness AK, et al. Hippocampal long-term depression mediates acute stress-induced spatial memory retrieval impairment. Proc Natl Acad Sci. 2007 Jul 3;104(27):11471–6.

248. Kemp N, McQueen J, Faulkes S, Bashir ZI. Different forms of LTD in the CA1 region of the hippocampus: role of age and stimulus protocol. Eur J Neurosci. 2000 Jan;12(1):360–6.

249. Lin SHN, Lien YR, Shibata K, Sasaki Y, Watanabe T, Lin CP, et al. The phase of plasticity-induced neurochemical changes of high-frequency repetitive transcranial magnetic stimulation are different from visual perceptual learning. Sci Rep. 2023 Apr 7;13(1):5720.

250. Jenks KR, Tsimring K, Ip JPK, Zepeda JC, Sur M. Heterosynaptic Plasticity and the Experience-Dependent Refinement of Developing Neuronal Circuits. Front Neural Circuits [Internet]. 2021 [cited 2023 May 28];15. Available from: https://www.frontiersin.org/articles/10.3389/fncir.2021.803401

251. Chistiakova M, Bannon NM, Bazhenov M, Volgushev M. Heterosynaptic Plasticity: Multiple Mechanisms and Multiple Roles. Neurosci Rev J Bringing Neurobiol Neurol Psychiatry. 2014 Oct;20(5):483–98.

252. Trivino-Paredes JS, Nahirney PC, Pinar C, Grandes P, Christie BR. Acute slice preparation for electrophysiology increases spine numbers equivalently in the male and female juvenile hippocampus: a DiI labeling study. https://doi.org/101152/jn003322019. 2019;122(3):958–69.

253. ChatGPT. ChatGPT. 2023.

254. Breit KR, Zamudio B, Thomas JD. Altered motor development following late gestational alcohol and cannabinoid exposure in rats. Neurotoxicol Teratol. 2019 May;73:31–41.

255. Metna-Laurent M, Mondésir M, Grel A, Vallée M, Piazza PV. Cannabinoid-Induced Tetrad in Mice. Curr Protoc Neurosci. 2017 Jul 5;80:9.59.1-9.59.10.

256. Traccis F, Frau R, Melis M. Gender Differences in the Outcome of Offspring Prenatally Exposed to Drugs of Abuse. Front Behav Neurosci. 2020;14:72.

257. Manzanedo C, Mateos-García A, Miñarro J, Arenas MC. The negative allosteric modulator of mGluR5, MPEP, potentiates the rewarding properties of cocaine in priming-induced reinstatement of CPP. Adicciones. 2020 Jul 1;32(3):193–201.

258. Niswender CM, Conn PJ. Metabotropic glutamate receptors: physiology, pharmacology, and disease. Annu Rev Pharmacol Toxicol. 2010;50:295–322.

259. Munakata Y, Pfaffly J. Hebbian learning and development. Dev Sci. 2004;7(2):141–8.

260. Choii G, Ko J. Gephyrin: a central GABAergic synapse organizer. Exp Mol Med. 2015 Apr;47(4):e158–e158.

261. Mahmood U, Ahn S, Yang EJ, Choi M, Kim H, Regan P, et al. Dendritic spine anomalies and PTEN alterations in a mouse model of VPA-induced autism spectrum disorder. Pharmacol Res. 2018 Feb 1;128:110–21.

262. Contreras D, Piña R, Carvallo C, Godoy F, Ugarte G, Zeise M, et al. Methylphenidate Restores Behavioral and Neuroplasticity Impairments in the Prenatal Nicotine Exposure Mouse Model of ADHD: Evidence for Involvement of AMPA Receptor Subunit Composition and Synaptic Spine Morphology in the Hippocampus. Int J Mol Sci. 2022 Jan;23(13):7099.

263. Pchitskaya E, Bezprozvanny I. Dendritic Spines Shape Analysis—Classification or Clusterization? Perspective. Front Synaptic Neurosci [Internet]. 2020 [cited 2023 Jun 22];12. Available from: https://www.frontiersin.org/articles/10.3389/fnsyn.2020.00031

264. Castelli MP, Piras AP, D'Agostino A, Pibiri F, Perra S, Gessa GL, et al. Dysregulation of the endogenous cannabinoid system in adult rats prenatally treated with the cannabinoid agonist WIN 55,212-2. Eur J Pharmacol. 2007 Nov;573(1–3):11–9.

265. Glavas MM, Ellis L, Yu WK, Weinberg J. Effects of prenatal ethanol exposure on basal limbic-hypothalamic-pituitary-adrenal regulation: Role of corticosterone. Alcohol-Clin Exp Res. 2007 Sep;31(9):1598–610.

266. Naseer M, Ullah I, Rasool M, Ansari S, Sheikh I, Bibi F, et al. Erratum to: Downregulation of dopamine D1 receptors and increased neuronal apoptosis upon ethanol and PTZ exposure in prenatal rat cortical and hippocampal neurons. Springer Nature; 2014.

267. Climent E, Pascual M, Renau-Piqueras J, Guerri C. Ethanol exposure enhances cell death in the developing cerebral cortex: Role of brain-derived neurotrophic factor and its signaling pathways. J Neurosci Res. 2002 Apr;68(2):213–25.

268. Kajimoto K, Allan A, Cunningham LA. Fate Analysis of Adult Hippocampal Progenitors in a Murine Model of Fetal Alcohol Spectrum Disorder (FASD). PLOS ONE. 2013 Sep;8(9).

269. Tanner DC, Githinji AW, Young EA, Meiri K, Savage DD, Perrone-Bizzozero NI. Fetal alcohol exposure alters GAP-43 phosphorylation and protein kinase C responses to contextual fear conditioning in the hippocampus of adult rat offspring. Alcohol-Clin Exp Res. 2004 Jan;28(1):113–22.

270. Sun H, Su R, Zhang X, Wen J, Yao D, Gao X, et al. HIPPOCAMPAL GR-AND CBI-MEDIATED MGLUR5 DIFFERENTIALLY PRODUCES SUSCEPTIBILITY AND RESILIENCE TO ACUTE AND CHRONIC MILD STRESS IN RATS. NEUROSCIENCE. 2017 Aug;357:295–302.

271. Samudio-Ruiz SL, Allan AM, Sheema S, Caldwell KK. Hippocampal N-Methyl-D-Aspartate Receptor Subunit Expression Profiles in a Mouse Model of Prenatal Alcohol Exposure. Alcohol-Clin Exp Res. 2010 Feb;34(2):342–53.

272. Davies S, Ballesteros-Merino C, Allen NA, Porch MW, Pruitt ME, Christensen KH, et al. Impact of moderate prenatal alcohol exposure on histaminergic neurons, histidine decarboxylase levels and histamine H2 receptors in adult rat offspring. Alcohol Fayettev N. 2019 May;76:47–57.

273. Bhattacharya D, Dunaway EP, Bhattacharya S, Bloemer J, Buabeid M, Escobar M, et al. Impaired ILK Function Is Associated with Deficits in Hippocampal Based Memory and Synaptic Plasticity in a FASD Rat Model. PLOS ONE. 2015 Aug;10(8).

274. Patten AR, Brocardo PS, Sakiyama C, Wortman RC, Noonan A, Gil-Mohapel J, et al. Impairments in hippocampal synaptic plasticity following prenatal ethanol exposure are dependent on glutathione levels. Hippocampus. 2013 Dec;23(12):1463–75.

275. de Ferron BS, Vilpoux C, Kervern M, Robert A, Antol J, Naassila M, et al. Increase of KCC2 in hippocampal synaptic plasticity disturbances after perinatal ethanol exposure. Addict Biol. 2017 Nov;22(6):1870–82.

276. Jamali-Raeufy N, Nasehi M, Zarrindast MR. Influence of N-methyl D-aspartate receptor mechanism on WIN55,212-2-induced amnesia in rat dorsal hippocampus. Behav Pharmacol. 2011 Oct;22(7):645–54.

277. Beggiato S, Borelli AC, Tomasini MC, Morgano L, Antonelli T, Tanganelli S, et al. Long-lasting alterations of hippocampal GABAergic neurotransmis adult rats following perinatal Delta(9)-THC exposure. Neurobiol Learn Mem. 2017 Mar;139:135–43.

278. Dandekar MP, Bharne AP, Borkar PD, Subhedar NK, Kokare DM. Maternal ethanol exposure reshapes CART system in the rat brain: Correlation with development of anxiety, depression and memory deficits. NEUROSCIENCE. 2019 May;406:126–39.

279. Brady ML, Diaz MR, Iuso A, Everett JC, Valenzuela CF, Caldwell KK. Moderate prenatal alcohol exposure reduces plasticity and alters NMDA receptor subunit composition in the dentate gyrus. J Neurosci Off J Soc Neurosci. 2013 Jan;33(3):1062–7.

280. Contreras ML, de la Fuente-Ortega E, Vargas-Roberts S, Munoz DC, Goic CA, Haeger PA. NADPH Oxidase Isoform 2 (NOX2) Is Involved in Drug Addiction Vulnerability in Progeny Developmentally Exposed to Ethanol. Front Neurosci. 2017 Jun;11.

281. Goodfellow MJ, Abdulla KA, Lindquist DH. Neonatal Ethanol Exposure Impairs Trace Fear Conditioning and Alters NMDA Receptor Subunit Expression in Adult Male and Female Rats. Alcohol-Clin Exp Res. 2016 Feb;40(2):309–18.

282. Raineki C, Hellemans KGC, Bodnar T, Lavigne KM, Ellis L, Woodward TS, et al. Neurocircuitry underlying stress and emotional regulation in animals prenatally exposed to alcohol and subjected to chronic mild stress in adulthood. Front Endocrinol. 2014;5.

283. Ngai YF, Sulistyoningrum DC, O'Neill R, Innis SM, Weinberg J, Devlin AM. Prenatal alcohol exposure alters methyl metabolism and programs serotonin transporter and glucocorticoid receptor expression in brain. Am J Physiol-Regul Integr Comp Physiol. 2015 Sep;309(5):R613–22.

284. Cunningham LA, Newville J, Li L, Tapia P, Allan AM, Valenzuela CF. Prenatal Alcohol Exposure Leads to Enhanced Serine 9 Phosphorylation of Glycogen Synthase Kinase-3beta (GSK-3beta) in the Hippocampal Dentate Gyrus of Adult Mouse. Alcohol Clin Exp Res. 2017 Nov;41(11):1907–16.

285. Zhang CR, Ho MF, Vega MCS, Burne THJ, Chong S. Prenatal ethanol exposure alters adult hippocampal VGLUT2 expression with concomitant changes in promoter DNA methylation, H3K4 trimethylation and miR-467b-5p levels. EPIGENETICS CHROMATIN. 2015 Sep;8.

286. Samudio-Ruiz SL, Allan AM, Valenzuela CF, Perrone-Bizzozero NI, Caldwell KK. Prenatal ethanol exposure persistently impairs NMDA receptor-dependent activation of extracellular signal-regulated kinase in the mouse dentate gyrus. J Neurochem. 2009 Jun;109(5):1311–23.

287. Sluyter F, Jamot L, Bertholet JY, Crusio WE. Prenatal exposure to alcohol does not affect radial maze learning and hippocampal mossy fiber sizes in three inbred strains of mouse. Behav Brain Funct. 2005 Jan;1:5–10.

Supplementary

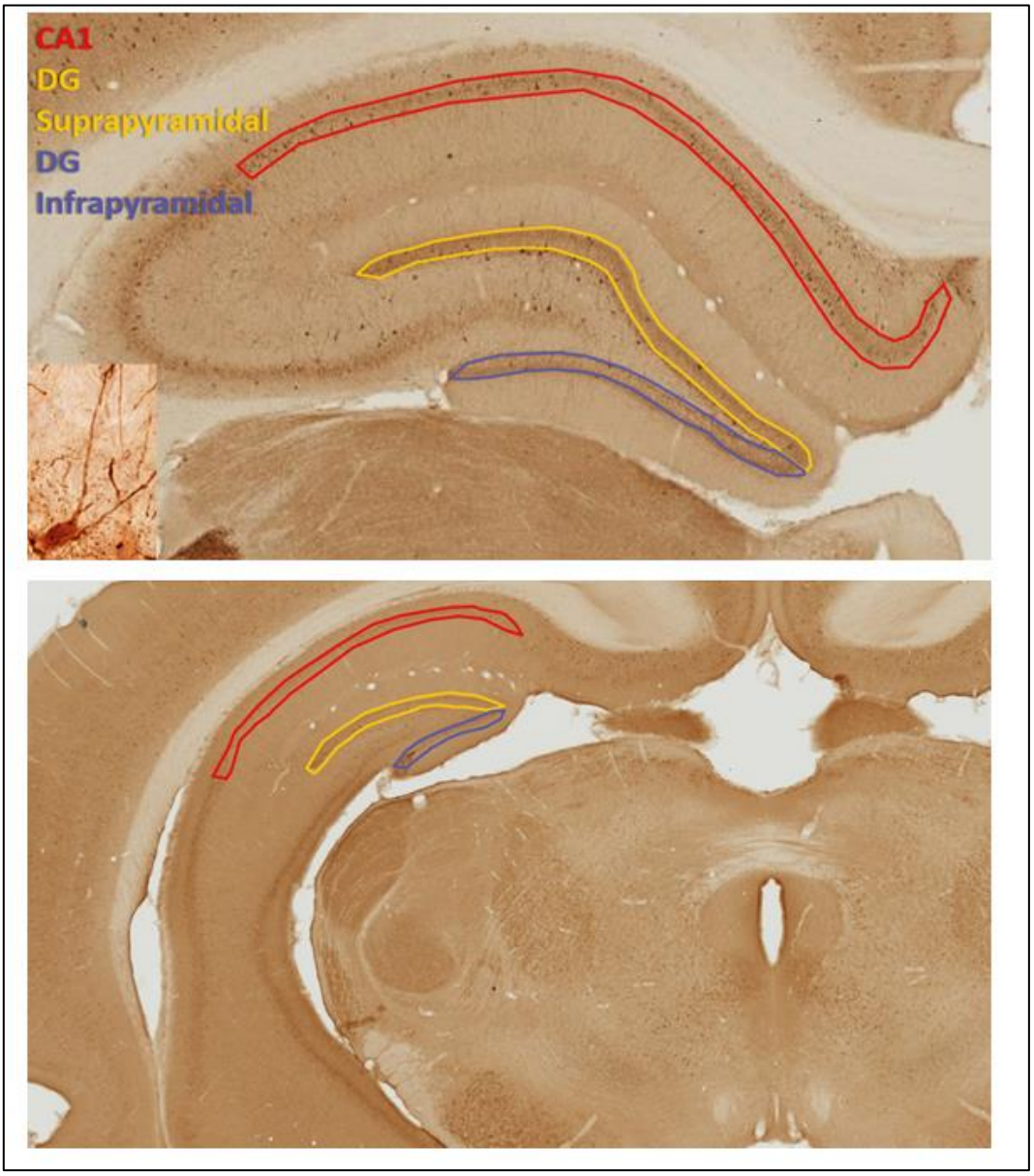

Figure S1: : Photomicrograph of a coronal hippocampal slice from a p70 Sprague Dawley rat showing how areas were traced during Image J analysis in DAB developed parvalbumin immunohistochemistry. Suprapyramidal and infrapyramidal measurements were taken separately, but pooled during final analysis. Inlay in bottom left is a photomicrograph of how cells appeared during counting.

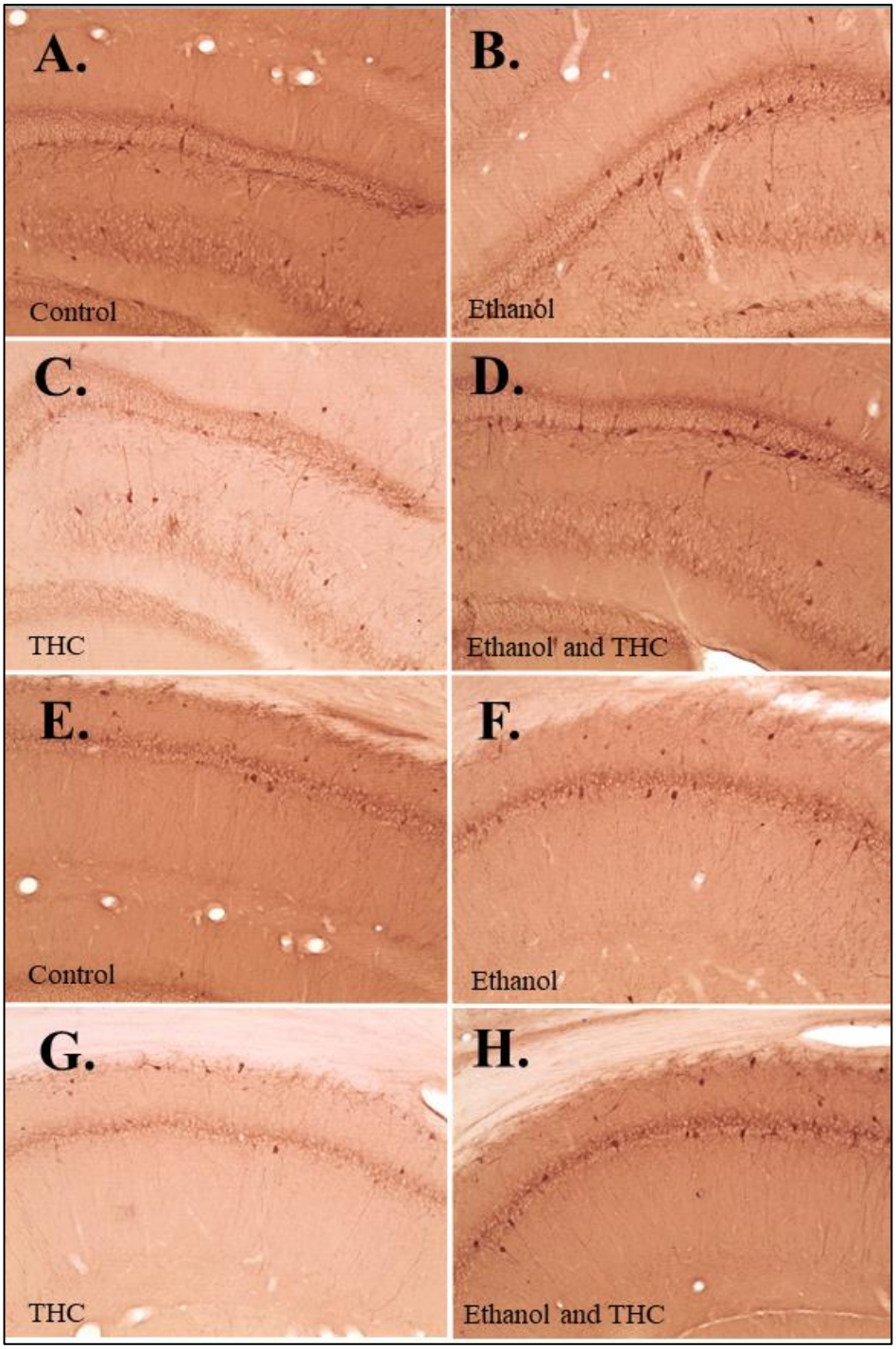

Figure S2: Representative images of parvalbumin-positive cells developed in DAB. A-D.: Dentate gyrus E-H.: CA1.

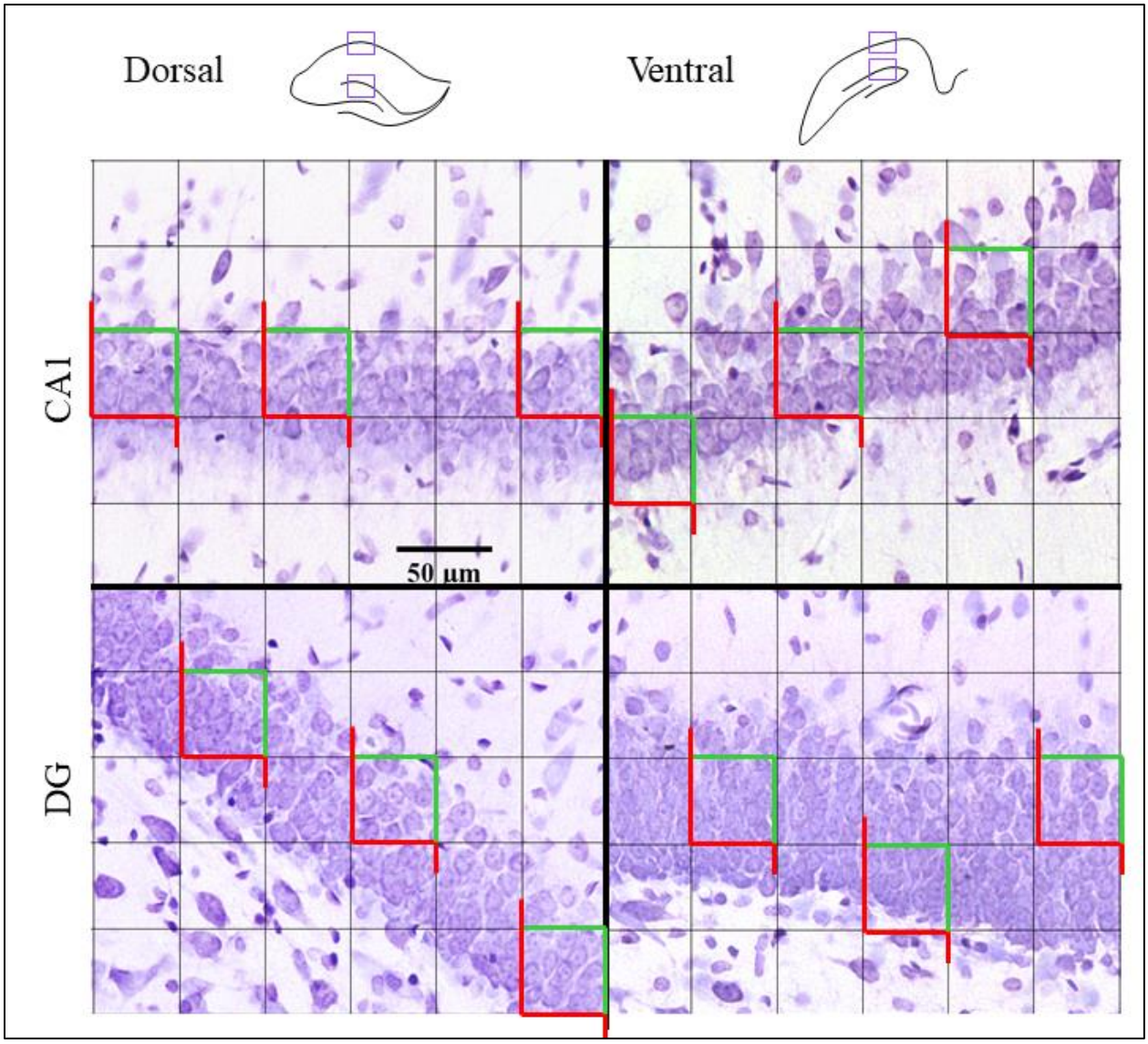

Figure S3: Example of Cresyl Violet counting method. Dorsal and ventral traces at the top of the image show the anatomy of each slice selected, and purple boxes show where each representative image was taken from. For each image, a 2000 um^2 grid was added in ImageJ using Tools> Analyse> Grid. Three boxes from each image were chosen for analysis, one aligned to the top, middle, and bottom of the cell layer to the best of the counter's ability. The red and green lines illustrate how the counter selected cells that were counted as in and out of the box; cells touching the green line were counted as in and cells touching the red line were counted as out. The "multipoint selection tool" in ImageJ was used to keep track of counted cells. Note that images shown have been cropped to allow for a closer view of the cell layer.

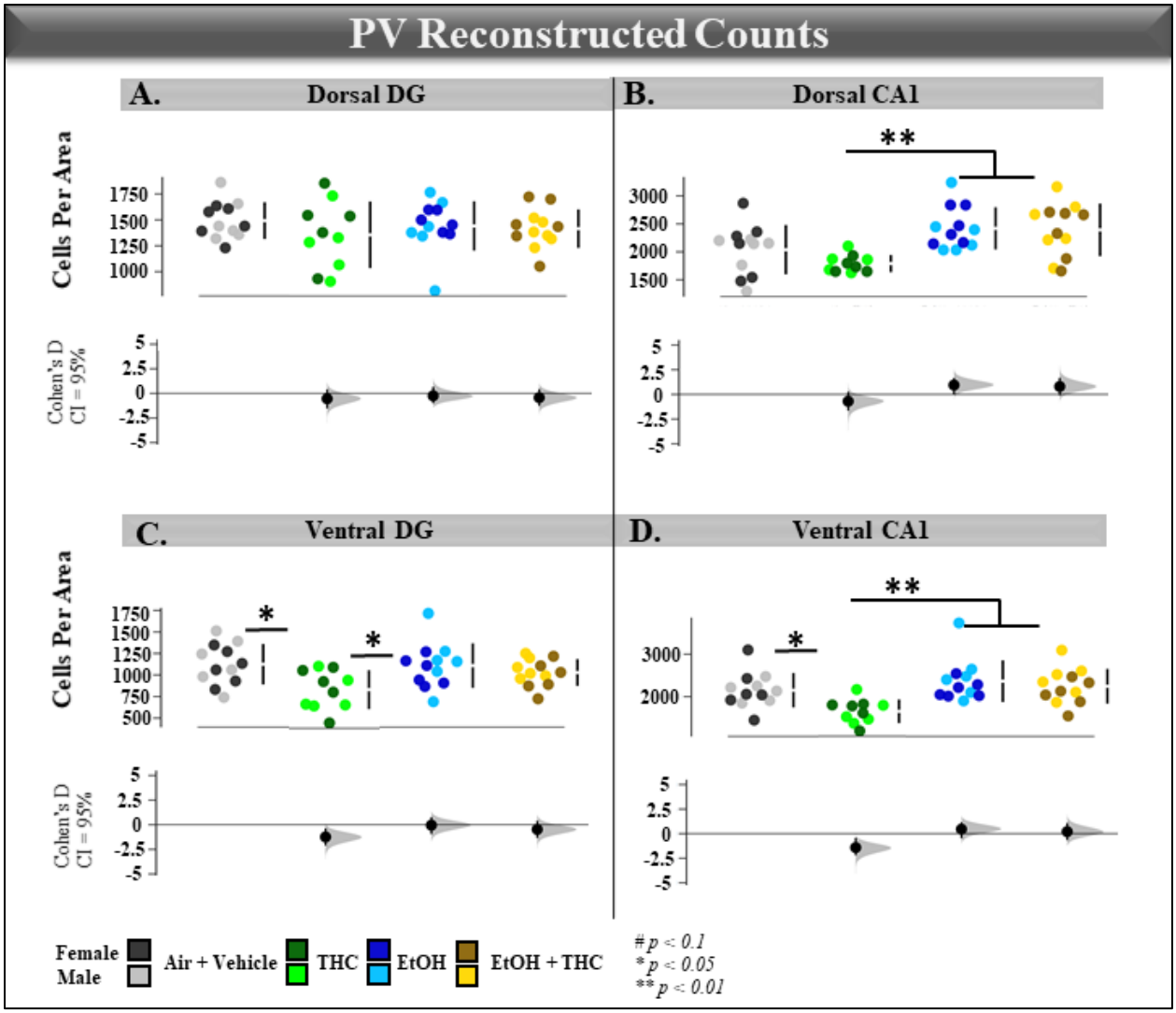

Figure S4: Reconstructed cell counts of the pyramidal cell layer of the CA1 region and the dentate granule cell layer. Each point represents one animal. Cohen's D of effect size shown where each experimental group is compared with control.

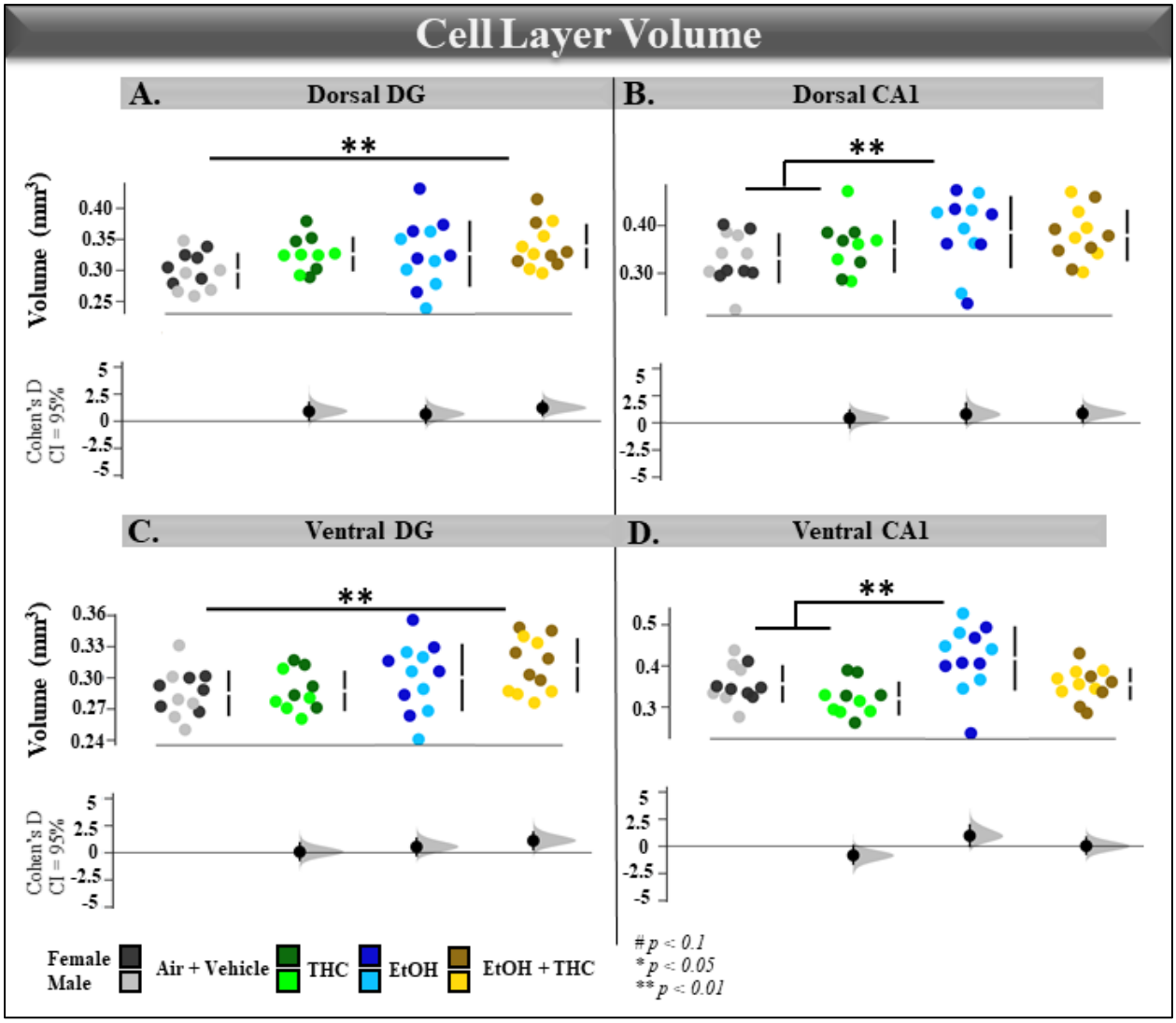

Figure S5: Reconstructed areas of the pyramidal cell layer of the CA1 region and the dentate granule cell layer. Each point represents one animal. Cohen's D of effect size shown where each experimental group is compared with control.

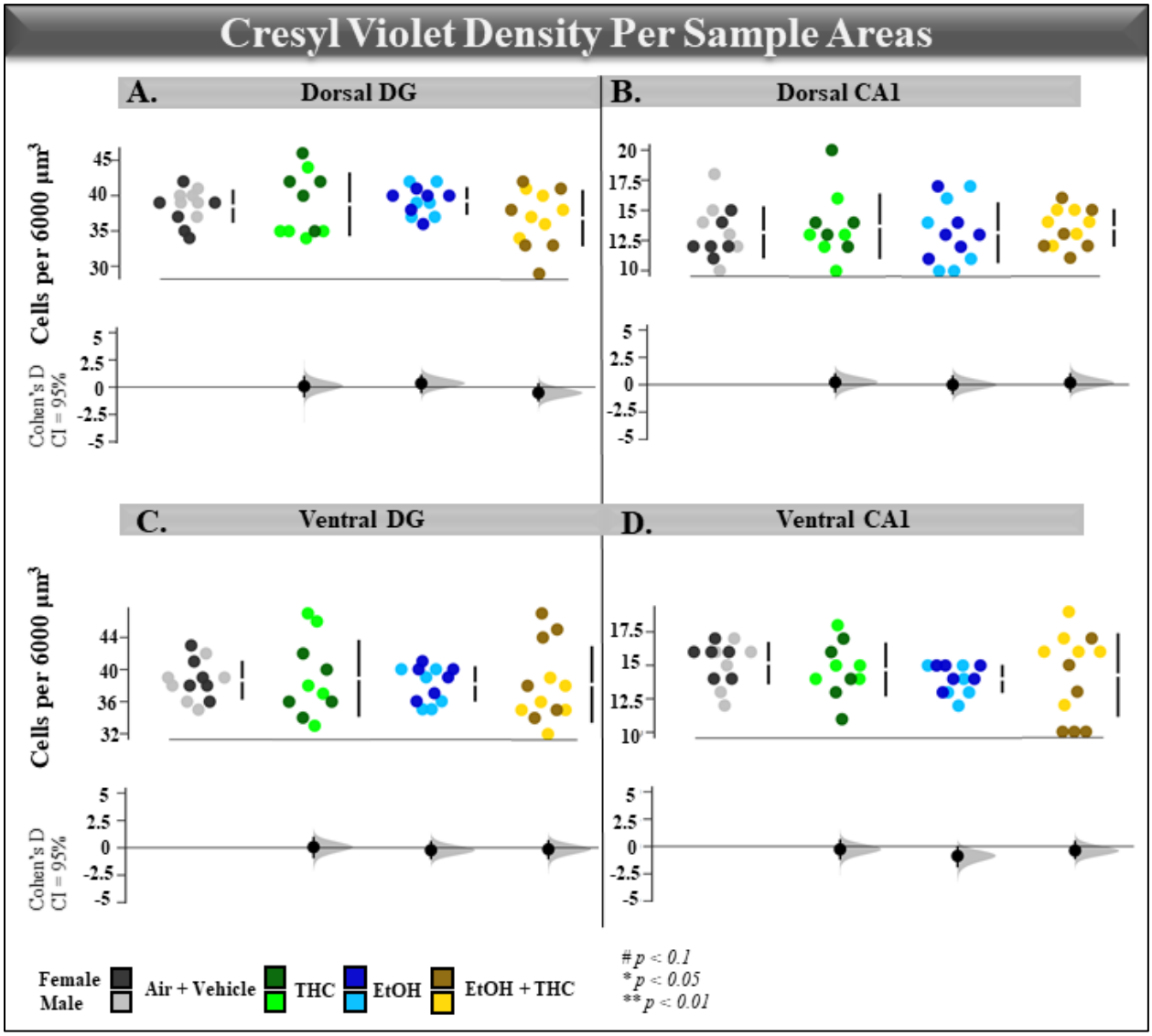

Figure S6: Number of Cresyl Violet stained cells in 3 2000 µm² boxes over the pyramidal cell layer of the CA1 region and the suprapyramidal blade of the dentate granule cell layer. Cohen's D of effect size shown where each experimental group is compared with control.

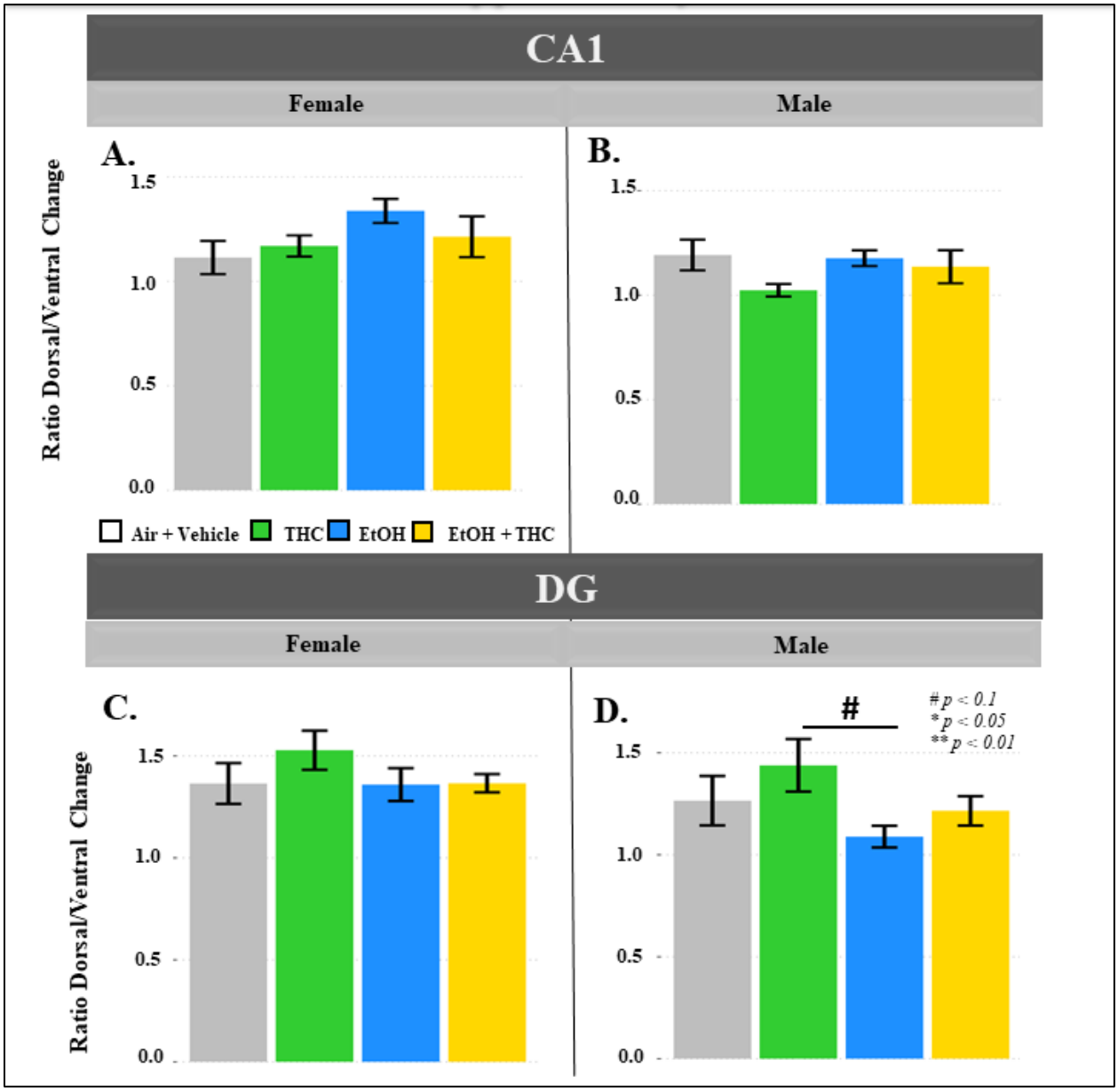

Figure S7: Ratio of dorsal to ventral parvalbumin neuron density in rats exposed to air, THC, EtOH, and EtOH + THC from GD5-20 in the dorsal and ventral cornu ammonis 1 region. C-D. Ratio of dorsal to ventral parvalbumin neuron density in rats exposed to air, THC, EtOH, and EtOH + THC from GD5-20 in the dorsal and ventral dentate gyrus.

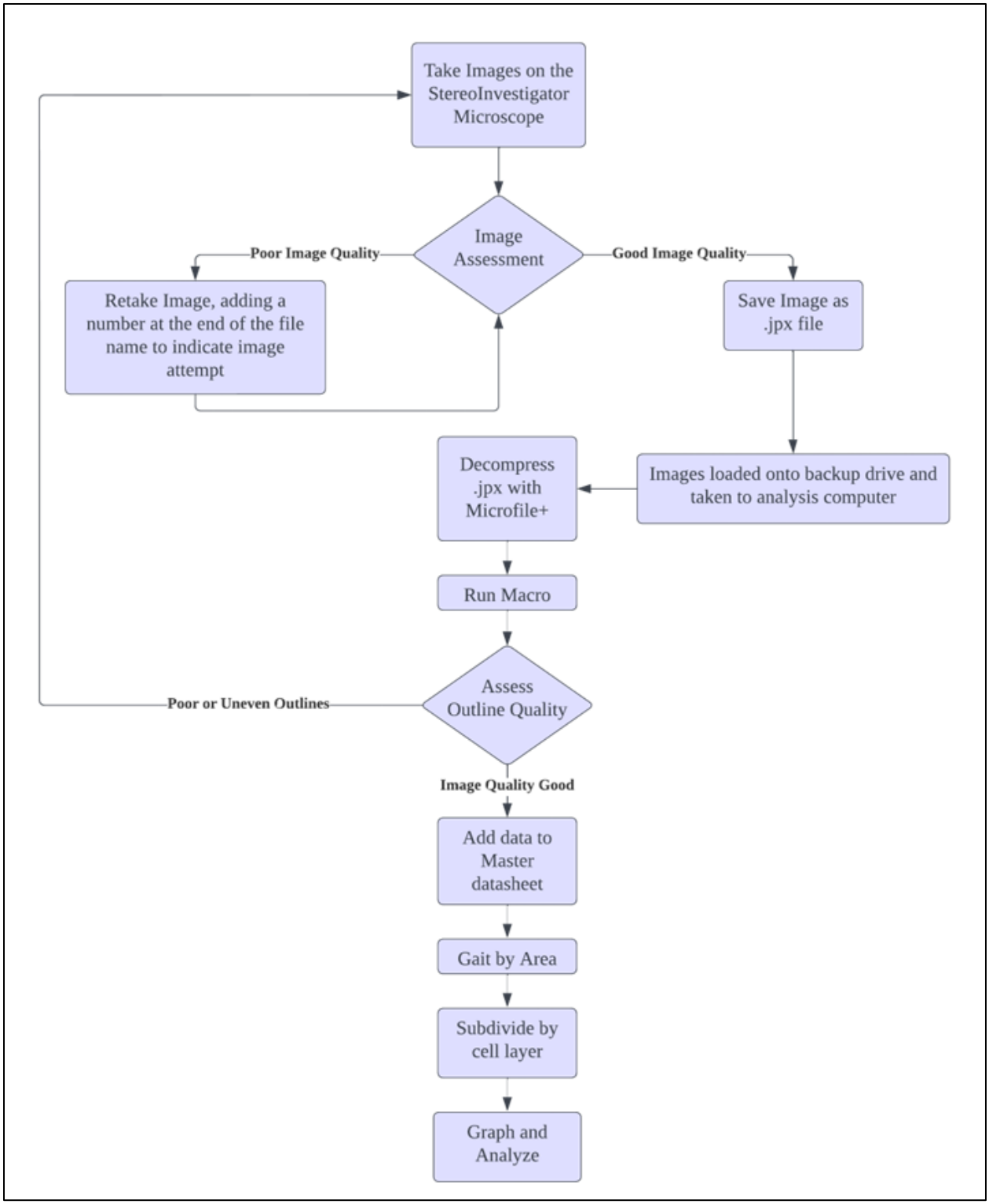

Figure S 5.1 Flow diagram of image acquisition

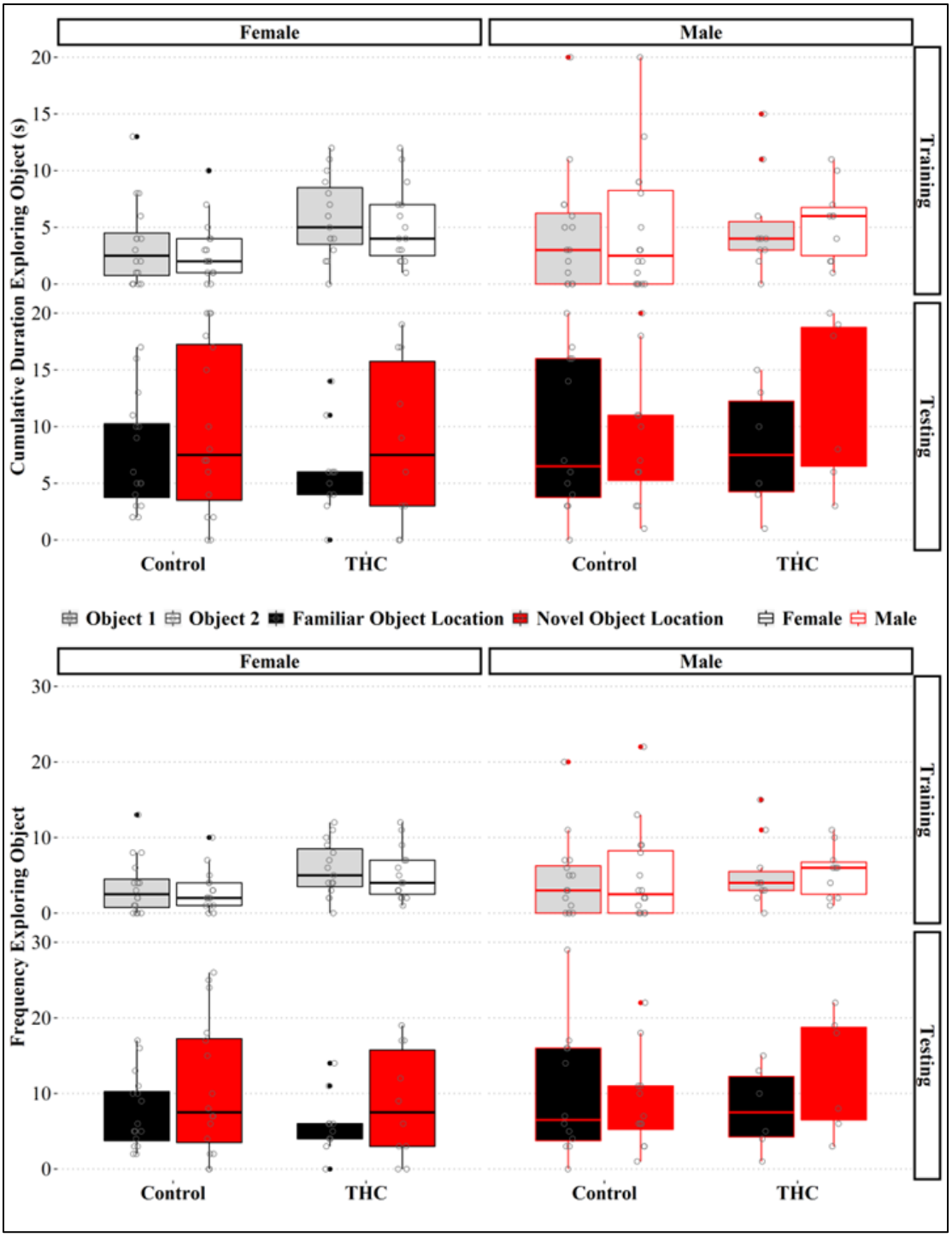

Figure S 6.1 Additional Novel Location Recognition Analysis

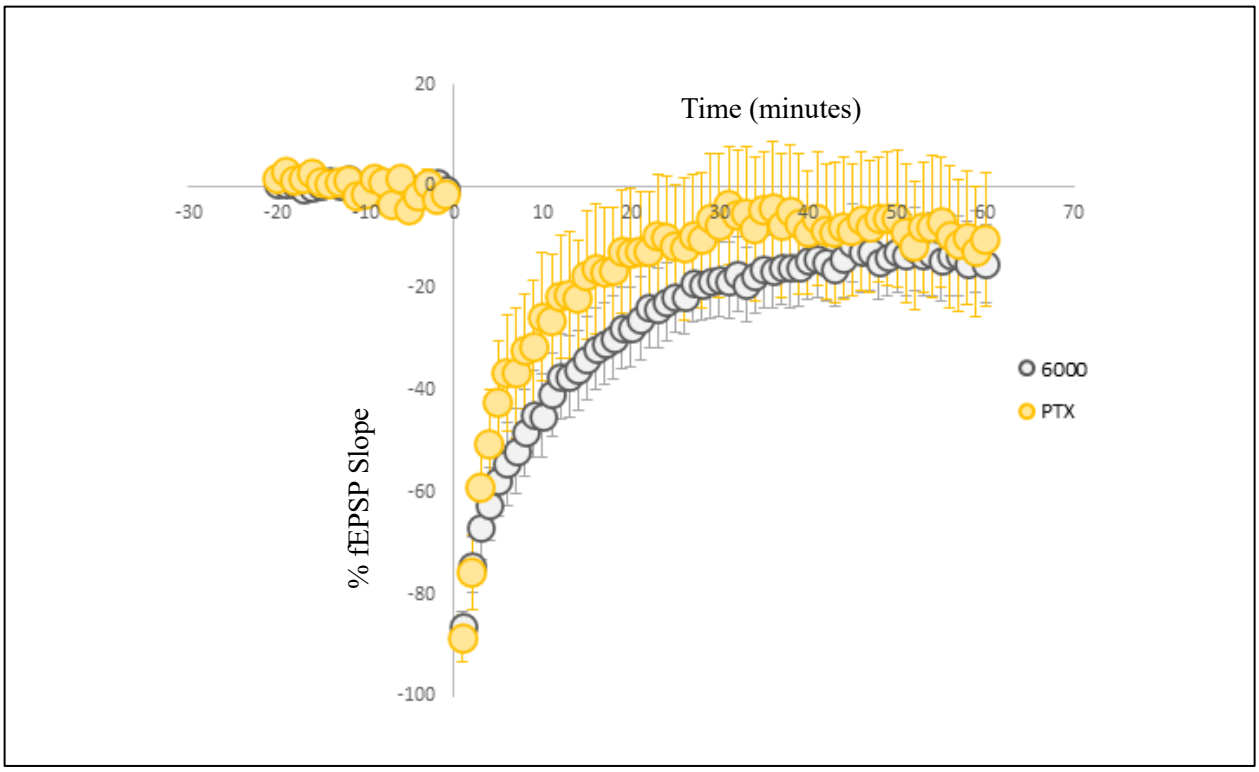

Figure S 6.2 Picrotoxin is not necessary for the induction of LTD in the 10 Hz protocol. All animals are male.

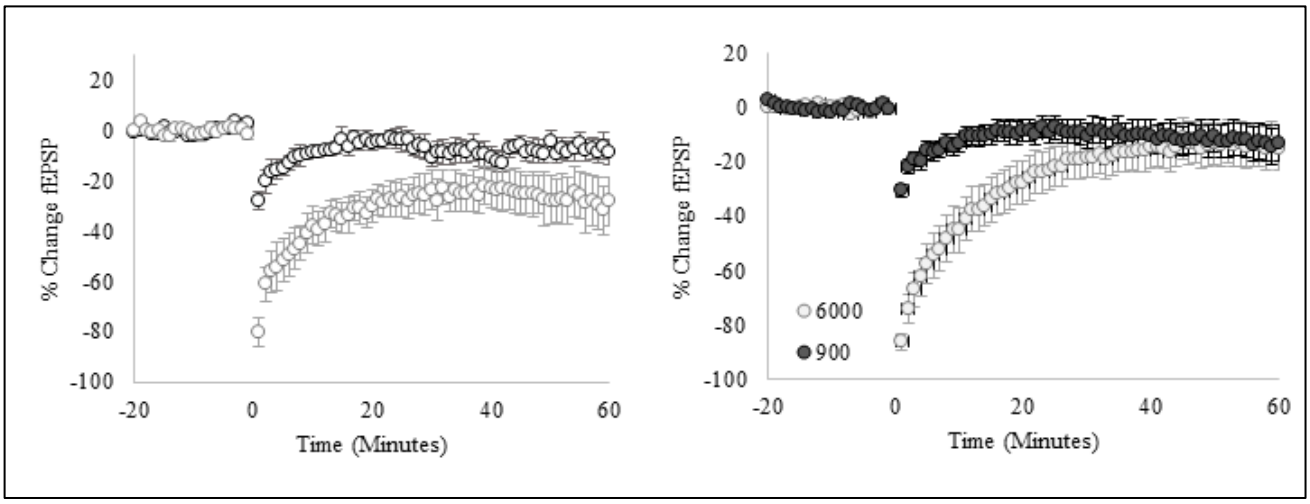

Figure S 6.3 Comparison of paradigms types in female (open circles) and male (closed circles) animals.

Table S 2.1 PRISMA search terms

Search Term Blocks	Search Terms
Specifies Prenatal	"Antenatal" OR "antepartum" OR "fetal" OR "prenatal"
Specifies brain region	"Hippocamp*" OR "dentate" OR "dentate gyrus" OR "CA1" OR "CA2" OR "CA3" OR "LPP" OR "MPP" OR "perforant pathway" OR "fimbria-fornix" OR "Schaffer collaterals" OR "Commisural pathway"
Specifies cytoarchitecture	"Genetic" OR "gene" OR "mRNA" OR "methylation" OR "hypermethylation" OR "acetylation"OR "hypomethylation" OR "methyl mark" OR "epigenetic" OR "NDMA" OR "nicotinic" OR "muscarinic" OR "CB2" OR "CB1" OR "GPCR" OR "G-protein" OR "G protein" OR "AMPA" OR "Calcium channel" OR "sodium channel" OR "chloride channel" OR "cAMP" OR "cyclic AMP" OR "PKA" OR "Signal transduction" OR "neurogenesis" OR "granule cell" OR "proliferation" OR "apoptosis" OR "neural stem cell" OR "neural stem cells" OR "cellular migration" OR "Immunohistochemistry" OR "IHC" OR "Ki-67" OR "PCNA" OR "Sox2" OR "BrdU" OR "DCX" OR "GFAP"

Specifies Alcohol	"PNEE" OR "Prenatal ethanol" OR "Prenatal alcohol" OR "PAE" OR "prenatal alcohol exposure" OR "FASD" OR "FAS" OR "fetal alcohol spectrum disorder" OR "fetal alcohol syndrome" OR "fetal alcohol exposure" OR "prenatal ethanol" OR "fetal ethanol" OR "ethanol" OR "alcohol"
Specifies Cannabis	"cannabis" OR "marijuana" or "THC" OR "Tetrahydrocannabinol" OR "Δ⁹-tetrahydrocannabinol" OR "cannabinoid" OR "WIN 55,212-2" OR "PME"

Table S 2.2 PRISMA inclusion and exclusion criteria

Inclusion Criteria	Exclusion Criteria
Must be a journal article	No behavior only paper
Must have cellular-level data (IHC, western, etc.)	No non-English papers
Must have prenatal equivalent exposure	Not in brain
Must include hippocampus or dentate gyrus	No review papers
Must mention Alcohol or Cannabinoid system in the abstract	Not injection alcohol
Must be mouse or rat	Electrophysiology only
	No drugs used to cure phenotype
	No other diseases
	No papers published before 2000
	No preliminary data papers

Table S 2.3 Short-listed papers that were excluded from the PRISMA, with reasons

Supplementary: Short-listed Papers that Were Excluded from the Final PRISMA, with Reasons					
Author	Title	Year	Methods	Main Findings	Reason for Exclusion
(264)	Dysregulation of the endogenous cannabinoid system in adult rats prenatally treated with the cannabinoid agonist WIN 55,212-2	2007	[35S]GTPγS binding assay, [3H]CP 55,940 binding assay, HPLC, hydrolysis of [3H]anandamide by fatty acid amide hydrolase, synthesis of anandamide through the activity of N-acyl-phosphatidylethanolamines (NAPE)-hydrolysing phospholipase D, Motor activity	EC50 values for WIN 55,212-2-stimulated [35S]GTPγS binding were significantly different in hippocampus (– 26%) and striatum (+ 27%) in WIN 55,212-2-treated rats. Cannabinoid CB1 receptor density and affinity were not affected in any analyzed region. In the striatum, increased anandamide levels were associated with reduced FAAH and enhanced NAPE-PLD activities. Opposite changes in anandamide levels and enzymatic activities were detected in limbic areas of WIN 55,212-2-treated rats. Ambulatory activity between WIN 55,212-2- and vehicle-treated adult offspring did not vary.	No immunohistochemistry
(265)	Effects of prenatal ethanol exposure on basal limbic-hypothalamic-pituitary-adrenal regulation: Role of corticosterone	2007	Adrenalectomy and Corticosterone Replacement; blood CORT and ACTH levels; Corticosterone and ACTH Radioimmunoassay; Antisense oligonucleotide probes for AVP, CRH, and POMC; Densitometric Analysis	Prenatal ethanol exposure induces HPA dysregulation under basal conditions at multiple levels of the axis, resulting in alterations in both HPA drive and feedback regulation and/or in the balance between drive and feedback. While some effects may be nutritionally mediated, it appears that the mechanisms underlying basal HPA dysregulation may differ between E and PF animals rather than occurring along a continuum of effects on the same pathway.	No immunohistochemistry, includes a treatment: cort removal and replacement
(266)	Downregulation of dopamine D1 receptors and increased neuronal apoptosis upon ethanol and PTZ	2013	Primary cell culture and drug treatment, RT-PCR, Western blotting, TUNEL staining	Ethanol and PTZ exposure down regulate the D1R expression and induced apoptotic neuronal death in prenatal rat brain. Therefore, our results suggested that exposure of ethanol and PTZ in primary neuronal cell culture leads to significant decrease in the expression of D1R and further	No immunohistochemistry

	exposure in prenatal rat cortical and hippocampal neurons.			leads to apoptotic neuronal cell death by significantly increasing the expression of pro apoptotic Bax, Bak and significantly decreasing the anti-apoptotic protein Bcl-2 leading to the increase in the expression of cleaved caspase-3 protein	
(267)	Ethanol exposure enhances cell death in the developing cerebral cortex: Role of brain-derived neurotrophic factor and its signaling pathways	2002	DNA Isolation and Determination of Fragmentation Associated With Apoptosis; RNA Extraction and Ribonuclease Protection Assay; BDNF ELISA; Western Blot for Analysis of PARP, Caspase 3, TrkB Receptors, and Bcl2; Electron Microscopy Analysis	Results support the hypothesis that alterations in the availability of neurotrophins and/or the correct functioning of their survival signaling receptors, as well as astroglial damage, may impair the establishment of neural connection and synaptic stabilization, leading to cell death	No immunohistochemistry
(268)	Fate Analysis of Adult Hippocampal Progenitors in a Murine Model of Fetal Alcohol Spectrum Disorder (FASD)	2013	Environmental Enrichment (EE); histology: DCX, PCNA, GFAP, S-100b	Moderate exposure to gestational alcohol can result in resistance to the neurogenic benefits of [environmentally enriched] in mice.	Contains a treatment: environmental enrichment
(269)	Fetal alcohol exposure alters GAP-43 phosphorylation and protein kinase C responses to contextual fear conditioning in the hippocampus of adult rat offspring	2004	Contextual Fear Conditioning, PKC Activity Assay, Western Blot Analysis of GAP-43, Phospho-GAP-43, and PKC Subtypes	Considering the role of PKC activation and GAP-43 phosphorylation in synaptic plasticity,our results suggest that deficient translocation of PKCbeta2and PKCbeta in the hippocampus may mediate theelectrophysiological and behavioral deficits observed in fetal alcohol exposed animals.	No immunohistochemistry

(270)	Hippocampal GR-and CBI-mediated MGluR5 differentially produces susceptibility and resilience to acute and chronic mild stress in rats	2017	Microinjection of WIN55,212-2; Stress protocol; Sucrose preference test; Open field test; RT-PCR; Western blotting: GR, CB1, mGluR5, and β-actin	GR was associated with the lower mGluR5 mRNA and protein in susceptibility rats of CMS group. CB1 was related to the lower mGluR5 mRNA and protein in susceptibility rats of AS group. Glucocorticoid and cannabinoid systems in hippocampus may regulate susceptibility and resilience to stress.	No immunohistochemistry, includes a treatment: stress protocol
(271)	Hippocampal N-Methyl-D-Aspartate Receptor Subunit Expression Profiles in a Mouse Model of Prenatal Alcohol Exposure	2010	RT-PCR; Immunoblotting of NMDA Receptor Subunits; Synaptosomal Membrane (LP1) Preparation and Immunoblotting of NMDA; Immunoprecipitation	Prenatal alcohol exposure induces selective changes in NMDA receptor subunit levels in specific subcellular locations in the adult mouse hippocampal formation. Of particular interest is the finding of decreased PSD-95-associated NR2B levels, suggesting that synaptic NR2B-containing NMDA receptor concentrations are reduced in FAE animals	No immunohistochemistry, dams given ethanol outside of pre-determined exposure period for this systematic review
(272)	Impact of moderate prenatal alcohol exposure on histaminergic neurons, histidine decarboxylase levels and histamine H 2 receptors in adult rat offspring	2019	Ethanol consumption study; Maternal serum ethanol assessment; Histidine decarboxylase (HDC) immunohistochemistry, HDC western blotting, Specific [125I]-iodoaminopotentidine binding to histamine H2 receptors, Amthamine-stimulated cAMP accumulation	Prenatal alcohol exposure (PAE) reduced histidine decarboxylase (HDC) in dentate gyrus, frontal cortex, and cerebellum of adult offspring. The number of HDC-positive neurons in ventral hypothalamus, the source of all histaminergic neural projections in brain, was not altered by PAE. Histamine H2 receptor density and H2 receptor-effector coupling were not altered by PAE. The PAE-induced reductions in HDC occurred in brain regions where heightened H3 receptor-effector coupling was observed previously.	Ethanol given to dams outside of gestation
(273)	Impaired ILK Function Is Associated with Deficits in Hippocampal Based	2015	Contextual fear conditioning; Electrophysiology recording; Immunoprecipitation (IP) assay, Western Blot	From this study, we conclude a close association of impaired ILK pathway and synaptic plasticity deficits in prenatal alcohol exposed rat model. Reduced ILK activity could be due to reduced BDNF to proBDNF ratio. The	No immunohistochemistry

	Memory and Synaptic Plasticity in a FASD Rat Model		analysis, ILK activity assay	reduced kinase activity and diminished interaction to GluR2 AMPAR could be responsible for increased stabilization of GluR2 containing receptors at the synapse. The increased calcium impermeable AMPAR is responsible for impaired LTP induction and maintenance. Reduced LTP can also be due to increased GSK3β activation which could affect receptor trafficking and protein expression required for LTP maintenance.	
(274)	Impairments in hippocampal synaptic plasticity following prenatal ethanol exposure are dependent on glutathione levels.	2013	Blood alcohol concentration assay; N-Acetyl-Cysteine Supplementation; Electrophysiology; Determination of Glutathione Levels	Study demonstrates the existence of a relationship between intracellular GSH levels and LTP in the DG of the hippocampus. With PNEE, long-term deficits in GSH occur and these lead to a decrease in LTP specifically in male animals. Supplementing PNEE animals with NAC to boost GSH concentrations is able to restore LTP in males	No immunohistochemistry
(275)	Increase of KCC2 in hippocampal synaptic plasticity disturbances after perinatal ethanol exposure	2017	Electrophysiology; In vitro drug applications; Autoradiography; KCC2 Immunofluorescence; KCC2 and NKCC1 western blotting	perinatal ethanol exposure in rats disturbs the role of GABAA inhibitions in modulating both NMDA-dependent LTP and LTD type of synaptic plasticity in CA1 area of the hippocampus. Such disturbances are accompanied with an upregulation of KCC2 co-transporter expression and can be corrected with acute bath application of bumetanide.	Ethanol given to dams outside of gestation
(276)	Influence of N-methyl D-aspartate receptor mechanism on WIN55,212-2-induced amnesia in rat dorsal hippocampus.	2011	Intra-CA1 injections of WIN55,212-2; Retrieval test; Elevated plus maze	These results suggest a possible relationship between NMDA receptor function and WIN responses. It is proposed that both NMDA receptor agonist and antagonist may restore memory in WIN-induced amnesia, but through different mechanisms. Although MK restores memory impairment induced by MK itself or by WIN through a state-dependent mechanism, NMDA may improve memory through	No immunohistochemistry, is behavior only

				glycine sites, which may be involved in spatial memory through their modulatory action on hippocampal NMDA receptors	
(277)	Long-lasting alterations of hippocampal GABAergic neurotransmis adult rats following perinatal Delta(9)-THC exposure	2017	[3H]-GABA outflow experiments; [3H]-GABA uptake experiments; Binding experiments	Maternal exposure to THC induces long-term alterations of hippocampal GABA system. Maternal exposure to THC permanently decreases hippocampal CB1 receptor. Hippocampal GABAergic alterations might underlie cognitive deficits of marijuana user offspring.	No immunohistochemistry
(278)	Maternal ethanol exposure reshapes CART system in the rat brain: Correlation with development of anxiety, depression and memory deficits	2019	Assessment of anxiety-like behavior employing EPM test; Assessment of depression-like behavior in FST; Assessment of cognition behavior using NORT; CART Immunohistochemistry; Morphometric analysis	This study investigates the effect of the alcohol abuse by the female rat on her offspring. Rat's chronic maternal ethanol ingestion model is employed, and her offspring at the age of 25 and 85 days are assessed. Alcoholic dam's offspring displayed a sign of memory impairment, and anxiety- and depression-like behaviors. Region-specific change is noticed in the CART expression of the offspring of alcoholic dams. The behavioral and neurological deficits may be correlated to abnormal expression of CART.	Ethanol given to dams outside of gestation
(279)	Moderate prenatal alcohol exposure reduces plasticity and alters NMDA receptor subunit composition in the dentate gyrus.	2013	Electrophysiological recordings; Synaptic and nonsynaptic fraction preparation and immunoblotting of NMDAR subunits; Crosslinking of surface receptors	We found that MPAE mice exhibit deficits in NMDA receptor (NMDAR)-dependent long-term potentiation (LTP) in the dentate gyrus. Further, using semiquantitative immunoblotting techniques, we found that the levels of GluN2B subunits were decreased in the synaptic membrane, while levels of C2′-containing GluN1 and GluN3A subunits were increased, in the dentate gyrus of MPAE mice.	Ethanol given to dams outside of gestation
(280)	NADPH Oxidase Isoform 2 (NOX2) Is Involved in Drug Addiction	2017	Western Blot; RNA Isolation and RT-PCR; Conditioned Place Preference (CPP); Free Choice Protocol (Two-Bottle Choice Protocol);	Our results support the role of redox homeostasis in the pathophysiology of drug addiction and show, for first time, that NOX2 could be involved in alcohol seeking behavior in mammals, specifically in the	Ethanol given to dams outside of gestation

	Vulnerability in Progeny Developmentally Exposed to Ethanol			vulnerability associated with problematic alcohol consumption.	
(281)	Neonatal Ethanol Exposure Impairs Trace Fear Conditioning and Alters NMDA Receptor Subunit Expression in Adult Male and Female Rats	2016	Trace Fear Conditioning; Western Blotting	EtOH-induced changes in DH NMDAR subunit expression—particularly synaptic GluN2B, which is critical for TFC—are proposed to weaken long-term memory consolidation and, during behavioral testing, diminish CS-evoked freezing behavior.	No immunohistochemistry
(282)	Neurocircuitry underlying stress and emotional regulation in animals prenatally exposed to alcohol and subjected to chronic mild stress in adulthood	2014	Chronic Mild Stress; Elevated Plus Maze; Neural Assessment of c-fos mRNA by in situ Hybridization;	Control males rely more on the amygdala and hippocampal formation, PAE males rely more on the mPFC and mpdPVN when facing a stressful situation. In contrast, the functional neural networks underlying stress and emotional regulation in females are more restricted, as PAE females rely primarily on the mPFC and amygdala. Additionally, our results indicate that CMS differentially affected the neural networks regulating stress and emotion in PAE and control animals. Indeed, exposure to CMS reduced the activity of the Amygdala + Hippocampal Formation network in control males, but reduced the activity of the Prefrontal Cortex + Paraventricular Nucleus network in PAE males. For females, CMS only reduced the activity of the Prefrontal Cortex network in PAE animals. Together, our results suggest that PAE, regardless of its association with CMS, results in a sexually dimorphic dysregulation of the neurocircuitry that underlies stress and emotional	No immunohistochemistry

				regulation, which may be implicated in the stress hyperresponsivity and increased vulnerability to anxiety and depressive disorders observed among individuals exposed to alcohol during gestation	
(50)	Neurodevelopmental alcohol exposure elicits long-term changes to gene expression that alter distinct molecular pathways dependent on timing of exposure	2013	RNA isolation and microarray hybridization; Gene ontology and gene network analysis; Quantitative RT-PCR	These changes to brain gene expression represent a 'molecular footprint' of neurodevelopmental alcohol exposure that is long-lasting and correlates with active processes disrupted at the time of exposure. This study provides further support that there is no neurodevelopmental time when alcohol cannot adversely affect the developing brain.	No immunohistochemistry
(283)	Prenatal alcohol exposure alters methyl metabolism and programs serotonin transporter and glucocorticoid receptor expression in brain	2015	Real-time PCR; Quantification of DNA methylation by bisulfite pyrosequencing; Immunoblot analysis.	We report for the first time that PAE is associated with altered plasma levels of methyl metabolites, altered one-carbon metabolism enzyme gene expression in liver and brain, and changes in the expression of two genes central to HPA axis function. These findings provide molecular evidence that supports and significantly extends previous studies on the effects of prenatal alcohol exposure on gene expression and epigenetic mechanisms, and advances our understanding of the pathophysiology of FASD.	No immunohistochemistry
(284)	Prenatal Alcohol Exposure Leads to Enhanced Serine 9 Phosphorylation of Glycogen Synthase Kinase-3beta	2017	Western Blot Analysis; Immunohistochemistry	These findings suggest that PAE may lead to a long-term disruption of GSK-3b signaling within the DG, and implicate mossy cells, GABAergic interneurons, and CA primary neurons as major targets of this dysregulation.	Ethanol given to dams outside of gestation

	(GSK-3beta) in the Hippocampal Dentate Gyrus of Adult Mouse.				
(285)	Prenatal ethanol exposure alters adult hippocampal VGLUT2 expression with concomitant changes in promoter DNA methylation, H3K4 trimethylation and miR-467b-5p levels	2015	Microarray-based analysis of gene expression; qPCR validation of differential gene expression; Clonal bisulphite sequencing; In vitro reporter assays of promoter function; ChIP-qPCR; Western blotting; MicroRNA profiling; TaqMan qPCR validation of differential miRNA expression; Luciferase reporter assay of miRNA–target mRNA interaction; Analysis of alcohol-sensitive miRNAs in serum	Prenatal ethanol exposure affects hippocampal gene expression and epigenetic state at multiple levels. Further, these effects are observed following a relatively moderate exposure early in pregnancy, and only in adult male offspring. Our findings are consistent with the idea that some of the cognitive and behavioural phenotypes observed in foetal alcohol spectrum disorders may be due to altered epigenetic and/or miRNA-mediated control of glutamate neurotransmission in the hippocampus.	No immunohistochemistry
(286)	Prenatal ethanol exposure persistently impairs NMDA receptor-dependent activation of extracellular signal-regulated kinase in the mouse dentate gyrus.	2009	Electrophysiology; Immunoblotting for ERK; Western blot data analysis; Immunohistochemistry of re-sectioned hippocampal slices	Found that FAE mice have decreased hippocampal NMDA receptor-dependent ERK activation that was not because of inherent deficiencies in PKA (Rap1-B-Raf-MEK) or PKC (Ras-Raf1-MEK) signaling. Immunohistochemical studies demonstrated that the deficit was localized to the DG	Ethanol given to dams outside of gestation
(287)	Prenatal exposure to alcohol does not affect radial maze	2005	Radial Maze; Timm's stain	Prenatal alcohol exposure influenced neither radial maze performance nor the sizes of the IIPMF terminal fields. We believe that future research should be	Ethanol given to dams outside of gestation

	learning and hippocampal mossy fiber sizes in three inbred strains of mouse.			pointed either at different targets when using mouse models for Fetal Alcohol Syndrome (e.g. more complicated behavioral paradigms, different hippocampal substructures, or other brain structures) or involve different animal models.	
(102)	Programming for increased expression of hippocampal GAD67 mediated the hypersensitivity of the hypothalamic-pituitary-adrenal axis in male offspring rats with prenatal ethanol exposure	2018	Serum ACTH and corticosterone detection; Hippocampal haematoxylin-eosin (HE) staining and transmission electron microscopy (TEM) analysis; Analysis of hypothalamic and hippocampal function-associated gene mRNA expression; Immunohistochemistry analysis of hippocampal GAD67; Analysis of hippocampal neurotransmitters, glutamate and GABA; Immunofluorescence analysis of hippocampal glutamatergic neurons and GABAergic neurons; DNA extraction and BSP; Rat hippocampus cell line H19-7 culture and treatment	High-glucocorticoid level mediated the intrauterine programming mechanism responsible for the hypersensitivity of the HPAA in male PEE-induced IUGR offspring…these intrauterine changes may alleviate the hippocampal excitatory effects on the glutamate-GABA synaptic connections, resulting in weakening negative regulation of the hypothalamus, ultimately leading to an increased excitatory ability of the hypothalamus. Increased expression of GAD67 as a compensatory effect was programmed in utero by epigenetic modifications, which continued until after birth or even into adulthood, and mediated the hypersensitivity of the HPAA to CS in the PEE male offspring.	Offstring assayed were GD20, for this paper they must be P30 or older

Table S 3.1: Statistics table, PV cell density, CA1

Tests of Between-Subjects Effects					
Dependent Variable: Density					
Source	Type III Sum of Squares	df	Mean Square	F	Sig.
Corrected Model	29132.467[a]	15	1942.164	2.115	.018
Intercept	2435997.732	1	2435997.732	2653.390	.000
Exposure	11805.214	3	3935.071	4.286	.008
Sex	553.038	1	553.038	.602	.440
DV	12841.272	1	12841.272	13.987	.000
Exposure * Sex	498.796	3	166.265	.181	.909
Exposure * DV	1545.583	3	515.194	.561	.642

Sex * DV	464.981	1	464.981	.506	.479
Exposure * Sex * DV	833.433	3	277.811	.303	.823
Error	69773.317	76	918.070		
Total	2575096.786	92			
Corrected Total a. R Squared = .295 (Adjusted R Squared = .155)	98905.784	91			

Table S 3.2: Statistics table, PV cell density, DG

Tests of Between-Subjects Effects
Dependent Variable: Inhibition

Source	Type III Sum of Squares	df	Mean Square	F	Sig.
Corrected Model	.001[a]	15	4.331E-5	4.044	.000
Intercept	.023	1	.023	2115.208	.000
Exposure	.000	3	5.376E-5	5.019	.003
Sex	1.741E-5	1	1.741E-5	1.625	.206
DV	.000	1	.000	35.527	.000
Exposure * Sex	4.386E-6	3	1.462E-6	.137	.938
Exposure * DV	2.131E-5	3	7.102E-6	.663	.577
Sex * DV	4.041E-5	1	4.041E-5	3.773	.056
Exposure * Sex * DV	2.709E-5	3	9.030E-6	.843	.475
Error	.001	76	1.071E-5		
Total	.024	92			

Corrected Total a. R Squared = .444 (Adjusted R Squared = .334)	.001	91			